

NUMERICAL INTEGRATION OF
LARGE DEFLECTION ELASTIC-PLASTIC
AXISYMMETRIC SHELLS OF REVOLUTION

Habib Uddin Ahmed

NOTICE

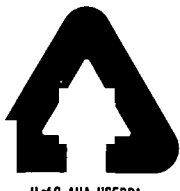
This report was prepared as an account of work sponsored by the United States Government. Neither the United States nor the United States Energy Research and Development Administration, nor any of their employees, nor any of their contractors, subcontractors, or their employees, makes any warranty, express or implied, or assumes any legal liability or responsibility for the accuracy, completeness or usefulness of any information, apparatus, product or process disclosed, or represents that its use would not infringe privately owned rights.

December, 1976

MASTER

EB

DISTRIBUTION OF THIS DOCUMENT IS UNLIMITED



ARGONNE NATIONAL LABORATORY, ARGONNE, ILLINOIS

operated under contract W-31-109-Eng-38 for the
U. S. ENERGY RESEARCH AND DEVELOPMENT ADMINISTRATION

DISCLAIMER

This report was prepared as an account of work sponsored by an agency of the United States Government. Neither the United States Government nor any agency Thereof, nor any of their employees, makes any warranty, express or implied, or assumes any legal liability or responsibility for the accuracy, completeness, or usefulness of any information, apparatus, product, or process disclosed, or represents that its use would not infringe privately owned rights. Reference herein to any specific commercial product, process, or service by trade name, trademark, manufacturer, or otherwise does not necessarily constitute or imply its endorsement, recommendation, or favoring by the United States Government or any agency thereof. The views and opinions of authors expressed herein do not necessarily state or reflect those of the United States Government or any agency thereof.

DISCLAIMER

Portions of this document may be illegible in electronic image products. Images are produced from the best available original document.

The facilities of Argonne National Laboratory are owned by the United States Government. Under the terms of a contract (W-31-109-Eng-38) between the U. S. Energy Research and Development Administration, Argonne Universities Association and The University of Chicago, the University employs the staff and operates the Laboratory in accordance with policies and programs formulated, approved and reviewed by the Association.

MEMBERS OF ARGONNE UNIVERSITIES ASSOCIATION

The University of Arizona	Kansas State University	The Ohio State University
Carnegie-Mellon University	The University of Kansas	Ohio University
Case Western Reserve University	Loyola University	The Pennsylvania State University
The University of Chicago	Marquette University	Purdue University
University of Cincinnati	Michigan State University	Saint Louis University
Illinois Institute of Technology	The University of Michigan	Southern Illinois University
University of Illinois	University of Minnesota	The University of Texas at Austin
Indiana University	University of Missouri	Washington University
Iowa State University	Northwestern University	Wayne State University
The University of Iowa	University of Notre Dame	The University of Wisconsin

NOTICE

This report was prepared as an account of work sponsored by the United States Government. Neither the United States nor the United States Energy Research and Development Administration, nor any of their employees, nor any of their contractors, subcontractors, or their employees, makes any warranty, express or implied, or assumes any legal liability or responsibility for the accuracy, completeness or usefulness of any information, apparatus, product or process disclosed, or represents that its use would not infringe privately-owned rights. Mention of commercial products, their manufacturers, or their suppliers in this publication does not imply or connote approval or disapproval of the product by Argonne National Laboratory or the U. S. Energy Research and Development Administration.

ABSTRACT

The improvement in the method of large deflection elastic-plastic analysis of shells and other structures appears to have continued interest. With the development in this work an improved numerical suppression scheme is now available for the large deflection elastic-plastic analysis of axisymmetric shells of revolution subjected to symmetric loadings. Quazilinearization of Sander's non-linear shell equations is presented for the first time. With these quazilinearized equations the suppression scheme has been developed to solve non-linear boundary-value problems. This suppression scheme has been used in conjunction with a Newton-Raphson method to improve a stable convergence process at the yield surface in elastic-plastic problems. Results presented indicate the accuracy of this numerical scheme. It appears to be possible to extend this method for more complicated situations.

NUMERICAL INTEGRATION OF
LARGE DEFLECTION ELASTIC-PLASTIC
AXISYMMETRIC SHELLS OF REVOLUTION

BY

HABIB UDDIN AHMED

Submitted in partial fulfillment of the
requirements for the degree of
Doctor of Philosophy in Civil Engineering
in the Graduate School of
Illinois Institute of Technology

Approved


J.W. Leonard

Advisor

Chicago, Illinois
December, 1976

MASTER

DEDICATED
TO
MY FATHER AND MY LATE MOTHER

ACKNOWLEDGEMENTS

The writer expresses his gratitude and sincere appreciation to his research advisor, Professor J. W. Leonard, Chairman of Civil Engineering Department of Illinois Institute of Technology, for his continuous encouragement and able guidance during the entire scope of this work.

The writer is thankful to Dr. C. H. Chu, Dr. R. A. Malek of Civil Engineering Department, Dr. A. F. D'Souza of Mechanics and Mechanical and Aerospace Engineering Department of Illinois Institute of Technology and Mr. K. D. Kuczen of Argonne National Laboratory for useful advises and reading the manuscript. The writer is also thankful to Dr. J. Gerdeen of Michigan Technological University for useful discussions. Thanks are due also to Mr. D'anjou of Illinois Institute of Technology for directing the format of this manuscript.

The writer is also very grateful to number of facilities provided by Argonne National Laboratory during the course of this effort.

The writer expresses special appreciation to his wife, Nasreen, for her perseverance, patience and cooperation without which it would have been impossible to complete this task. For her hard work in typing this manuscript and encouragement, which has been invaluable. The writer expresses his appreciation to his children who cooperated in every possible way and who must now think that their father is a professional student.

H. U. A

TABLE OF CONTENTS

	Page
ACKNOWLEDGEMENT	iii
LIST OF TABLES	vii
LIST OF FIGURES	viii
NOMENCLATURE	x
CHAPTER	
I. INTRODUCTION	1
Previous Research	1
Non-Linear Shell Theory	1
Plasticity	2
Numerical Methods	4
Scope of Study	7
II. EQUILIBRIUM AND KINEMATIC EQUATION FOR SHELLS OF REVOLUTION	9
Intent of Chapter	9
Shell Geometry	9
General Equilibrium Equations	10
General Strain Displacement Relations	19
General Boundary Conditions	20
Simplification to Shell of Revolution	21
Simplified Equation of Motion	22
Specialized Strain-Displacement Relations	23
Inclusion of Constitutive Relations	24
Reordering of Equations	25
III. ELASTO-PLASTIC CONSTITUTIVE RELATIONS	27
Intent of Chapter	27
Material Behavior and Properties	27
Yield Surface	29
Hardening Modulus	31
Review of Elastic-Plastic Method of Analysis	34
Incremental Plasticity for Shells of Revolution	36
Definition of Stress-Strain Relation	36
Partial Stiffness Coefficients	39
Transition Case	40
Determination of Partial Stiffness Coefficients	42
Newton-Raphson Scheme	44
Consistency of Function	50
Shell Incremental Plasticity	52
Treatment of Shell Apex	57

	Page
CHAPTER	
IV. INCREMENTAL SOLUTION OF ELASTIC-PLASTIC PROBLEMS.	59
Intent of Chapter	59
Bases of Solution.	59
Reformulation of Initial Value Problems.	60
Quasilinearization	62
Theory	62
Application.	65
Final form of Equations.	69
Statement of Chapter	77
V. NUMERICAL INTEGRATION SCHEME FOR LINEAR ANALYSIS.	78
Intent of Chapter.	78
Linear Analysis Method-Background.	78
Description of Suppression Process	80
Basic Suppression Technique.	81
Statement of Chapter	87
VI. NUMERICAL INTEGRATION OF QUASILINEARIZED EQUATIONS	88
Intent of Chapter.	88
Suppression Scheme for Non-linear Elastic Analysis	88
Application of Quasilinearization.	88
Application of Suppression Scheme.	89
Complexities of Non-linear Elastic-Plastic Analysis	91
Non-linear Multisegment Numerical Integration Technique.	92
Suppression Scheme vs Multisegment Method.	95
Statement of Chapter	97
VII. RESULTS	98
Boundary Conditions.	98
Torus Under External Pressure.	101
Spherical Membrane Under External Pressure	110
Cylindrical Membrane Under External Pressure	112
Annular Plate Subjected to Inner Edge Deflection	115
VIII. CONCLUSIONS AND RECOMMENDATIONS	122
Summary of Study	122

CHAPTER	Page
Discussion of Results	122
Limitations	123
Possible Extensions	124
General Conclusions	124
APPENDIX	
A. STRESS PRELIMINARIES	126
Stress Tensor	127
Stress Invariant.	129
Effective Stress.	130
Strain Preliminaries.	131
Deviatoric Stress Tensor.	134
B. NON-DIMENSIONALIZED SHELL EQUATIONS AND TREATMENT OF SINGULARITIES AT SHELL APEX	136
Significance of Non-dimensionalization.	137
Non-dimensionalized Governing Shell Equations .	139
Singularities at the Apex of the Shell.	141
C. SHELL CONFIGURATIONS	144
Cylinder.	145
Sphere.	145
Torus	145
Cone.	146
Annular Plate	146
D. DEFINITION OF HARDENING.	148
BIBLIOGRAPHY	155

LIST OF TABLES

Table	Page
1. Components of Matrix	75

LIST OF FIGURES.

Figure	Page
2.1 Shell Surface Coordinates.	11
2.2 Shell Curvatures	13
2.3 Sign Convention of Stress Resultants	15
2.4 Sign Convention of Stress Components	17
3.1 Von-Mises Yield Surface Elastic to Plastic	30
3.2 Von Mises Yield Surface Plastic to Elastic	30
3.3 Bilinear Stress-Strain Curve	32
7.1 Shell Boundary Conditions Nomenclature	99
7.2 Shell Boundary Condition Nomenclature.	100
7.3 Torus Under External Pressure	102
7.4 Elastic Deflection Behavior of a Torus	104
7.5 Elastic Meridional Moment Distribution of a Torus. .	105
7.6 Elastic Circumferential Membrane Force Distribution in Torus.	106
7.7 Circumferential Bending Moment Distribution in Torus	107
7.8 Spherical Membrane Under External Pressure	109
7.9 Cylindrical Membrane Under External Pressure	109
7.10 Deflection Relationship of Spherical Membrane Under External Pressure.	111
7.11 Load Deflection Relationship of Cylindrical Membrane under External Pressure	113
7.12 Annular Plate Nomenclature	116
7.13 Relation Between Total Load and Deflection of Annular Plate.	118

Figure	Page
7.14 Elastic-Plastic Zones In Annular Plate	121
D.1 Bilinear Strain Hardening Properties of SS304 Material.	152

NOMENCLATURE

Following is a list of some important symbols as they are used in the text. Other symbols are defined appropriate parts of certain symbols have different meaning in different sections of the text. Where this occurs, the symbol is redefined for each section.

ϕ	= Angle between axis of revolution and normal to the shell.
r	= Radial distance from the axis of revolution to a point on the middle surface.
R_1 or R_ϕ	= Principal radius of curvature in the meridional plane.
R_2 or R_θ	= Principal radius of curvature in the plane perpendicular to the meridian.
s	= Coordinate length measured on the meridian.
R	= Shell configuration radius. When defined as superscript R refers to residual or previous solution state.
α, β	= Lame's Coefficients.
u, v, w	= Components of displacements at the middle surface of the shell.
h	= Shell thickness.
$*$	= When used as a superscript it refers to a non-dimensional quantity per the definitions in appendix B.
x_1, x_2, x_3	= Cartesian coordinate system used for the definition of shell configuration.
γ	= Angle of rotation of shell meridian.
z	= Shell thickness coordinate.

C_{ij}	= Membrane stiffness coefficients in shell stress-strain relations
D_{ij}	= Bending stiffness coefficients in shell stress-strain relations
E	= Modulus of elasticity.
E_{ij}	= Stiffness coefficients in incremental stress-strain relations.
$\epsilon_\phi, \epsilon_\theta$	= Meridional and circumferential membrane strains.
$\bar{\epsilon}_\phi, \bar{\epsilon}_\theta$	= Approximations to ϵ_ϕ and ϵ_θ resulting from the previous iteration of the quasilinearization algorithm.
ϵ_1, ϵ_2	= Principal strain.
$\epsilon_1^i, \epsilon_2^i$	= ϵ_1 and ϵ_2 at the beginning of an increment.
$\bar{\epsilon}_1, \bar{\epsilon}_2$	= Approximations to ϵ_1 and ϵ_2 resulting from the previous iteration of the quasilinearization algorithm.
H	= Strain hardening function.
H'	= Derivative of H with respect to its argument.
\bar{H}'	= Defined by Eq. (III.13)
K_{ij}	= Coupling stiffness coefficients in shell stress-strain relations.
x_s, x_θ	= Approximations to x_s and x_θ resulting from previous iteration of quasilinearization algorithm.
ν	= Poisson's ratio.
M_ϕ, M_θ	= Meridional and circumferential bending moments per unit length.
$\bar{M}_\phi, \bar{M}_\theta$	= Approximations to M_ϕ and M_θ resulting from previous iteration of quasilinearization algorithm.
M_o	= Yield bending moment, $\sigma_o h^2/4$ per unit length.

N_ϕ, N_θ	= Meridional and circumferential membrane forces per unit length.
$\bar{N}_\phi, \bar{N}_\theta$	= Approximations to N_ϕ and N_θ resulting from previous iteration of quasilinearization algorithm.
N_0	= Yield membrane force, $\sigma_0 h$ per unit length.
P_r, P_ϕ	= External surface loads per unit area of middle surface.
Q_ϕ	= Transverse shear force per unit length.
\bar{Q}_ϕ	= Approximation to Q_ϕ resulting from previous iteration of quasilinearization algorithm.
S_1, S_2	= Deviatoric Stress.
σ_1, σ_2	= Principal stresses.
σ_1^i, σ_2^i	= σ_1 and σ_2 at the beginning of an increment.
$\bar{\sigma}_1, \bar{\sigma}_2$	= Approximations to σ_1 and σ_2 resulting from previous iteration of quasilinearization algorithm.
σ_0	= Yield stress in simple tension.
x	= Independent variable.
$d(\cdot)$	= Infinitesimal increment.
$\Delta(\cdot)$	= Finite increment.
$(\cdot)'$	= $\frac{d(\cdot)}{ds}$ (Note exception for H' .)

CHAPTER I

INTRODUCTION

A direct integration numerical scheme has been developed for the large deflection elastic-plastic analysis of shells of revolution subjected to symmetric loadings. This numerical scheme appears to be advantageous to other existing numerical schemes for similar applications. The results obtained for some sample problems compare with existing theoretical and experimental results in the literature.

In the design of nuclear reactors and other industrial applications where size limitation on components are imposed, the structures must withstand large magnitude of loadings. This requires that their structural performance be investigated well into regions of potential yielding. Such investigations in the case of shells of revolution are more precise and economical with direct numerical integration schemes than with finite element or finite difference approaches.

1.1 Previous Research.

A summary of the literature on the subject is presented under various subtitles in the context of work performed.

1.1.1. Non-linear Shell Theory. Substantial progress has been made toward the development of the non-linear theory of elastic shells in the past ten years. It is interesting to note that the literature on this subject is divided into two different approaches, those that invoke Kirchoff's Hypothesis and those that assume

a state of plane stress. Under Kirchoff's Hypothesis the normal to the undeformed middle surface remain normal to the deformed middle surface of the shell.

Sander's (7) has based his non-linear shell theory on the Kirchoff's assumption and on the assumption of small rotations about the normal. Small strains are admitted. This theory is more generally accepted than others due to its simplicity and to the satisfactory results obtained therefrom. Koiter's (5) work is concentrated almost entirely on the assumption of the state of plane stress and of small strains. But, it was necessary for Koiter to lower the magnitude of corrections with respect to strain measures, to the fundamental forms of the middle surface to satisfy the Gauss-Codazzi relations of surface compatibility. Naghdi (6) has defined his strain measures as functions of the metric of the undeformed middle surface. Further, Naghdi (3) has chosen to couple his non-linear constitutive relations with strain measures and stress resultants. His derivations are based, like those of Sander's (7), on a strain energy density function corresponding to the undeformed middle surface with the assumption of the Kirchoff's Hypothesis.

1.1.2. Plasticity. Earlier work in plasticity theory was based on a perfectly plastic material behavior. Some of this is reported by Prager and Hodge (72). Scope of work hardening behavior in the earlier literature was limited. However, some fundamental research in this area was done by Drucker (73) and (74) and also by Hill (1).

A brief survey on the early developments in plasticity theory is available in Ref. (78).

Although many yield criteria have been proposed in the literature such as those by Hill (1), the Von-Mises yield criterion (75) has been supported by experimental observations. For the prediction of the onset of plastic flow, the flow rules advocated by Prandtl (76) and by Reuss (77) seems to agree closely with the Von-Mises yield criterion (75). Some of the experimental observations, such as in the Liquid Metal Fast Breeder Reactor material experiments (24), indicate that stainless steel (SS 304) obeys the Von-Mises yield criterion. These experiments also indicate that a combination of isotropic and kinematic hardening behaviour is observed in SS 304 material testing. For some high temperature applications Wu and Witmer (4) have developed constitutive relations based on the Von-Mises yield criterion and an isotropic hardening rule.

Since the work performed here used the incremental theory of plasticity, the information available in the literature for practical solution methods will be emphasized in the following. Hodge (62,63) adopted a quadratic programming approach in a solution algorithm using the finite element method of analysis. Marcal (15-18) provided a theory of incremental plasticity which was applicable to shells of revolution. Marcal also used the finite element approach in his development of an incremental plasticity solution algorithm.

Gerdeen (9) later used Marcal's approach in conjunction with the direct integration method. Hütula (65) used essentially the same approach as Gerdeen (9) but also presented an application of the Newton-Raphson scheme for predicting better approximations to stress and strain increments in the vicinity of the yield surface. In this definition, Hütula (65) used a special case of Marcal's (15-16) yield transition case.

1.1.3. Numerical Methods. There are several numerical methods including finite element method, finite difference method and direct numerical integration method that have been used for the elastic-plastic analysis of shells of revolution.

In the finite element method the structure is discretized into finite sized elements, and the stiffness of each of these elements is defined. By using the stiffness method of analysis and satisfying the compatibility at the node circle junctions of adjacent elements, solutions of a given problem are obtained.

In the finite difference method the structure is distributed with mesh points. For each of the mesh points the differential equations of the system are represented in finite difference form following a backward difference, a central difference or a forward difference approach. A system of simultaneous equations are developed and a boundary value problem is solved.

In the elastic-plastic analysis of structures both the finite element and the finite difference approaches have been used. In many instances a combination of finite-element and finite-difference

methods has been proved useful. The finite element method is highly versatile and does not have the inherent stability problems of the finite difference methods. In the finite-difference method, it is difficult to select an appropriate mesh size that is simultaneously convergent and efficient. Various applications with finite element, finite difference and their combinations is given in Refs. (26 - 59).

Significant contributions in the application of finite elements to large deflection analyses of elastic-plastic shells were given by Marcal (16 - 18) and by Poppov and Yaghammi (19). Both studies used the curved shell element of Khajasteh-Bakht.

Marcal (18) also uses a triangular plate element known as the De Veneke element. Wu and Witmer (4) have applied the finite-element method to transient large deflection elastic-plastic analyses of simple structures, but this investigation was limited to the use of ring and beam elements. One significant feature of the work of Wu and Witmer in (4) is the development of plasticity flow theory relations from direct considerations of the high temperature applications.

Direct numerical integration methods, when appropriately developed to apply to complicated problems, prove to be computationally advantageous to the finite-element and finite difference methods. Goldberg and Bogdanoff (11) were the first to develop the multi-segment method of numerical integration. Kalnins and Lestini (66) have applied this technique to non-linear analysis of elastic shells of revolution. Gerdeen (9) used the multisegment method of direct

numerical integration for the large deflection analysis of elastic-plastic shells of revolution. The suppression technique of Goldberg (11) and Zarghami and Robinson (80) was used by Carter, Robinson and Schnobrich (14) and by Leonard (13) for the dynamic response of elastic shells. Marcal and Pilgrim (15) used a numerical integration method for the elastic-plastic analysis, but it was limited to small deflection theory assumptions.

Numerical Integration enables a direct solution to non-linear differential equations by converting a boundary value problem to a set of initial value problems in a form such that these initial value problems are integrated numerically and recombined to satisfy the boundary conditions.

However, in shell analysis a problem arises in the use of numerical integration. The solutions are of exponential type and accuracy is lost in integration over long path lengths. To overcome this problem, the multi-segment (12) or the suppression technique (13) (14) can be used. These methods provide uniform accuracy everywhere along the integration path. It has been shown that the suppression method is a more efficient means to achieve that accuracy.

Where large deflections of shells are accompanied by plastic strains, an accurate analysis requires that partial yielding through the shell thickness be considered. For the Von-Mises criterion of yielding the stiffness is determined by integration over the shell thickness following the work of Marcal and Pilgrim (15) who considered small deflections only. This requires storage of stress at several

points through the thickness of the shell at each station along the meridian. Gerdeen (9) and Hutula (65) adopted the multisegment method of direct integration for large deflection elastic-plastic analysis of shells of revolution. There has been no work reported in the literature for the large deflection elastic-plastic analysis of shells of revolution using a suppression technique.

1.2 Scope of Study.

The following assumptions are made in this study:

- (i) Large deflections and small strains.
- (ii) Axisymmetric shell of revolution with arbitrary meridional contours.
- (iii) Symmetrical loadings.
- (iv) Isotropic material behavior.
- (v) Von-Mises yield criterion.

A quazilinearization method along with Sander's non-linear shell theory is used in developing a set of quazilinearized governing equations. The constitutive relations for elastic-plastic behavior have a more general form than those presented by Hutula (65). In treating the elastic-plastic interface problem, Marcal's (15,16) approach has been generally followed. Much of the work on the development of a numerical scheme was directed towards the development of a suppression technique for non-linear elastic-plastic behavior. It is shown analytically that the suppression technique is a more efficient technique than the multisegment method.

1.3 Organization of Study.

Equilibrium and kinematic equations for non-linear shells of

revolution are presented in Chapter II. Incremental elastic-plastic constitutive relations is the subject of Chapter III. In Chapter IV a quasilinearization technique is applied to the non-linear shell equations and the resulting equations are organized in a form necessary for the solution algorithm.

In Chapter V the suppression technique for the linear elastic analysis of shells is reviewed. In Chapter VI a non-linear method of analysis with the suppression scheme for large deflection elastic and elastic-plastic analysis of shells of revolution is developed and compared to the multisegment method of numerical integration.

A set of examples for the verification of the linear elastic, non-linear elastic and non-linear elastic-plastic solutions algorithm is given in Chapter VII. Chapter VIII provides conclusions and recommendations resulting from this study.

CHAPTER II

EQUILIBRIUM AND KINEMATIC EQUATIONS FOR SHELLS OF REVOLUTION

2.0 Intent of Chapter.

Of the most recently developed shell theories, Sander's shell theory (7) appears to be most advantageous due to its simplicity in application. In this chapter the governing equations for a general shell are presented followed by their reductions to those for axisymmetrically loaded shells of revolutions. Those equations consist of equilibrium, strain-displacement and constitutive relations. Only a basic treatment of constitutive relations is given here. A more detailed treatment of plasticity is left for a later chapter. The governing equations are represented as a set of first order ordinary differential equations suitable for numerical integration.

2.1 Shell Geometry.

Let the undeformed middle surface of the shell be as shown in Fig (II.1) upon which the orthogonal curvilinear coordinate lines ξ_1 and ξ_2 are defined by the dotted lines. Let the coordinate system of the middle surface be defined as follows:

The position vector of a point on the shell middle surface is:

$$\vec{r} = x_i \hat{e}_i$$

$$x_i = f_i (\xi_1, \xi_2) ; i=1,2,3 \quad (\text{II.1})$$

Where f_i is a single valued function, and \hat{e}_i are the unit Cartesian base vectors.

The position of any point in the shell is specified by the coordinates ξ_1, ξ_2 and z , where ξ_1 and ξ_2 specify position on the middle surface while z measures the distance along the outward normal from the middle surface to the point (See Fig. 2.1).

The outward directed unit normal vector at a point of the middle surface is denoted by \hat{n} . The coordinates ξ_1 and ξ_2 are to be chosen in such a way that the system is right handed. The unit tangent vectors to the ξ_1 and ξ_2 curves are denoted by \hat{t}_1 and \hat{t}_2 respectively.

Let the displacement vector \bar{U} of the material points on the middle surface of the shell be resolved into components tangential and normal to the undeformed middle surface as follows.

$$\bar{U} = u \hat{t}_1 + v \hat{t}_2 + w \hat{n} \quad (\text{II.2})$$

2.2 General Equilibrium Equations.

The equilibrium equations of a three dimensional medium referred to orthogonal curvilinear coordinates corresponding to the deformed body are obtained from Sanders (7). The equations of equilibrium in terms of stresses are reduced to the force and moment equilibrium equations by integrating the stress equilibrium equations through the thickness and using the relationships between the stresses and the stress resultants. Sander (7) adopted Kirchoff's Hypotheses with some reference to small strain assumption and small rotations about the normal. He also defined modified force resultants which

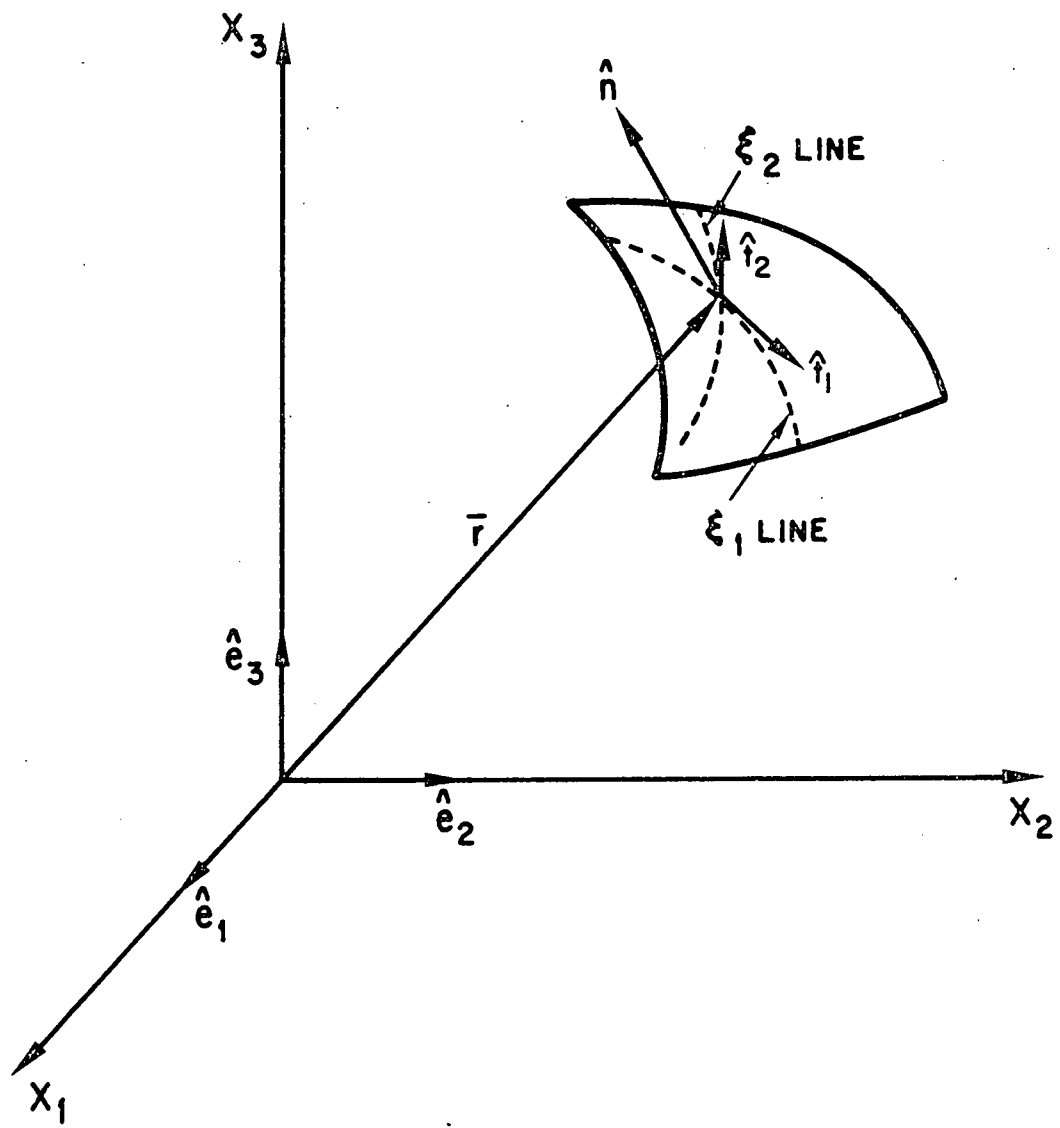


Figure 2.1. Shell Surface Coordinates

include contributions from the moment resultants multiplied by the deformed radii of curvature. With these assumptions pertinent non-linear terms are retained. The governing equations are given by:

$$\begin{aligned}
 & (\beta N_{11})_{,1} + (\alpha N_{12})_{,2} + \alpha_{,2} N_{12} - \beta_{,1} N_{22} + \alpha \beta R_1^{-1} Q_1 \\
 & + \frac{1}{2} \alpha \left(R_1^{-1} - R_2^{-1} \right) M_{12} ,_2 - \alpha \beta R_1^{-1} (\gamma_1 N_{11} + \gamma_2 N_{12}) \\
 & + \alpha \beta P_1 = 0
 \end{aligned} \tag{II.3}$$

$$\begin{aligned}
 & (\alpha N_{22})_{,2} + (\beta N_{21})_{,1} + \beta_{,1} N_{21} - \alpha_{,2} N_{11} + \alpha \beta R_2^{-1} Q_2 \\
 & + \frac{1}{2} \beta \left((R_2^{-1} - R_1^{-1}) M_{21} \right) ,_1 - \alpha \beta R_2^{-1} (\gamma_2 N_{22} + \gamma_1 N_{21}) \\
 & + \alpha \beta P_2 = 0
 \end{aligned} \tag{II.4}$$

$$\begin{aligned}
 & (\beta Q_1)_{,1} + (\alpha Q_2)_{,2} - \alpha \beta (R_1^{-1} N_{11} + R_2^{-1} N_{22}) - \\
 & (\beta \gamma_1 N_{11} + \gamma_2 N_{12})_{,1} - (\alpha \gamma_1 N_{12} + \alpha \gamma_2 N_{22})_{,2} + \alpha \beta P = 0
 \end{aligned} \tag{II.5}$$

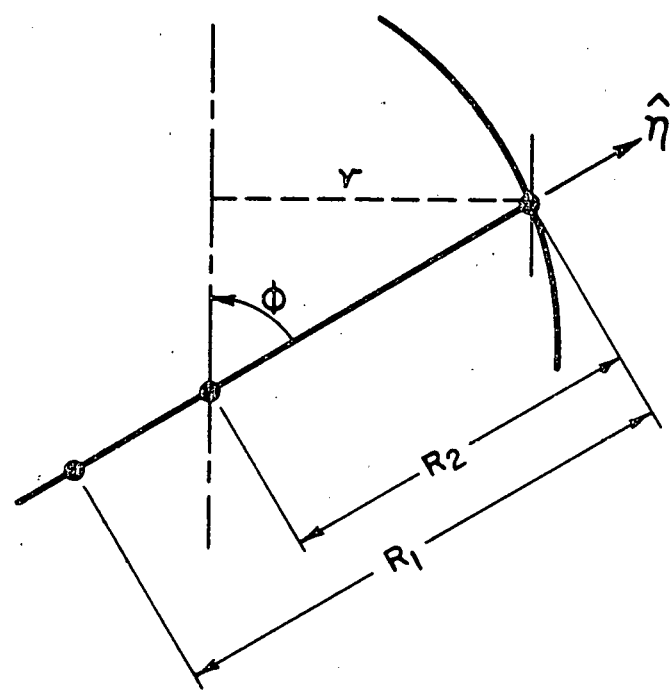


Figure 2.2. Shell Curvatures

$$(\beta M_{11}),_1 + (\alpha M_{12}),_2 + \alpha, 2 M_{12} - \beta, 1 M_{22} - \alpha \beta Q_1 = 0 \quad (II.6)$$

$$(\alpha M_{22}),_2 + (\beta M_{21}),_1 + \beta, 1 M_{21} - \alpha, 2 M_{11} - \alpha \beta Q_2 = 0 \quad (II.7)$$

Where α, β are Lame's coefficients of the surface metric of an orthogonal curvilinear coordinate system; P_1, P_2, P = tractions in 1,2, normal directions; R_1, R_2 are radii of principle curvature; P is the mass density; $\gamma_1, \gamma_2, \gamma$ are rotation quantities defined in Sec. 2.3 commas denote partial derivatives ($f,\alpha = \partial f / \partial \xi \alpha$); and $N\alpha\beta, M\alpha\beta, Q\alpha$ are modified resultants of the stress distribution σ_{ij} integrated through the thickness. The modified moment resultants are:

$$M_{11} = \int_{-h/2}^{+h/2} \sigma_{11} (1 + z/R_2) zdz \quad (II.8)$$

$$M_{21} = M_{12} = \frac{1}{2} \int_{-h/2}^{+h/2} \sigma_{12} (2 + z/R_2 + z/R_1) zdz \quad (II.9)$$

$$M_{22} = \int_{-h/2}^{+h/2} \sigma_{22} (1 + z/R_1) zdz \quad (II.10)$$

If k_{ij} are curvatures (defined in Sec. 2.3), and N_{ij_0} are

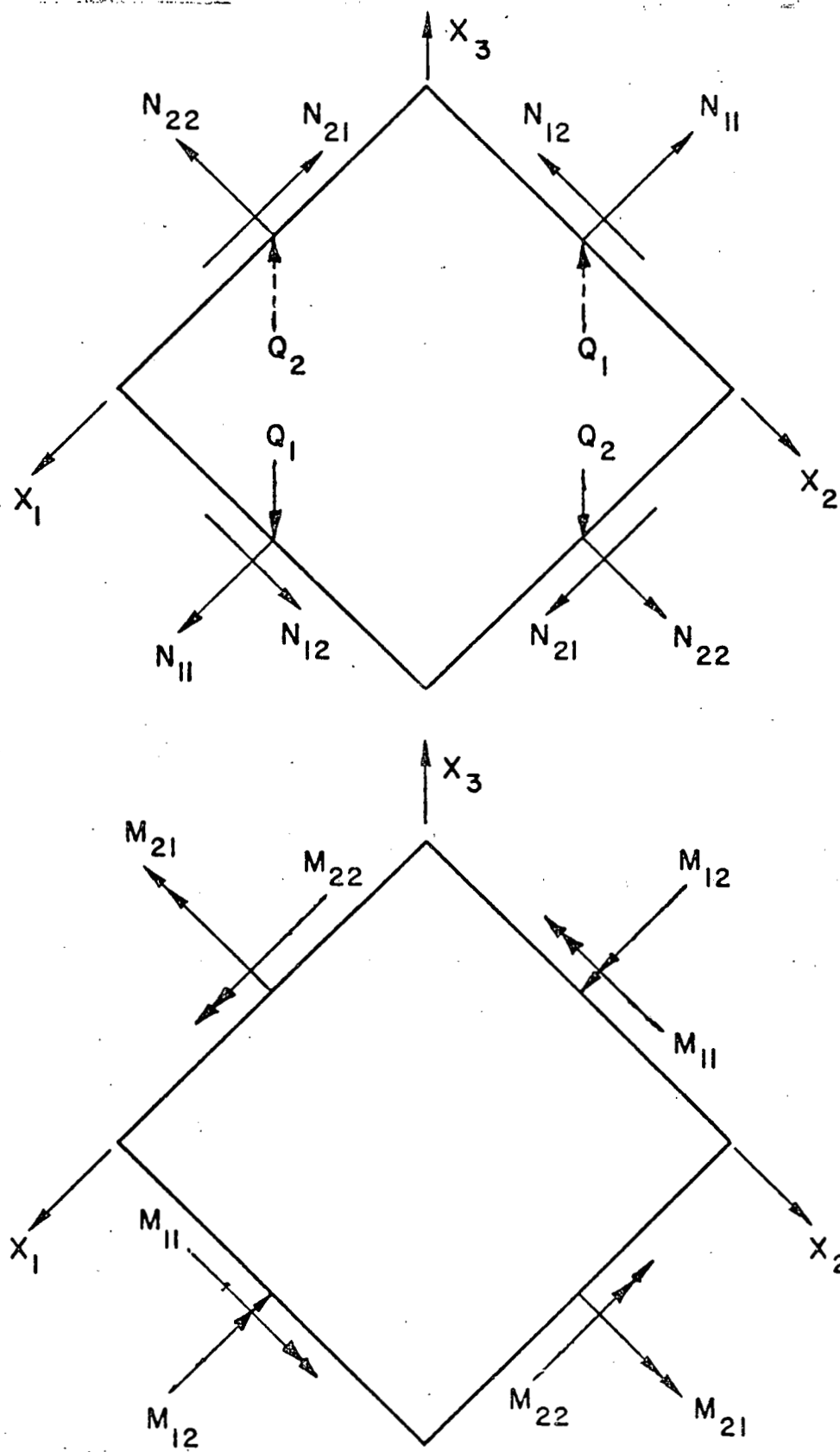


Figure 2.3. Sign Convention of Stress Resultants

the classical membrane force resultants:

$$N_{11o} = \int_{-h/2}^{+h/2} \sigma_{11} (1 + z/R_2) dz \quad (II.11)$$

$$N_{22o} = \int_{-h/2}^{+h/2} \sigma_{22} (1 + z/R_1) dz \quad (II.12)$$

$$N_{12o} = \int_{-h/2}^{+h/2} \sigma_{12} (1 + z/R_2) dz \quad (II.13)$$

$$N_{21o} = \int_{-h/2}^{+h/2} \sigma_{21} (1 + z/R_1) dz \quad (II.14)$$

The modified force resultants of Eqs. (II.3) to (II.7) are given by Sanders (7) as:

$$N_{11} = N_{11o} + M_{11} \left(\frac{1}{R_1} + k_{11} \right) \quad (II.15)$$

$$N_{22} = N_{22o} + M_{22} \left(\frac{1}{R_2} + k_{22} \right) \quad (II.16)$$

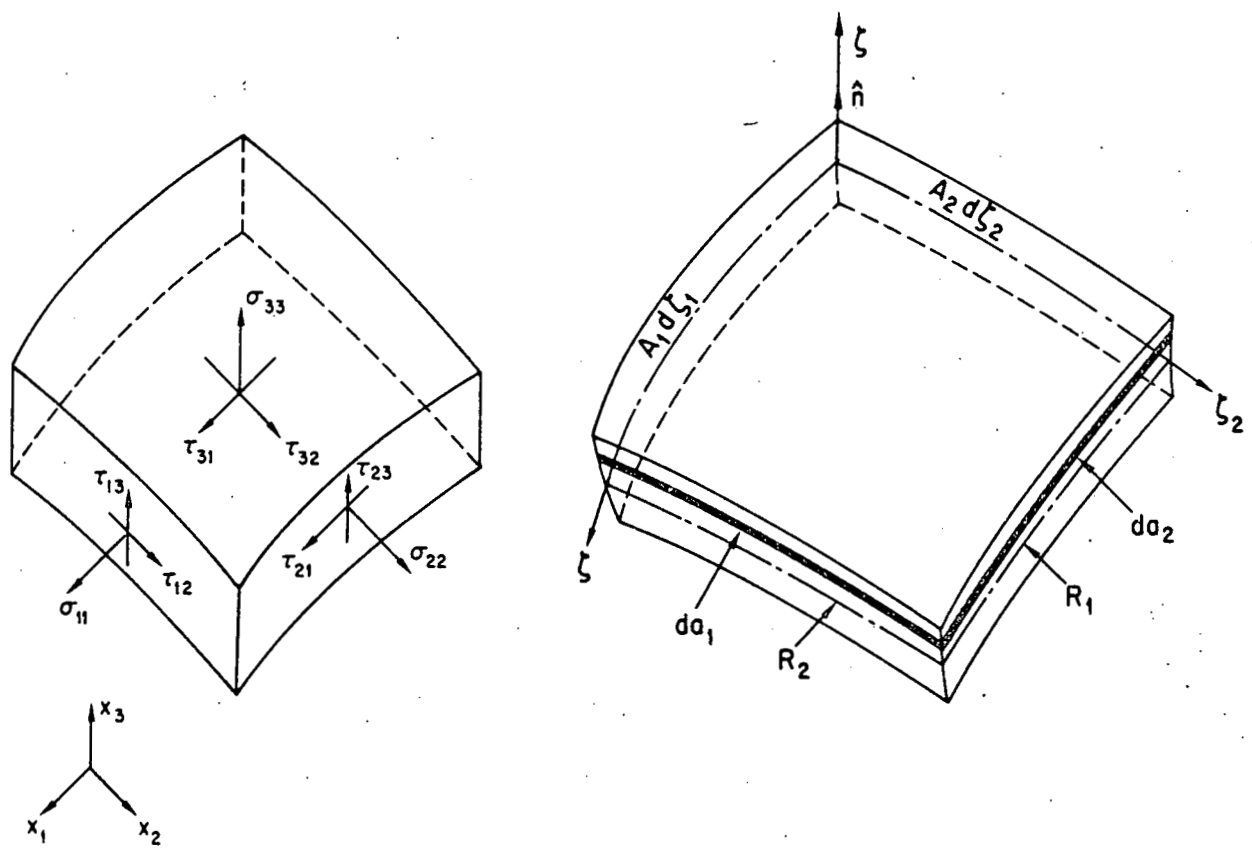


Figure 2.4. Sign Convention of Stress Components

$$N_{12} = N_{22o} + M_{22} \left(\frac{i}{R_2} + k_{12} \right) \quad (\text{II.17})$$

$$N_{21} = N_{21o} + M_{21} \left(\frac{1}{R_1} + k_{21} \right) \quad (\text{II.18})$$

The transverse shear resultants are:

$$Q_1 = \int_{-h/2}^{+h/2} \sigma_{13} (1 + z/R_2) dz \quad (\text{II.19})$$

$$Q_2 = \int_{-h/2}^{+h/2} \sigma_{23} (1 + z/R_1) dz \quad (\text{II.20})$$

The sign convention of various stress resultants is as shown in Fig. (II.2)

The sign convention of various stress components is as shown in Fig. (II.3)

In Fig. III.3 and as given in Eqs. (II.8) to (II.20) the various stress components are integrated with reference to the middle surface of the shell.

2.3 General Strain Displacement Relations.

Sander's theory (7) is based on small strains and small rotations about the normal. Through the thickness a linear distribution of strain is assumed, viz:

$$\bar{\epsilon}_{ij} = \epsilon_{ij} + z k_{ij} \quad (\text{II.21})$$

Where $\bar{\epsilon}_{ij}$ are strains of a point not on the middle surface, k_{ij} are curvatures and ϵ_{ij} are strains of the corresponding point on the middle surface:

$$\epsilon_{11} = (\alpha \beta)^{-1} \left[\beta u_{,1} + \alpha v_{,2} + \alpha \beta R_1^{-1} w + \frac{1}{2} \alpha \beta \gamma_1^2 \right] \quad (\text{II.22})$$

$$\epsilon_{22} = (\alpha \beta)^{-1} \left[\alpha v_{,2} + \beta u_{,1} + \alpha \beta R_2^{-1} w + \frac{1}{2} \alpha \beta \gamma_2^2 \right]$$

(II.23)

$$\epsilon_{12} = \frac{1}{2} (\alpha \beta)^{-1} \left[\beta v_{,1} + \alpha u_{,2} - \alpha v_{,2} - \beta u_{,1} + \alpha \beta \gamma_1 \gamma_2 \right] \quad (\text{II.24})$$

$$k_{11} = (\alpha \beta)^{-1} \left[\beta \gamma_{1,1} + \alpha \gamma_2 \right]$$

$$k_{22} = (\alpha \beta)^{-1} \left[\alpha \gamma_{2,2} + \beta, \gamma_1 \right] \quad (\text{II.25})$$

$$k_{12} = \frac{1}{2} (\alpha \beta)^{-1} \left[\beta \gamma_{2,1} + \alpha \gamma_{1,2} - \alpha, \gamma_1 - \beta, \gamma_2 \right. \\ \left. + \alpha \beta (R_2^{-1} - R_1^{-1}) \gamma \right] \quad (\text{II.26})$$

$$k_{21} = \frac{1}{2} (\alpha \beta)^{-1} \left[\alpha \gamma_{1,2} + \beta \gamma_{2,1} - \beta, \gamma_2 - \alpha, \gamma_1 \right. \\ \left. - \alpha \beta (R_2^{-1} - R_1^{-1}) \gamma \right] \quad (\text{II.27})$$

The rotational terms are given by:

$$\gamma_1 = -\alpha^{-1} w_{,1} + R_1^{-1} u \quad (\text{II.28})$$

$$\gamma_2 = -\beta^{-1} w_{,2} + R_2^{-1} v \quad (\text{II.29})$$

2.4 General Boundary Condition.

Four conditions are necessary on each edge to provide boundary conditions for the field equations of a general shell.

On an edge $\xi_1 = \text{constant}$:

$$1. \quad N_{11} \text{ or } u \text{ specified} \quad (\text{II.30})$$

$$2. \quad N_{12} + \frac{1}{2} (3 R_2^{-1} - R_1^{-1}) M_{12} + \frac{1}{2} (N_{11} + N_{22}) \gamma$$

$$\text{or } v \text{ specified} \quad (\text{II.31})$$

$$3. \quad Q_1 + \beta^{-1} M_{12,2} - \gamma_1 N_{11} - \gamma_2 N_{12}$$

$$\text{or } w \text{ specified} \quad (\text{II.32})$$

$$4. \quad M_{11} \text{ or } \gamma_1 \text{ specified} \quad (\text{II.33})$$

2.5 Simplification to Shell of Revolution.

The geometry of a shell of revolution is shown in Fig. (2.2).

The coordinate ξ_1 is taken as the arc length s ; and the coordinate ξ_2 as the circumferential angle θ . Thus, if the derivatives are taken with respect to the arc lengths:

$$\alpha = 1 \quad (\text{II.34})$$

$$\beta = r \quad (\text{II.35})$$

$$\alpha,2 = 0 \quad (\text{II.36})$$

$$\beta_{,1} = \frac{dr}{ds} = \cos\phi \quad (II.37)$$

$$r = \frac{R_1}{2} \sin\phi \quad (II.38)$$

$$ds = R_1 d\phi \quad (II.39)$$

$$\beta_{,2} = 0 \quad (II.40)$$

Where $R_\phi = R_1$, $R_\theta = R_2$, ϕ = angle the normal to the shell makes with the axis of revolution and r is the perpendicular distance of the meridional point from the axis of revolution.

2.6 Simplified Equations of Motion.

If axisymmetric behavior is assumed, Eqs. (II.3) to (II.7) become:

$$N_{\phi,s} + \frac{\cos\phi}{r} (N_\phi - N_\theta) + \frac{1}{R_\phi} (Q_\phi - \gamma_\phi N_\phi) + P_\phi = 0 \quad (II.41)$$

$$Q_{\phi,s} + \frac{\cos\phi}{r} Q_\phi - \left(K_\theta + \frac{\sin\phi}{r} \right) N_\theta + \frac{1}{R_\phi} Q_\phi \gamma_\phi$$

$$- \gamma_{\phi,s} + \frac{1}{R_\phi} (1 + \gamma_\phi^2) N_\phi + P = 0 \quad (II.42)$$

$$M_{\phi,s} + \frac{\cos\phi}{r} (M_{\phi} - M_{\theta}) - Q_{\phi} = 0 \quad (\text{II.43})$$

2.7 Specialized Strain-Displacement Relations.

For a shell of revolution:

$$\epsilon_{\theta} = \frac{1}{r} (u \cos\phi + w \sin\phi) \quad (\text{II.44})$$

$$\epsilon_{\phi} = u_{,s} + \frac{w}{R_{\phi}} + \frac{1}{2} \gamma_{\phi}^2 \quad (\text{II.45})$$

$$\gamma_{\phi} = \frac{1}{R_{\phi}} u - w_{,s} \quad (\text{II.46})$$

$$k_{\theta} = \frac{1}{r} \gamma_{\phi} \cos\phi \quad (\text{II.47})$$

$$K_{\phi} = \gamma_{\phi,s} \quad (\text{II.48})$$

2.8 Inclusion of Constitutive Relations.

Hookean behavior will be assumed for the elastic part of the response. The Von Mises yield criteria associated with the Prandt-Reuss flow rule will be adopted for elastic-plastic behavior. A detailed treatment of incremental constitutive relations for elastic-plastic behavior will be the subject of a separate chapter. Only a brief treatment of these relations is given in the following.

The incremental stress-strain relations are given by:

$$\left\{ \begin{array}{l} d\sigma_\theta \\ d\sigma_\phi \\ d\bar{\varepsilon}_p \end{array} \right\} = \left[\begin{array}{cc} \frac{\partial \sigma_\theta}{\partial \varepsilon_\theta} & \frac{\partial \sigma_\theta}{\partial \varepsilon_\phi} \\ \frac{\partial \sigma_\phi}{\partial \varepsilon_\theta} & \frac{\partial \sigma_\phi}{\partial \varepsilon_\phi} \\ \frac{\partial \bar{\varepsilon}_p}{\partial \varepsilon_\theta} & \frac{\partial \bar{\varepsilon}_p}{\partial \varepsilon_\phi} \end{array} \right] \left\{ \begin{array}{l} d\varepsilon_\theta \\ d\varepsilon_\phi \end{array} \right\} \quad (II.49)$$

Where $d\bar{\varepsilon}_p$ is the effective plastic strain differential, the terms in the matrix are called partial stiffness coefficients and are described in detail in Chapter III for plastic behavior.

For Hookean elastic behavior the incremental stress and strain

values reduce to total stress and strain values, and:

$$\frac{\partial \sigma_\theta}{\partial \epsilon_\theta} = \frac{\partial \sigma_\phi}{\partial \epsilon_\phi} = \frac{E}{1-v^2} \quad (II.50)$$

$$\frac{\partial \sigma_\theta}{\partial \epsilon_\phi} = \frac{\partial \sigma_\phi}{\partial \epsilon_\theta} = \frac{vE}{1-v^2} \quad (II.51)$$

2.9 Reordering of Equations.

The solution techniques detailed in subsequent chapters requires that the governing equations for the two point boundary problems of a shell of revolution be written in the form of an initial value problem in terms of fundamental variables appearing in the natural boundary conditions, i.e. w , Q_ϕ , N_ϕ , γ_ϕ , u and M_ϕ . The remaining variables are termed auxiliary variables: ϵ_θ , k_θ , N_θ , M_θ , ϵ_ϕ and K_ϕ . Rearranging the governing shell equilibrium and kinematic equations, Eqs. (II.39) to (II.46) gives the required set of six ordered first order nonlinear differential equations in terms of the six auxiliary and six fundamental variables. The remaining six equations are to be obtained from the constitutive equations.

$$w_s = \frac{U_\phi}{R_\phi} - \gamma_\phi \quad (II.52)$$

$$\gamma_{\phi,s} = k_{\phi} \quad (II.53)$$

$$M_{\phi,s} = \frac{\cos\phi}{r} (M_{\theta} - M_{\phi}) + Q_{\phi} \quad (II.54)$$

$$Q_{\phi,s} = N_{\theta} \left(\frac{\sin\phi}{r} + K_{\theta} \right) + N_{\phi} \frac{1}{R_{\phi}} (1 + \gamma_{\phi}^2) + k_{\phi} \quad (II.55)$$

$$- Q_{\phi} \left(\frac{\cos\phi}{r} + \frac{1}{R} \gamma_{\phi} \right) - P \quad (II.56)$$

$$U_{\phi,s} = \varepsilon_{\phi} - \frac{w}{R_{\phi}} - \frac{1}{2} \gamma_{\phi}^2 \quad (II.57)$$

$$N_{\phi,s} = \frac{\cos\phi}{r} (N_{\theta} - N_{\phi}) + \frac{1}{R_{\phi}} (N_{\phi} \gamma_{\phi} - Q_{\phi}) - P_{\phi} \quad (II.58)$$

The set of first order ordinary differential equations presented above can not be integrated because they contain non-linearities.

The treatment of material and geometric non-linearities will be the subject of the following chapters.

CHAPTER III

ELASTO - PLASTIC CONSTITUTIVE RELATIONS

3.0 Intent of Chapter.

In this chapter are derived the constitutive relations to be used with the equilibrium and kinematic shell equations in the preceding chapter. A brief description of material behavior is followed by a summary of the method of analysis. The incremental constitutive relations are presented along with an iterative scheme for predicting improved stress increments.

3.1 Material Behavior and Properties.

The importance of material characteristics in the consideration of elastic-plastic behavior is obvious, particularly when strain hardening effects are considered. In this study a limitation is imposed in that a bilinear stress-strain representation is assumed. It is, therefore, necessary to construct a bilinear stress-strain representation from the available isochronous material curves. One difficulty in such a construction is that almost all material curves have been based on tests of uniaxially loaded specimens. The method recommended by Oak Ridge National Laboratory (24) is adopted in this study: that representation is shown in Fig. D.1 of Appendix D.

Elastic-plastic analysis requires consideration of several aspects of material response other than the selection of a bilinear stress-strain representation. These include:

- (a) a yield stress corresponding to the onset of plastic flow.
- (b) equations relating plastic strain increments to stress and strains subsequent to yielding; and
- (c) a hardening rule specifying the change in yield stress in the course of plastic flow, etc.

This work has been largely devoted to analytical developments and hence limited to mechanical and monotonic loading applications. A Von-Mises yield criterion with the associated flow rule that follow isotropic hardening is used in this analysis. This combination of material behavior has generally agreed with experimental observations.

A Newton-Raphson scheme, which was initially used by Hutula (65) is used to aid convergence of elastic-plastic constitutive relations. Marcal's (15) approach for the elastic to plastic transition case is used in conjunction with this Newton-Raphson procedure.

It should be noted that Marcal (15) was the first to propose a stiffness approach to plasticity for shells of revolution. Hutula (65) and this work have generally followed Marcal's approach in developing analysis procedures.

3.1.1 Yield Surface. From the stress preliminaries of Appendix A the second invariant of the stress tensor J_2 is defined as:

$$J_2 = \frac{1}{3} \left\{ \sigma_{\phi}^2 - \sigma_{\phi} \sigma_{\theta} + \sigma_{\theta}^2 \right\} = \frac{1}{3} \sigma_e^2 \quad (\text{III.1})$$

where σ_e is the effective stress. According to distortion energy theory, the distortion energy density in the real system equals the distortion energy density at yield in an equivalent simple tension test.

$$U_d = \frac{1}{2G} J_2 = \frac{3}{4G} \tau_{\text{oct}}^2 \quad (\text{III.2})$$

Where G is the shear modulus and τ_{oct} is the octahedral shear stress. For the simple tension test at the yield point in simple tension:

$$J_2 = \frac{1}{3} \sigma_0^2 \quad (\text{III.3})$$

Where σ_0 is the yield stress in simple tension. Hence, the yield condition for the biaxial state of stress becomes:

$$\sigma_{\phi}^2 - \sigma_{\phi} \sigma_{\theta} + \sigma_{\theta}^2 = \sigma_0^2 \quad (\text{III.4})$$

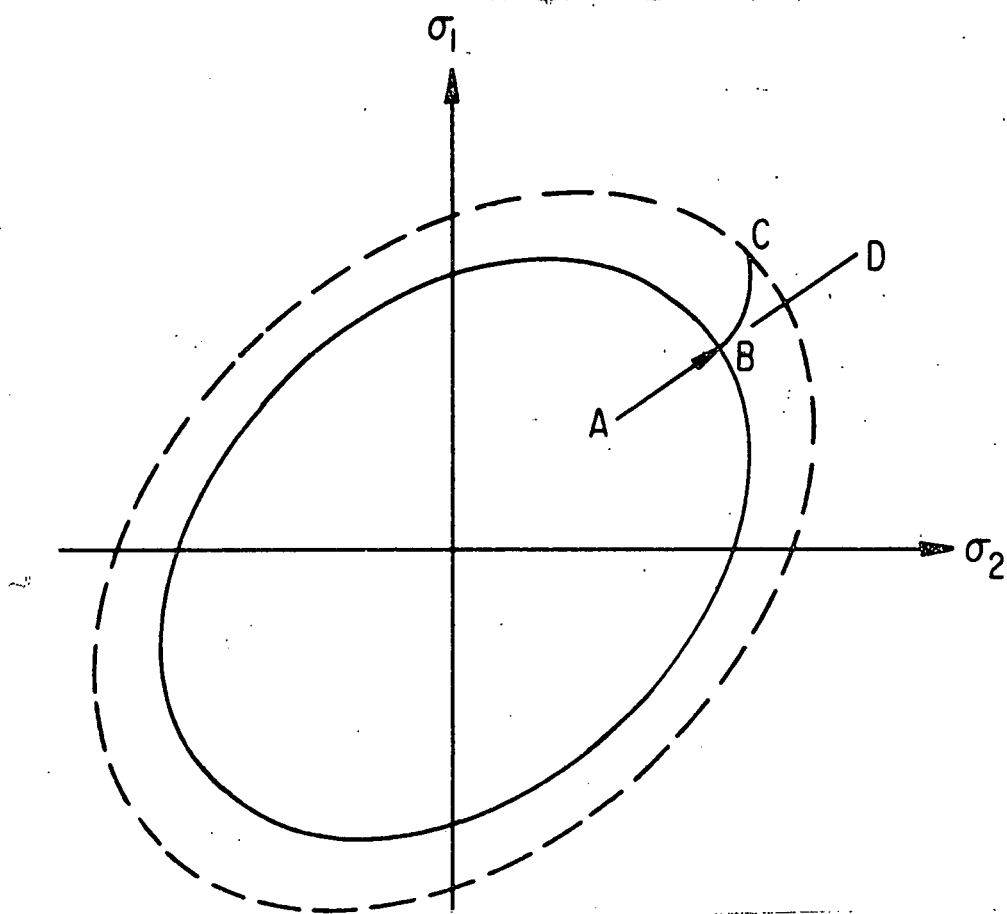


Figure 3.1. Von Mises Yield Surface Elastic to Plastic.

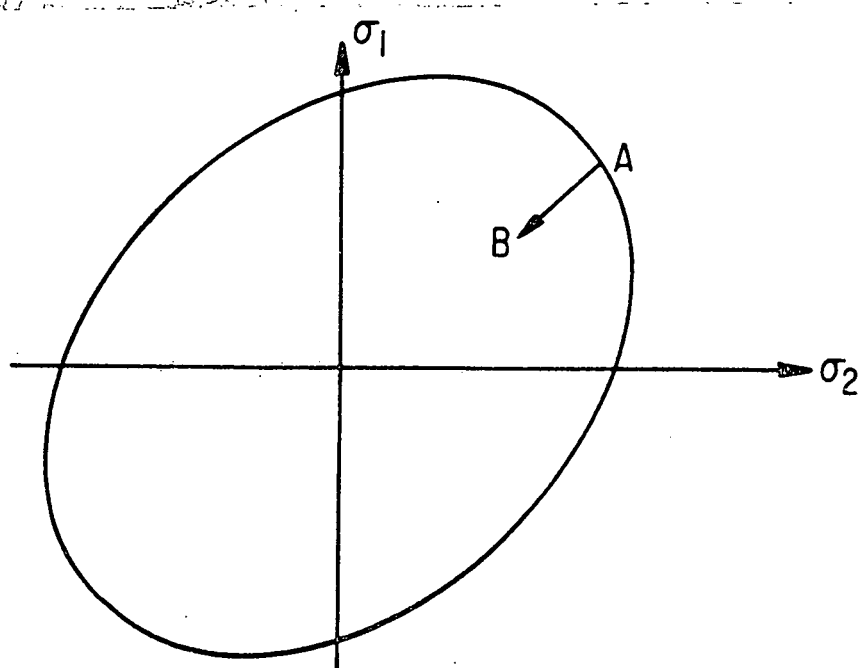


Figure 3.2. Von Mises Yield Surface Plastic to Elastic.

For the case of pure shear:

$$\sigma_{\phi} = -\sigma_{\theta} = A \quad (\text{III.5})$$

Where A is the yield stress in pure shear.

The second invariant of stress tensor is given by Eq. (III.3) and Eq. (III.4) as :

$$\frac{1}{3} \sigma_0^2 = \frac{1}{3} (\sigma_{\phi}^2 - \sigma_{\phi} \sigma_{\theta} + \sigma_{\theta}^2) \quad (\text{III.6})$$

But if we use the pure shear condition of Eq. (III.5) on the right hand side of Eq. (III.6), we get:

$$\frac{1}{3} \sigma_0^2 = \sigma_{\phi}^2 = A^2 \quad (\text{III.7})$$

or

$$A = \frac{\sigma_0}{\sqrt{3}} \quad (\text{III.8})$$

indicating that the yield stress in pure shear is $\frac{1}{\sqrt{3}}$ times the yield stress in simple tension.

3.1.2 Hardening Modulus: For a strain hardening material obeying isotropic hardening law the yield surface grows with increase in

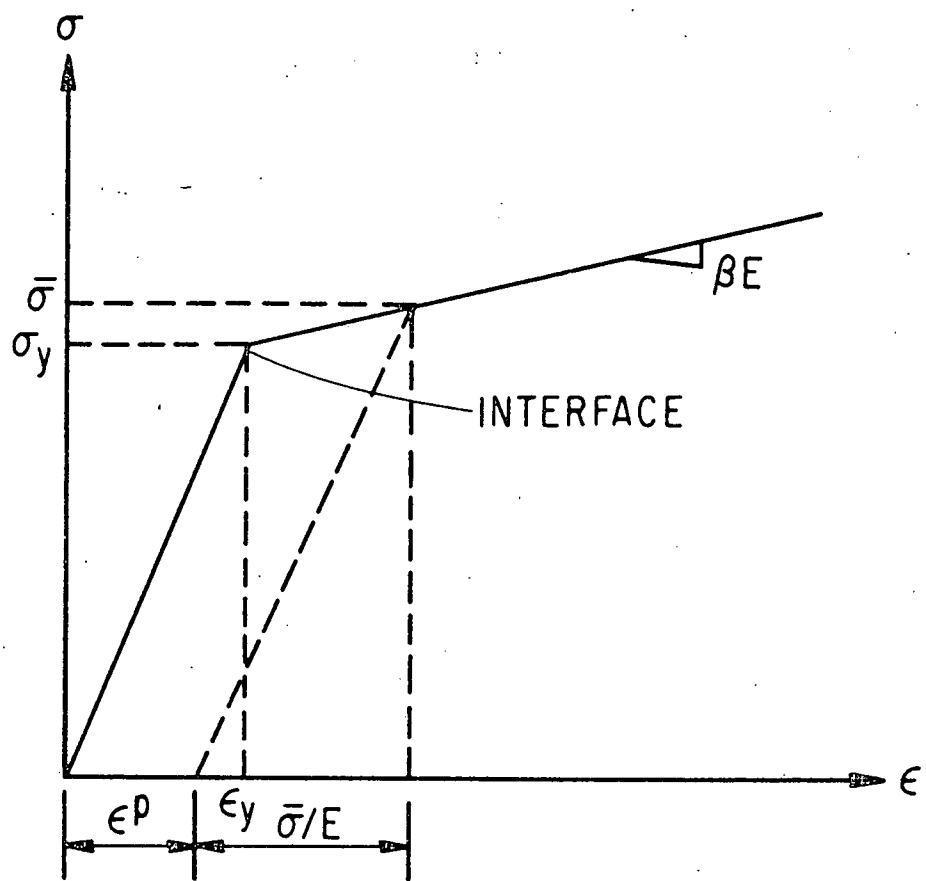


Figure 3.3. Bilinear Stress-Strain Curve

plastic strain. That is, when the material is subjected to plastic strain ϵ^P it attains a stress state $\bar{\sigma}$ given by:

$$\bar{\sigma} = \sigma_o + \frac{E\epsilon^P}{K} \quad (\text{III.9})$$

Where σ_o here is the initial yield stress of the material, E is the slope of elastic portion of the bilinear stress-strain curve of Fig. (D.1), then:

$$K = \frac{1-\beta}{\beta} \quad (\text{III.10})$$

In Eq. (III.9) the stress state $\bar{\sigma}$ describes the new yield surface or the new yield stress generally denoted as the hardening modulus H . Therefore, Eq. (III.9) can be written as:

$$H(\epsilon^P) = \sigma_o + \frac{E\epsilon^P}{K} \quad (\text{III.11})$$

Once a plastic strain ϵ^P is attained rather than using the yield condition of Eq. (III.4), a new yield condition is given by:

$$\sigma_\phi^2 - \sigma_\phi \sigma_\theta + \sigma_\theta^2 = H^2(\epsilon^P) \quad (\text{III.12})$$

Refer to Appendix D for a precise discussion on Eq. (III.9) to (III.11).

The slope of the effective stress-plastic strain diagram H is obtained by differentiating equation (III.11).

$$\frac{\partial \bar{\sigma}}{\partial \epsilon^p} = H = \frac{E}{K} \quad (\text{III.13})$$

The values of H are obtainable directly from the material data. Specifically, the values of K are obtained from the effective stress-effective plastic strain relationships. A selection of these values obtained from the nuclear reactor material data of Ref. (24a) is given in Appendix D.

3.2 Review of Elastic-Plastic Method of Analysis.

Elastic-plastic problems beyond the yield point on the stress-strain diagram require an incremental analysis since a closed form solution is not possible for complicated loadings and geometries. Strain hardening characteristics and effects are important. The non-linearities associated with large deflection shell theories and the Von-Mises criteria for yielding, compound the difficulties of the problem.

The plasticity theory presented here is based on the small strain assumption. The total strain is assumed as a linear combination of elastic ϵ_{ij}^e and plastic ϵ_{ij}^p strains.

$$d\epsilon_{ij} = d\epsilon_{ij}^e + d\epsilon_{ij}^p \quad (\text{III.14})$$

The Von-Mises yield condition used in the analysis is based on distortion energy theory. Using Eq. (III.12) a yield function can be defined as:

$$f = J_2 - \frac{H^2}{3} = 0 \quad (\text{III.15})$$

The yield envelope of Von-Mises is shown in Fig. (3.1) where ABC is the loading path from elastic to plastic state and ABD is the proportional loading path. In Fig. (3.2) the path AB defines plastic to elastic state.

$$J_2 = \frac{1}{2} \sigma_{ij}^T \sigma_{ij} \quad (\text{III.16})$$

In terms of this function, the general stress-strain relation in the differential form in the plastic region is:

$$d\epsilon_{ij}^P = \frac{\sqrt{3/2} \left(\frac{\partial f}{\partial \sigma_{ij}} \right) d\epsilon^P}{\sqrt{\left(\frac{\partial f}{\partial \sigma_{mn}} \right) \left(\frac{\partial f}{\partial \sigma} \right)}} \quad (\text{III.17})$$

Where $d\epsilon^P$ is the effective plastic strain increment corresponding to the equivalent strain increment in a simple tension test.

For the Von-Mises yield condition the above relation can be reduced to (Prandt-Reuss flow rule)

$$\frac{d\varepsilon_{ij}^P}{2} = \frac{3}{2} \sigma_{ij} \frac{d\varepsilon_e^P}{\sigma_e} \quad (\text{III.18})$$

3.3 Incremental Plasticity for Shells of Revolution.

3.3.1 Definition of Stress-Strain Relations. Marcal (15,16) has recommended an incremental form of the constitutive relations to be used with the governing axisymmetric shells of revolution equations with limitations to symmetric loadings. Marcal's partial stiffness approach in these references is useful in developing a convenient numerical algorithm which accounts for most of the difficulties in the elastic-plastic problem.

The total incremental strain is a linear sum of incremental elastic and incremental plastic strains. For shells of revolution (ignoring shear components) this is given by Marcal (15) in component form as:

$$d\varepsilon_\phi = d\varepsilon_\phi^e + d\varepsilon_\phi^p \quad (\text{III.19})$$

$$d\varepsilon_\theta = d\varepsilon_\theta^e + d\varepsilon_\theta^p \quad (\text{III.20})$$

or, substitutions for the elastic strains $d\varepsilon_{\phi}^e$ and $d\varepsilon_{\theta}^e$ in terms of corresponding stress increments, Poisson's ratio and Young's Modulus E gives:

$$d\varepsilon_{\phi} = \frac{1}{E} d\sigma_{\phi} - \frac{v}{E} d\sigma_{\theta} + d\varepsilon_{\phi}^p \quad (III.21)$$

$$d\varepsilon_{\theta} = \frac{1}{E} d\sigma_{\theta} - \frac{v}{E} d\sigma_{\phi} + d\varepsilon_{\theta}^p \quad (III.22)$$

If the Prandt-Reuss relations (III.20) are used, Eqs. (III.23) and (III.24) are written as:

$$d\varepsilon_{\phi} = \frac{1}{E} d\sigma_{\phi} - \frac{v}{E} d\sigma_{\theta} + \frac{3}{2} \frac{\sigma'_{\phi}}{\sigma_e} d\varepsilon^p \quad (III.23)$$

$$d\varepsilon_{\theta} = \frac{1}{E} d\sigma_{\theta} - \frac{v}{E} d\sigma_{\phi} + \frac{3}{2} \frac{\sigma'_{\theta}}{\sigma_e} d\varepsilon^p \quad (III.24)$$

σ'_{ϕ} and σ'_{θ} are the deviatoric component of stresses:

$$\sigma'_{\phi} = \frac{1}{3} (2\sigma_{\phi} - \sigma_{\theta}) \quad (III.25)$$

$$\sigma'_{\theta} = \frac{1}{3} (2\sigma_{\theta} - \sigma_{\phi}) \quad (III.26)$$

Another equation comes from the Von-Mises yield Criterion, as given by Marcal (15), when represented in differential form and then simplified using the slope of effective stress-effective plastic strain curve and neglecting the shear components,

$$H' d\bar{\epsilon}^p = -\frac{3}{2} \frac{\sigma'_\phi}{\sigma_e} d\epsilon_\phi + \frac{3}{2} \frac{\sigma'_\theta}{\sigma_e} d\epsilon_\theta \quad (\text{III.27})$$

Where H' is the slope of effective stress-effective plastic strain curve:

$$H' = \frac{\partial \sigma}{\partial \bar{\epsilon}^p} \quad (\text{III.28})$$

$$\text{and } \bar{\epsilon}^p = \int d\bar{\epsilon}^p \quad (\text{III.29})$$

Equations (III.25), (III.26) and (III.29) can be represented together as:

$$\begin{Bmatrix} d\epsilon_\phi \\ d\epsilon_\theta \\ 0 \end{Bmatrix} = \begin{bmatrix} \frac{1}{E} & -\frac{v}{E} & \frac{3}{2} \left(\frac{\sigma'_\phi}{\sigma_e} \right) \\ -\frac{v}{E} & \frac{1}{E} & \frac{3}{2} \left(\frac{\sigma'_\theta}{\sigma_e} \right) \\ \frac{3}{2} \left(\frac{\sigma'_\phi}{\sigma_e} \right) & \frac{3}{2} \left(\frac{\sigma'_\theta}{\sigma_e} \right) & -H' \end{bmatrix} \begin{Bmatrix} d\sigma_\phi \\ d\sigma_\theta \\ d\bar{\epsilon}^p \end{Bmatrix} \quad (\text{III.30})$$

or:

$$\begin{Bmatrix} d\sigma_\phi \\ d\sigma_\theta \\ d\sigma_e \end{Bmatrix} = [K] \begin{Bmatrix} d\epsilon_\phi \\ d\epsilon_\theta \\ 0 \end{Bmatrix} \quad (\text{III.31})$$

Where the plastic stiffness coefficient matrix:

$$[K] = \begin{bmatrix} \frac{1}{E} & -\frac{\nu}{E} & \frac{3}{2} \frac{\sigma'_\phi}{\sigma_e} \\ -\frac{\nu}{E} & \frac{1}{E} & \frac{3}{2} \frac{\sigma'_\theta}{\sigma_e} \\ \frac{3}{2} \frac{\sigma'_\phi}{\sigma_e} & \frac{3}{2} \frac{\sigma'_\theta}{\sigma_e} & -H \end{bmatrix} \quad (\text{III.32})$$

3.3.2. Partial Stiffness Coefficients. By the chain rule of differentiation we can also write:

$$d\sigma_\phi = \frac{\partial \sigma_\phi}{\partial \epsilon_\phi} d\epsilon_\phi + \frac{\partial \sigma_\phi}{\partial \epsilon_\theta} d\epsilon_\theta \quad (\text{III.33})$$

$$d\sigma_\theta = \frac{\partial \sigma_\theta}{\partial \epsilon_\phi} d\epsilon_\phi + \frac{\partial \sigma_\theta}{\partial \epsilon_\theta} d\epsilon_\theta \quad (\text{III.34})$$

$$d\bar{\varepsilon}^P = \frac{\partial \bar{\varepsilon}^P}{\partial \varepsilon_\phi} d\varepsilon_\phi + \frac{\partial \bar{\varepsilon}^P}{\partial \varepsilon_\theta} d\varepsilon_\theta \quad (\text{III.35})$$

or

$$\begin{Bmatrix} d\sigma_\phi \\ d\sigma_\theta \\ -p \\ d\varepsilon \end{Bmatrix} = \begin{bmatrix} \frac{\partial \sigma_\phi}{\partial \varepsilon_\phi} & \frac{\partial \sigma_\phi}{\partial \varepsilon_\theta} \\ \frac{\partial \sigma_\theta}{\partial \varepsilon_\phi} & \frac{\partial \sigma_\theta}{\partial \varepsilon_\theta} \\ \frac{\partial -p}{\partial \varepsilon_\phi} & \frac{\partial -p}{\partial \varepsilon_\theta} \end{bmatrix} \begin{Bmatrix} d\varepsilon_\phi \\ d\varepsilon_\theta \end{Bmatrix} \quad (\text{III.36})$$

By a comparison of Eq. (III.37) with the Eq. (III.32) the terms in the matrix of Eq. (III.37), called the partial stiffness coefficients as defined by Marcal (15), are determined from Eq. (III.33). Stiffness coefficients are only C^1 (class 1) functions of ε_ϕ and ε_θ as demonstrated by Hutzla (65).

3.3.3. Transition Case. The transition between elastic and plastic regimes of Fig (3.3) must be treated differently as follows. Partial stiffness coefficients at the transition are modified by considering a mean stiffness coefficient. The mean stiffness coefficient as defined by Marcal (15) is calculated from the proportional weighting of the elastic and plastic partial stiffness coefficients,

for instance:

$$\left. \frac{\partial \sigma_\phi}{\partial \varepsilon_\phi} \right|_{\text{mean}} = m \left. \frac{\partial \sigma_\phi}{\partial \varepsilon_\phi} \right|_{\text{elastic}} + (1-m) \left. \frac{\partial \sigma_\phi}{\partial \varepsilon_\phi} \right|_{\text{plastic}} \quad (\text{III.37})$$

Where m is a proportionality factor, $0 \leq m \leq 1$.

The value of m is obtained either from consideration of the maximum shear stress-strain curve for the Tresca Yield Criterion or from the effective stress-strain curve for the Von-Mises Yield Criterion.

Marcal (15) has defined m to be the ratio of plastic strain to the total strain at the yield transition for the load increment. Gerdeen (9) and Hutula (65) have found $m=\frac{1}{2}$ as a value for stable and reasonable solution which is used in this study.

In Eq. (III.32) the values of $(\frac{\sigma_\phi}{\sigma_e})$, $(\frac{\sigma_\theta}{\sigma_e})$ and H' at the transition can be determined as suggested by Hutula (65).

$$\left(\frac{\sigma_\phi}{\sigma_e} \right)^* = m \left(\frac{\sigma_{\phi 1}'}{\sigma_{e1}} \right) + (1-m) \left(\frac{\sigma_{\phi 1}' + \Delta \sigma_{\phi 1}'}{\sigma_{e1} + \Delta \sigma_{e2}} \right)$$

(III.38)

$$\left(\frac{\sigma'}{\sigma_e} \right)^* = m \left(\frac{\sigma_{\theta_1}}{\sigma_{e1}} \right) + (1-m) \left(\frac{\sigma'_{\theta_1} + \Delta\sigma'_{\theta}}{\sigma_{e1} + \Delta\sigma_e} \right) \quad (III.39)$$

$$(H')^* = m H' (\varepsilon_{p1}) + (1-m) H' (\varepsilon_{p1} + \Delta\varepsilon_p) \quad (III.40)$$

Where (Δ) identifies an incremental value for a given load increment and the subscript (i) refers to previous or residual solution state.

3.3.4. Determination of Partial Stiffness Coefficients. The quantities in the matrix of Eq. (III.31) are obtained by inverting the matrix of Eq. (III.32). The determinant of matrix (III.30) is given by:

$$D = -\frac{1}{E} (1-v^2) \frac{(H')^*}{E} + \frac{9}{4} \left(\frac{\sigma'}{\sigma_e} \right)^* 2 + \frac{9}{2} v \left(\frac{\sigma'}{\sigma_e} \right)^* \left(\frac{\sigma'}{\sigma_e} \right) + \frac{9}{4} \left(\frac{\sigma'}{\sigma_e} \right)^* 2 \quad (III.41)$$

Where an asterik denotes that at the transition the quantities with asterik must be determined from Eqs. (III.24) to (III.26) respectively.

Let:

$$D^* = -ED, \text{ then:}$$

$$E_{11} = \frac{\partial \sigma_\phi}{\partial \varepsilon_\phi} = \frac{1}{D^*} \left\{ H' + \frac{9}{4} \left(\frac{\sigma_\theta'}{\sigma_e} \right)^* 2 E \right\} \quad (\text{III.42})$$

$$E_{12} = \frac{\partial \sigma_\phi}{\partial \varepsilon_\theta} = \frac{1}{D^*} \left\{ v H' - \frac{9}{4} E \left(\frac{\sigma_\phi'}{\sigma_e} \right)^* \left(\frac{\sigma_\theta'}{\sigma_e} \right)^* \right\} \quad (\text{III.43})$$

$$E_{13} = \frac{\partial \sigma_\phi}{\partial \varepsilon_p} = \frac{3}{2D^*} \left\{ \left(\frac{\sigma_\phi'}{\sigma_e} \right)^* + v \left(\frac{\sigma_\theta'}{\sigma_e} \right)^* \right\} \quad (\text{III.44})$$

$$E_{21} = \frac{\partial \sigma_\theta}{\partial \varepsilon_\phi} = \frac{1}{D^*} \left\{ v H' - \frac{9}{4} E \left(\frac{\sigma_\phi'}{\sigma_e} \right)^* \left(\frac{\sigma_\theta'}{\sigma_e} \right)^* \right\} \quad (\text{III.45})$$

$$E_{22} = \frac{\partial \sigma_\theta}{\partial \varepsilon_\theta} = \frac{1}{D^*} \left\{ H' + \frac{9}{4} E \left(\frac{\sigma_\phi'}{\sigma_e} \right)^* 2 \right\} \quad (\text{III.46})$$

$$E_{23} = \frac{\partial \sigma_\theta}{\partial \epsilon_p} = \frac{3}{2D^*} \left\{ \left(\frac{\sigma_\theta}{\sigma_e} \right)^* + v \left(\frac{\sigma_\phi}{\sigma_e} \right)^* \right\} \quad (\text{III.47})$$

$$E_{31} = \frac{3}{2D^*} \left\{ \left(\frac{\sigma_\theta}{\sigma_e} \right)^* + v \left(\frac{\sigma_\theta}{\sigma_e} \right)^* \right\} \quad (\text{III.48})$$

$$E_{32} = \frac{3}{2D^*} \left\{ \left(\frac{\sigma_\theta}{\sigma_e} \right)^* + v \left(\frac{\sigma_\phi}{\sigma_e} \right)^* \right\} \quad (\text{III.49})$$

$$E_{33} = \frac{1}{D^*} \left\{ - \frac{(1-v)}{E} \right\} \quad (\text{III.50})$$

3.3.5 Newton-Raphson Scheme. In the incremental elastic-plastic analysis that is performed here it is necessary to select extremely small load steps in order to keep the stress point at the yield surface. The selection of a load step and thereby a stress increment varies for different problems depending upon the degree of accuracy desired. In order to achieve the desired accuracy for lesser load steps Hutzla (65) adopted a Newton-Raphson Scheme. This scheme is used in the incremental elastic-plastic analysis performed here. The formulation of the Newton-Raphson scheme for obtaining improved stress increments is presented here with generalizations

with respect to the yield transition parameter m defined earlier.

In this scheme three functions f_1 , f_2 and f_3 are defined and by means of these functions a Newton-Raphson algorithm is developed.

Define three functions:

$$f_1 = -\Delta\varepsilon_\phi + \frac{1}{E} \Delta\sigma_\phi - \frac{v}{E} \Delta\sigma_\theta + \frac{3}{2} \left(\frac{\sigma_\phi'}{\sigma_e} \right)^* \Delta\varepsilon_p \quad (III.51)$$

$$f_2 = -\Delta\varepsilon_\theta - \frac{v}{E} \Delta\sigma_\phi + \frac{1}{E} \Delta\sigma_\theta + \frac{3}{2} \left(\frac{\sigma_\theta'}{\sigma_e} \right)^* \Delta\varepsilon_p \quad (III.52)$$

$$f_3 = \left\{ \sigma_\phi^2 - \sigma_\phi \sigma_\theta + \sigma_\theta^2 - H (\varepsilon_p)^2 \right\} / 3 \quad (III.53)$$

Where :

$$\Delta\sigma_\phi = \sigma_\phi - \sigma_{\phi 1} \quad (III.54)$$

$$\Delta\sigma_\theta = \sigma_\theta - \sigma_{\theta 1} \quad (III.55)$$

$$\Delta\sigma_\phi' = \sigma_\phi' - \sigma_{\phi 1}' \quad (III.56)$$

$$\Delta\sigma_\theta' = \sigma_\theta' - \sigma_{\theta 1}' \quad (III.57)$$

$$\Delta \bar{\varepsilon}_p = \bar{\varepsilon}_p - \bar{\varepsilon}_{p1} \quad (III.58)$$

Two of the above functions, f_1 and f_2 of Eqs. (III.51) and (III.52) have been defined using the incremental form of Eqs. (III.23) and (III.24). The third function f_3 of Eq. (III.53) is defined using the definition of the yield function of Eq. (III.15) rather than using Eq. (III.27).

The consistency of using Eq. (III.15) for defining the function f_3 will be given toward the end of this chapter.

Above functions f_1 and f_2 have been defined using the incremental form of Eqs. (III.23) and (III.24). However, rather than defining a third function f_3 from Eq. (III.28) use of the yield function of Eq. (III.15) has been made.

Substituting for $(\frac{\sigma_\phi}{\sigma_e})^*$ and $(\frac{\sigma_\theta}{\sigma_e})^*$ from Eqs. (III.38) and (III.39) the functions of Eqs. (III.51) to (III.53) can be written as:

$$f_1 (\sigma_\phi, \sigma_\theta, \varepsilon_p)$$

$$= - \Delta \varepsilon_\phi + \frac{1}{E} (\sigma_\phi - \sigma_{\phi1}) - \frac{v}{E} (\sigma_\theta - \sigma_{\theta1})$$

$$+ \left[\frac{3m}{2} \left(\frac{\sigma'_{\phi_1}}{\sigma_{e1}} \right) + \frac{3}{2} (1-m) \left(\frac{\sigma'_{\phi}}{\sigma_e} \right) \right] (\bar{\epsilon}_p - \bar{\epsilon}_{p1}) \quad (III.59)$$

$$f_2 (\sigma_{\phi}, \sigma_{\theta}, \bar{\epsilon}_p) = - \Delta\epsilon_{\theta} + \frac{1}{E} (\sigma_{\theta} - \sigma_{\theta_1}) - \frac{v}{E} (\sigma_{\phi} - \sigma_{\phi_1})$$

$$+ \left[\frac{3m}{2} \left(\frac{\sigma'_{\theta_1}}{\sigma_{e1}} \right) + \frac{3}{2} (1-m) \left(\frac{\sigma'_{\theta}}{\sigma_e} \right) \right] (\epsilon_p - \epsilon_{p1}) \quad (III.60)$$

$$f_3 (\sigma_{\phi}, \sigma_{\theta}, \epsilon_p) = \left\{ \sigma_{\phi}^2 - \sigma_{\theta} \sigma_{\phi} + \sigma_{\theta}^2 - H (\bar{\epsilon}_p)^2 \right\} / 3 \quad (III.61)$$

Substituting for the deviatoric stress components for the residual as well as the current state:

$$f_1 (\sigma_{\phi}, \sigma_{\theta}, \bar{\epsilon}_p) = - \Delta\epsilon_{\phi} + \frac{1}{E} (\sigma_{\phi} - \sigma_{\phi_1}) - \frac{v}{E} (\sigma_{\theta} - \sigma_{\theta_1})$$

$$+ \left[\frac{m (\sigma_{\phi_1} - \frac{1}{2} \sigma_{\theta_1})}{H (\bar{\epsilon}_{p1})} + \frac{(1-m) (\sigma_{\phi} - \frac{1}{2} \sigma_{\theta})}{H (\bar{\epsilon}_p)} \right] (\bar{\epsilon}_p - \bar{\epsilon}_{p1}) \quad (III.62)$$

$$f_2 (\sigma_{\phi}, \sigma_{\theta}, \bar{\epsilon}_p) = - \Delta\epsilon_{\theta} + \frac{1}{E} (\sigma_{\theta} - \sigma_{\theta_1}) - \frac{v}{E} (\sigma_{\phi} - \sigma_{\phi_1})$$

(III.70)

$$\frac{\partial f_2}{\partial \theta} = \frac{d_{\theta}}{m(\partial_{\theta} - \frac{\partial}{\partial \phi})} - \left\{ \frac{(\frac{d_{\theta}}{d_{\phi}}) H}{(\frac{d_{\phi}}{d_{\theta}}) H} - 1 \right\} \frac{(\frac{d_{\theta}}{d_{\phi}}) H}{(1-m)(\partial_{\theta} - \frac{\partial}{\partial \phi})} + \frac{(\frac{d_{\theta}}{d_{\phi}}) H}{(1-m)(\partial_{\theta} - \frac{\partial}{\partial \phi})} =$$

$$\frac{\partial f_2}{\partial \theta} = \frac{d_{\theta}}{1 + \frac{(\frac{d_{\theta}}{d_{\phi}}) H}{(1-m)(\frac{d_{\phi}}{d_{\theta}} - \frac{d_{\theta}}{d_{\phi}})}} \quad \text{(III.69)}$$

$$\frac{\partial f_2}{\partial \phi} = \frac{d_{\phi}}{\sqrt{(1-m)(\frac{d_{\phi}}{d_{\theta}} - \frac{d_{\theta}}{d_{\phi}})}} \quad \text{(III.68)}$$

(III.67)

$$\frac{\partial f_1}{\partial \theta} = \frac{d_{\theta}}{m(\partial_{\theta} - \frac{\partial}{\partial \phi})} - \left\{ \frac{(\frac{d_{\theta}}{d_{\phi}}) H}{(\frac{d_{\phi}}{d_{\theta}}) H} - 1 \right\} \frac{(\frac{d_{\theta}}{d_{\phi}}) H}{(1-m)(\partial_{\theta} - \frac{\partial}{\partial \phi})} + \frac{(\frac{d_{\theta}}{d_{\phi}}) H}{(1-m)(\partial_{\theta} - \frac{\partial}{\partial \phi})} =$$

$$\frac{\partial f_1}{\partial \theta} = \frac{d_{\theta}}{1 + \frac{(\frac{d_{\theta}}{d_{\phi}}) H}{(1-m)(\frac{d_{\phi}}{d_{\theta}} - \frac{d_{\theta}}{d_{\phi}})}} \quad \text{(III.66)}$$

$$\frac{\partial f_1}{\partial \phi} = \frac{d_{\phi}}{1 + \frac{(\frac{d_{\theta}}{d_{\phi}}) H}{(1-m)(\frac{d_{\phi}}{d_{\theta}} - \frac{d_{\theta}}{d_{\phi}})}} \quad \text{(III.65)}$$

Various derivatives of these functions are:

$$f_3(\partial_{\phi}, \partial_{\theta}, \frac{d_{\theta}}{d_{\phi}}) = \left\{ \partial_{\phi}^2 - \partial_{\phi} \partial_{\theta} + \partial_{\theta}^2 - \left[H(\frac{d_{\theta}}{d_{\phi}}) \right]^2 \right\}^3 \quad \text{(III.64)}$$

$$(\frac{d_{\theta}}{d_{\phi}} - \frac{d_{\phi}}{d_{\theta}}) \left[\frac{(\frac{d_{\theta}}{d_{\phi}}) H}{m(\partial_{\theta} - \frac{\partial}{\partial \phi})} + \frac{(\frac{d_{\theta}}{d_{\phi}}) H}{(1-m)(\partial_{\theta} - \frac{\partial}{\partial \phi})} \right] +$$

$$\frac{\partial f_3}{\partial \sigma_\phi} = (2 \sigma_\phi - \sigma_\theta) / 3 = \sigma_\phi' \quad (III.71)$$

$$\frac{\partial f_3}{\partial \sigma_\theta} = (2 \sigma_\theta - \sigma_\phi) / 3 = \sigma_\theta' \quad (III.72)$$

$$\frac{\partial f_3}{\partial \bar{\epsilon}_p} = -\left\{ 2 H' (\bar{\epsilon}_p) H (\bar{\epsilon}_p) \right\} / 3 \quad (III.73)$$

and, thus the Newton-Raphson algorithm is given by:

$$\left\{ \begin{array}{c} \sigma_\phi \\ \sigma_\theta \\ \bar{\epsilon}_p \end{array} \right\}^{(n+1)} = \left\{ \begin{array}{c} \sigma_\phi \\ \sigma_\theta \\ \bar{\epsilon}_p \end{array} \right\}^{(n)} - \left[\begin{array}{ccc} \frac{\partial f_1}{\partial \sigma_\phi} & \frac{\partial f_1}{\partial \sigma_\theta} & \frac{\partial f_1}{\partial \bar{\epsilon}_p} \\ \frac{\partial f_2}{\partial \sigma_\phi} & \frac{\partial f_2}{\partial \sigma_\theta} & \frac{\partial f_2}{\partial \bar{\epsilon}_p} \\ \frac{\partial f_3}{\partial \sigma_\phi} & \frac{\partial f_3}{\partial \sigma_\theta} & \frac{\partial f_3}{\partial \bar{\epsilon}_p} \end{array} \right]^{-1} \left\{ \begin{array}{c} f_1 \\ f_2 \\ f_3 \end{array} \right\}$$

(III.74)

It can be easily seen that for $m = \frac{1}{2}$ these equations reduce to those given by Hutula (65).

Henceforth, our definition of the function f_3 on the previous pages, viz.

$$f_3 = J_2 - K = \frac{1}{3} \sigma_e^2 - \frac{1}{3} K^2$$

is consistent with the definition of the Von-Mises Criteria or the distortion energy theory. What remains to be seen now is whether this function is also consistent with the Prandt Reuss relations that were used in defining the plastic strain components in functions f_1 and f_2 .

3.3.6 Consistency of Function f_3 . From (64) the general plastic stress-strain relation is given by:

$$d\epsilon_{ij}^p = \frac{\sqrt{3/2} (\partial f_3 / \partial \sigma_{ij}) d\sigma^p}{\sqrt{(\partial f_3 / \partial \sigma_{mn}) (\partial f_3 / \partial \sigma_{mn})}} \quad (\text{III.75})$$

or:

$$d\epsilon_{ij}^p = \frac{3/2 (\partial f_3 / \partial \sigma_{ij})}{\sqrt{(\partial f_3 / \partial \sigma_{mn}) (\partial f_3 / \partial \sigma_{mn})}} \frac{d\sigma_e}{\sigma_e} \quad (\text{III.76})$$

and for the function f_3 defined as before, this reduces to:

$$d\epsilon_{ij}^p = \frac{3}{2} \frac{\sigma'_{ij}}{\sigma_e} d\epsilon^p$$

Which is same as the plastic strain components used in the definition of functions f_1 and f_2 .

The definition of the yield function is therefore consistent with Prandt-Reuss relations.

A further simplicity is achieved by noting the fact that the component plastic strains are directly obtainable from the derivatives of the defined function, for instance:

$$d\epsilon_\phi^p = \frac{3}{2} \frac{\partial f_3 / \partial \sigma_\phi}{\sigma_e} d\epsilon^p \quad (\text{III.78})$$

$$d\epsilon_\theta^p = \frac{3}{2} \frac{\partial f_3 / \partial \sigma_\theta}{\sigma_e} d\epsilon^p \quad (\text{III.79})$$

and:

$$d\epsilon^p = \sqrt{\frac{2}{\sqrt{3}} \left(d\epsilon_\phi^{p2} + d\epsilon_\phi^p d\epsilon_\theta^p + d\epsilon_\theta^{p2} \right)} \quad (\text{III.80})$$

3.4 Shell Incremental Plasticity.

The incremental elastic-plastic stress-strain relations presented in the previous section can not as yet be used directly with the governing shell equations. According to Eqs. (II.11) to (II.20) the stress components must be integrated through the thickness in order to determine the magnitudes of stress resultants at the meridional integration points. This is not quite straight forward for incremental plasticity. The incremental values of stress resultants N_ϕ , N_θ , M_ϕ , M_θ are represented as functions of strains ϵ_ϕ , ϵ_θ and of curvatures K_ϕ , K_θ defined by the following chain rule of differentiation.

For elastic-plastic behavior

$$\left\{ \begin{array}{l} \Delta N_\phi \\ \Delta N_\theta \\ \Delta M_\phi \\ \Delta M_\theta \end{array} \right\} = \begin{bmatrix} \frac{\partial N_\phi}{\partial \epsilon_\phi} & \frac{\partial N_\phi}{\partial \epsilon_\theta} & \frac{\partial N_\phi}{\partial K_\phi} & \frac{\partial N_\phi}{\partial K_\theta} \\ \frac{\partial N_\theta}{\partial \epsilon_\phi} & \frac{\partial N_\theta}{\partial \epsilon_\theta} & \frac{\partial N_\theta}{\partial K_\phi} & \frac{\partial N_\theta}{\partial K_\theta} \\ \frac{\partial M_\phi}{\partial \epsilon_\phi} & \frac{\partial M_\phi}{\partial \epsilon_\theta} & \frac{\partial M_\phi}{\partial K_\phi} & \frac{\partial M_\phi}{\partial K_\theta} \\ \frac{\partial M_\theta}{\partial \epsilon_\phi} & \frac{\partial M_\theta}{\partial \epsilon_\theta} & \frac{\partial M_\theta}{\partial K_\phi} & \frac{\partial M_\theta}{\partial K_\theta} \end{bmatrix} \left\{ \begin{array}{l} \Delta \epsilon_\phi \\ \Delta \epsilon_\theta \\ \Delta K_\phi \\ \Delta K_\theta \end{array} \right\}$$

(III.81)

Let:

$$C_{11} = \frac{\partial N}{\partial \varepsilon} \quad (III.82)$$

$$\phi$$

$$C_{12} = \frac{\partial N}{\partial \varepsilon_\theta} = \frac{\partial N_\theta}{\partial \varepsilon_\phi} \quad (III.83)$$

$$C_{22} = \frac{\partial N_\theta}{\partial \varepsilon_\theta} = \frac{\partial M}{\partial \varepsilon_\phi} \quad (III.84)$$

$$K_{11} = \frac{\partial N}{\partial K_\phi} = \frac{\partial M}{\partial \varepsilon_\phi} \quad (III.85)$$

$$K_{12} = \frac{\partial N_\phi}{\partial \theta} = \frac{\partial N}{\partial K_\phi} = \frac{\partial M}{\partial \varepsilon_\theta} = \frac{\partial M_\theta}{\partial \varepsilon_\phi} \quad (III.86)$$

$$K_{22} = \frac{\partial N_\theta}{\partial K_\theta} = \frac{\partial M_\theta}{\partial \varepsilon_\theta} \quad (III.87)$$

$$D_{11} = \frac{\partial M_\phi}{\partial K_\phi} \quad (III.88)$$

$$D_{12} = \frac{\partial M_\phi}{\partial K_\theta} = \frac{\partial M_\theta}{\partial K_\phi} \quad (III.89)$$

$$D_{22} = \frac{\partial M_\theta}{\partial K_\theta} \quad (III.90)$$

Thus:

$$\Delta N_\phi = C_{11} \Delta \varepsilon_\phi + C_{12} \Delta \varepsilon_\theta + K_{11} \Delta K_\phi + K_{12} \Delta K_\theta \quad (\text{III.91})$$

$$\Delta N_\theta = C_{12} \Delta \varepsilon_\phi + C_{22} \Delta \varepsilon_\theta + K_{12} \Delta K_\phi + K_{22} \Delta K_\theta \quad (\text{III.92})$$

$$\Delta M_\phi = K_{11} \Delta \varepsilon_\phi + K_{12} \Delta \varepsilon_\theta + D_{11} \Delta K_\phi + D_{12} \Delta K_\theta \quad (\text{III.93})$$

$$\Delta M_\theta = K_{12} \Delta \varepsilon_\phi + K_{22} \Delta \varepsilon_\theta + D_{12} \Delta K_\phi + D_{22} \Delta K_\theta \quad (\text{III.94})$$

Eqs. (III.91) to (III.94) can be solved for $\Delta \varepsilon_\phi$ and ΔK_ϕ

$$\Delta \varepsilon_\phi = \left[\begin{array}{l} (\Delta N_\phi - C_{12} \Delta \varepsilon_\theta - K_{12} \Delta K_\theta) D_{11} \\ - (\Delta M_\phi - K_{12} \Delta \varepsilon_\theta - D_{12} \Delta K_\theta) K_{11} \end{array} \right] \frac{1}{A_{11}} \quad (\text{III.95})$$

$$\text{Where } A_{11} = C_{11} D_{11} - K_{11}^2$$

$$\Delta K_\phi = \left[\left(\Delta M_\phi - K_{12} \Delta \varepsilon_\theta - D_{12} \Delta K_\theta - \right. \right. \\ \left. \left. - \left(\Delta N_\phi - C_{12} \Delta \varepsilon_\theta - K_{12} \Delta K_\theta - \right) \right] \right] / A_{11} \quad (\text{III.96})$$

$$\text{Where : } A_{11} = C_{11} D_{11} - K_{11}^2$$

The various coefficients in Eqs. (III.91) to (III.94) are determined from the definitions of the stress resultants.

$$C_{11} = \int_{-h/2}^{+h/2} \frac{\partial \sigma_\phi}{\partial \varepsilon_\phi} dz$$

$$C_{12} = \int_{-h/2}^{+h/2} \frac{\partial \sigma_\phi}{\partial \varepsilon_\theta} dz$$

$$C_{22} = \int_{-h/2}^{+h/2} \frac{\partial \sigma_\theta}{\partial \varepsilon_\theta} dz$$

$$D_{11} = \int_{-h/2}^{+h/2} \frac{\partial \sigma_\phi}{\partial \varepsilon_\phi} z dz$$

$$D_{12} = \int_{-h/2}^{+h/2} \frac{\partial \sigma_\phi}{\partial \varepsilon_\theta} z dz$$

$$D_{22} = \int_{-h/2}^{+h/2} \frac{\partial \sigma_\theta}{\partial \varepsilon_\theta} z dz$$

$$C_{21} = C_{12}$$

$$D_{21} = D_{12}$$

$$\begin{aligned}
 K_{11} &= \int_{-h/2}^{+h/2} \frac{\partial \sigma_\phi}{\partial \epsilon_\phi} z^2 dz & , & \quad K_{12} = \int_{-h/2}^{+h/2} \frac{\partial \sigma_\phi}{\partial \epsilon_\theta} z^2 dz \\
 K_{22} &= \int_{-h/2}^{+h/2} \frac{\partial \sigma_\theta}{\partial \epsilon_\theta} z^2 dz & & \quad (III.97)
 \end{aligned}$$

For elastic-behavior Eqs. (III.97) simply reduce to:

$$\begin{aligned}
 C_{11} &= C_{22} = \frac{Eh}{1-v^2} \\
 C_{12} &= \frac{Ehv}{(1-v^2)} & & \quad (III.98)
 \end{aligned}$$

$$K_{11} = K_{12} = K_{22} = 0$$

$$D_{11} = D_{22} = \frac{Eh^3}{12(1-v^2)}$$

$$D_{12} = \frac{vEh^3}{12(1-v^2)}$$

3.5 Treatment at Shell Apex.

Constitutive relations Eqs. (III.91) to (III.95) must be treated differently at an umbelical shell apex because of singularities in the equations. In the special case of singularities of an umbelical point,

$$\Delta\epsilon_\theta = \Delta\epsilon_\phi \text{ and } \Delta K_\theta = \Delta K_\phi$$

Therefore Eqs. (III.90) and (III.92) become:

$$\Delta N_\phi = (c_{11} + c_{12})\Delta\epsilon_\phi + (K_{11} + K_{12})\Delta K_\phi \quad (\text{III.99})$$

$$\Delta M_\phi = (D_{11} + D_{12})\Delta K_\phi + (K_{11} + K_{12})\Delta\epsilon_\phi \quad (\text{III.100})$$

From which:

$$\left[\Delta\epsilon_\phi = (D_{11} + D_{12}) \{ \Delta N_\phi \} - (K_{11} + K_{12}) \{ \Delta M_\phi \} \right] \quad \left. \right|_{A_{22}} \quad (\text{III.101})$$

$$\left[\Delta K_\phi = (c_{11} + c_{12}) \{ \Delta M_\phi \} - (K_{11} + K_{12}) \{ \Delta N \} \right] \quad \left. \right|_{A_{22}} \quad (\text{III.102})$$

Where:

$$A_{22} = (c_{11} + c_{12})(d_{11} + d_{12}) - (k_{11} + k_{12})^2 \quad (\text{III.103})$$

$$\Delta N_\phi = \Delta N_\phi \quad (\text{III.104})$$

$$\Delta M_\theta = \Delta M_\phi \quad (\text{III.105})$$

CHAPTER IV

INCREMENTAL SOLUTION OF ELASTIC-PLASTIC PROBLEMS

4.0 Intent of Chapter.

The equations derived in the previous chapters must be organized in a form such that they are integrable. It is intended to present a complete set of equations in a form independent of the numerical integration scheme adopted.

4.1 Bases for Solution.

The set of first order ordinary differential equation, Eqs. (II.52) to (II.58) can not as yet be integrated since they contain non-linearities. The method adopted to treat these non-linearities requires that they be reorganized. The incorporation with the constitutive relations of chapter III must also be detailed.

The method of analysis for treating the non-linearities in shell equations is simplified in such a way that direct integration with the aid of a suppression scheme (Chapter V) is possible. To obtain the nonlinear elastic solutions, this integration is performed directly for the total applied loading and a number of iterations are required to converge to the non-linear elastic solution. For elastic-plastic material behavior this integration and iterative procedure is carried out for every increment of the load.

The direct numerical integration of shell equations is possible separately for all homogeneous as well as particular solutions followed by their recombinations. For elastic-plastic analysis this is

accomplished for each increment of the load. Further, the elastic-plastic constitutive relations are used accordingly during each homogeneous and particular solution integration.

It is in general extremely difficult to obtain solutions to non-linear differential equations of the boundary value type such as those posed for a shell of revolution in the previous chapters. Direct numerical integration of the non-linear differential equations can be made possible in various ways such as:

- (i) Using an incremental approach throughout:
- (ii) Application of a Newton-Raphson procedure:
- (iii) Application of quazilinearization methods:

The first of the above is generally tedious and may lead to propagation of errors due to truncation within each of the series of increment. A Newton-Raphson Procedure has been used with the multi-segment method by Kalnins and Lestini (67) to obtain solutions to non-linear-elastic shell problems. Later Gerdeen (9) applied the Newton-Raphson Procedure with a multisegment method to solutions to non-linear elastic-plastic problems.

Hutula (65) obtained a set of quasilinearized shell equations using Reissner-Meissner's Shell Theory. The set of first order ordinary differential equations due to Sanders (7) presented in Chapter II will be quasilinearized and organized to be made amenable to use.

4.2 Reformulation of Initial Value Problems.

The solution to a symmetrically loaded shell of revolution

problem between the initial and final edges is obtained by converting a boundary value problem to an initial value problem. For a system of $2n$ variables, at the initial edge only n boundary conditions are known for a given problem. Linearly independent values of the remaining n variables at the initial edge are chosen. The prescription of n boundary values and n arbitrarily chosen values at the initial edge for each homogeneous and particular solution integration thus constitutes an initial value problem. When these integrations are carried out to the final edge n boundary conditions are satisfied and a set of coefficients determined that are used to appropriately combine the linearly independent homogeneous and the particular solutions. This is valid for iterative non-linear elastic solutions since the non-linear shell equations are quasilinearized within each iterate. This is also possible for an incremental non-linear elastic-plastic solutions due to the assumed linear behavior within each increment in this range.

Direct numerical integration of linear or non-linear shell governing equations is difficult since these equations tend to provide extraneous exponentially growing functions which must be controlled in order to obtain a correct solution to the problem. The numerical integration of shell equations which starts by conversion of a boundary value problem to an initial value problem, must be assisted by a technique to control the extraneous solutions. Two such techniques have been developed, which provide uniform accuracy everywhere along

the integration path: the multisegment method and the suppression technique.

4.3 Quasilinearization.

4.3.1 Theory. The quasilinearization technique was developed by Bellman (68), Kalaba (69) and applied to chemical engineering problems by Lee (70).

In the quasilinearization technique the non-linear differential equation are first represented by a set of simultaneous first order differential equations. Each of the first order differential equations is linearized using Taylor series expansions with second and higher order terms omitted. Iterative solutions of the resulting linearized differential equations usually converge quadratically to the solution of the original equations such that each iteration approximately doubles the number of digits of accuracy. For example, let us consider the following set of non-linear first order differential equation:

$$\frac{dy_i}{dx} = f_i(x, y_j); \quad (IV.1)$$

i, j = 1, 2, ..., n

with boundary conditions:

$$y_i(0) = \alpha_i \quad (IV.2)$$

where $f_i(x, y_j)$ are non-linear functions which can be linearized around $y_i = y_i^*$ as follows:

$$f_i(x, y_j) = f_i(x, y_j^*) + \left\{ \frac{\partial f_i(x, y_j)}{\partial y_k} \right\}_{y_j=y_j^*} (y_k - y_k^*) \quad (IV.3)$$

In other words, the differential equations can be represented around $y_i = y_i^*$, as:

$$\frac{dy_i}{dx} = f_i(x, y_j^*) + j_{ik} (y_k - y_k^*) \quad (IV.4)$$

where:

$$j_{ik} = \left\{ \frac{\partial f_i}{\partial y_k} \right\}_{y_j=y_j^*} \quad (IV.5)$$

If y is represented in the vector form (y_1, y_2, \dots, y_n) and f represented in vector form (f_1, f_2, \dots, f_n) , and if y^* is taken as a previous iteration $y^{(n)}$ to the solution. then the differential equation, Eq. (IV.1) can be written as:

$$\frac{dy}{dx} = f(x, y^{(n)}) + J(y^{(n)}) (y^{(n+1)} - y^{(n)}) \quad (IV.6)$$

Eq. (IV.6) now constitutes a linear initial value problem for $y^{(n+1)}$.

Once $y^{(n+1)}$ has been determined, successive iterates $y^{(r)}$, $r=n+2, n+3, \dots$, can be obtained from successive solutions of Eq. (IV.6). The initial iterate $y^{(0)}$ can be taken as the linear elastic solution.

The Jacobian J is given by:

$$J(y^{(n)}) = \begin{bmatrix} \frac{\partial f_1^{(n)}}{\partial y_1} & \frac{\partial f_1^{(n)}}{\partial y_2} & \dots & \frac{\partial f_1^{(n)}}{\partial y_m} \\ \frac{\partial f_2^{(n)}}{\partial y_1} & \frac{\partial f_2^{(n)}}{\partial y_2} & \dots & \frac{\partial f_2^{(n)}}{\partial y_m} \\ \vdots & \vdots & \ddots & \vdots \\ \vdots & \vdots & \ddots & \vdots \\ \frac{\partial f_m^{(n)}}{\partial y_1} & \frac{\partial f_m^{(n)}}{\partial y_2} & \dots & \frac{\partial f_m^{(n)}}{\partial y_m} \end{bmatrix} \quad (IV.7)$$

4.3.2 Application. It is now possible to apply this method to the set of first order shell differential equations given in Chapters II and III.

The application of the quasilinearized method does not alter the linear terms in the shell governing equations. For example, the first order ordinary differential equation.

$$w_s = \frac{u}{R_\phi} - \gamma_\phi \quad (IV.8)$$

when quasilinearized becomes:

$$w_s^{(n+1)} = \frac{1}{R_\phi} \left\{ u^{(n)} + \frac{\partial u^{(n)}}{\partial u} (u^{(n+1)} - u^{(n)}) \right\}$$

$$- \left\{ \gamma_\phi^{(n)} + \frac{\partial \gamma_\phi^{(n)}}{\partial \gamma_\phi} (\gamma_\phi^{(n+1)} - \gamma_\phi^{(n)}) \right\}$$

$$= \frac{u_\phi^{(n+1)}}{R_\phi} - \gamma_\phi^{(n+1)} \quad (IV.9)$$

To illustrate the quasilinearization process, consider the non-linear equation:

$$U_{\phi,s} = \varepsilon_{\phi} - \frac{W}{R_{\phi}} - \frac{1}{2} \gamma_{\phi}^2 \quad (IV.10)$$

Application of the quasilinearization method to this equation gives:

$$\begin{aligned} U_{\phi,s}^{(n+1)} &= \varepsilon_{\phi}^{(n+1)} - \frac{W^{(n+1)}}{R_{\phi}} - \frac{1}{2} \left\{ \left(\gamma_{\phi}^{(n)} \right)^2 + \left(\frac{\partial \gamma_{\phi}}{\partial \gamma_{\phi}} \right)^{(n)} \left(\gamma_{\phi}^{(n+1)} - \gamma_{\phi}^{(n)} \right) \right\} \\ &= \varepsilon_{\phi}^{(n)} - \frac{W^{(n)}}{R_{\phi}} - \frac{1}{2} \left\{ \left(\gamma_{\phi}^{(n)} \right)^2 + 2 \left(\gamma_{\phi}^{(n)} \right)^n \left(\gamma_{\phi}^{(n+1)} - \gamma_{\phi}^{(n)} \right) \right\} \\ U_{\phi,s}^{(n+1)} &= - \frac{W}{R_{\phi}} - \gamma_{\phi}^{(n+1)} \gamma_{\phi}^{(n)} + \frac{1}{2} \left(\gamma_{\phi}^{(n)} \right)^2 \quad (IV.11) \end{aligned}$$

where the superscript (n) represents the value of the previous iterate. The quasilinearized version of the complete set of governing shell equations, Eq. (II.52) to Eq. (II.58), is given by:

$$W_{s}^{(n+1)} = \frac{U^{(n+1)}}{R_{\phi}} - \gamma_{\phi}^{(n+1)} \quad (IV.12)$$

$$\gamma_{\phi, s}^{(n+1)} = K_{\phi}^{(n+1)} \quad (IV.13)$$

$$M_{\phi, s}^{(n+1)} = \frac{\cos \phi}{r} \left\{ M_{\theta}^{(n+1)} - M_{\phi}^{(n+1)} \right\} + Q_{\phi}^{(n+1)} \quad (IV.14)$$

$$(rQ_{\phi})_{s}^{(n+1)} = \frac{r}{R_{\phi}} \left\{ 2 \gamma_{\phi}^{(n)} N_{\phi}^{(n)} \right\} \gamma_{\phi}^{(n+1)} + rN_{\theta}^{(n)} K_{\phi}^{(n+1)} + rN_{\phi}^{(n)} K_{\theta}^{(n+1)}$$

$$+ \left\{ \sin \phi + rK_{\theta}^{(n)} \right\} N_{\theta}^{(n+1)} - \frac{r}{R_{\phi}} \gamma_{\phi}^{(n)} Q_{\phi}^{(n+1)} - \frac{r}{R_{\phi}} Q_{\phi}^{(n)} \gamma_{\phi}^{(n+1)}$$

$$+ r \left\{ \frac{1}{R_{\phi}} + \frac{(\gamma_{\phi}^2)^{(n)}}{R_{\phi}} + K_{\phi}^{(n)} \right\} N_{\phi}^{(n+1)}$$

$$+ r \left\{ K_{\phi}^{(n)} N_{\phi}^{(n)} - K_{\theta}^{(n)} N_{\theta}^{(n)} - \frac{2}{R_{\phi}} (\gamma_{\phi}^2)^{(n)} (N_{\phi}^{(n)}) \right\}$$

$$+ \frac{\gamma_{\phi}^{(n)} Q_{\phi}^{(n)}}{R_{\phi}} - P \} \quad (IV.15)$$

$$U_{s}^{(n+1)} = \varepsilon_{\phi}^{(n+1)} - \frac{w}{R_{\phi}} - \gamma_{\phi}^{(n)} \gamma_{\phi}^{(n+1)} + \frac{1}{2} (\gamma_{\phi}^2)^{(n)} \quad (IV.16)$$

$$\begin{aligned}
 N_{\phi's}^{(n+1)} &= \frac{\cos\phi}{r} N_{\theta}^{(n+1)} - \frac{\cos\phi}{r} N_{\phi}^{(n+1)} - \frac{Q_{\phi}^{(n+1)}}{R_{\phi}} - \frac{\gamma_{\phi}^{(n)} N_{\phi}^{(n)}}{R_{\phi}} \\
 &+ \frac{1}{R_{\phi}} \left\{ \gamma_{\phi}^{(n)} N_{\phi}^{(n+1)} + N_{\phi}^{(n)} \gamma_{\phi}^{(n+1)} \right\} - P_{\phi} \quad (IV.17)
 \end{aligned}$$

It is to be noted that the above set of equations contain auxiliary variables, such as $\epsilon_{\theta}, K_{\theta}, \epsilon_{\phi}, K_{\phi}, N_{\theta}$ and M_{θ} , along with the fundamental variables that were defined in Chapter II. These auxiliary variables are determined using the constitutive relations. Since no prior use of constitutive relations was made in deriving the set of quasilinearized governing differential equations, Eqs. (IV.12) to (IV.17), generality with respect to material behavior is retained.

In the foregoing derivation of Eqs. (II.52) to (II.58) the iterate values corresponding to a previous solution state are represented with superscript (n) whereas the current iteration variables are represented with superscript (n+1). An obvious choice for the trial iterates during the first iteration of the non-linear solution is the linear elastic solution. Subsequently, the current iteration variables defined by the superscript (n+1) become iterate values for future iterations. Such iterations are repeated until a desired accuracy is obtained.

4.4 Final Form of Equations.

A brief description of the method of large deflection elastic-plastic analysis is presented in the following chapter.

Emphasis is given to organizing previously derived equations in a form suitable for integrations. Since only a general method of analysis can be presented here many of the previously derived equations have been referenced to indicate their usability.

The procedure for the scaling of loads to the yield point and a method of assuming strains to start the solution algorithm is outlined in Appendix D.

Once the strains are known for the current iteration of a load increment then the functions f_1 , f_2 , f_3 and their derivatives are evaluated from (III.50) to (III.61).

For each load step the initial trial solution $(\sigma_\phi, \sigma_\theta, \bar{\epsilon}^p)_0$ corresponds to initial iteration number zero. In this case the best choice happens to be Eq. (III.31). Note that if the transition factor $m=1$ is used in Eqs. (III.62) to (III.73) they reduce to Eq.(III.31).

The current values of stresses and effective plastic strain are evaluated from Eq. (III.62), given by:

$$\begin{Bmatrix} \sigma_\phi \\ \sigma_\theta \\ \bar{\epsilon}_p \end{Bmatrix}^{(n+1)} = \begin{Bmatrix} \sigma_\phi \\ \sigma_\theta \\ \bar{\epsilon}_p \end{Bmatrix}^{(n)} - \begin{bmatrix} \frac{\partial f_1}{\partial \sigma_\phi} & \frac{\partial f_1}{\partial \sigma_\theta} & \frac{\partial f_1}{\partial \bar{\epsilon}_p} \\ \frac{\partial f_2}{\partial \sigma_\phi} & \frac{\partial f_2}{\partial \sigma_\theta} & \frac{\partial f_2}{\partial \bar{\epsilon}_p} \\ \frac{\partial f_3}{\partial \sigma_\phi} & \frac{\partial f_3}{\partial \sigma_\theta} & \frac{\partial f_3}{\partial \bar{\epsilon}_p} \end{bmatrix}^{-1} \begin{Bmatrix} f_1 \\ f_2 \\ f_3 \end{Bmatrix}$$

(IV.18)

The plastic stiffness coefficients are then evaluated from (III.25) to (III.34) and the coefficients C_{11} , C_{22} , C_{21} , D_{11} , D_{12} , D_{22} , D_{21} , K_{11} , K_{12} , K_{21} , A_{11} are evaluated at each meridional integration point from Eq. (III.99) or (III.100) to (III.104) for singular points.

The auxiliary variables are determined from:

$$\epsilon_\theta^j = (u_\phi^j \cos\phi + w_\phi^j \sin\phi) / r \quad (IV.19)$$

$$K_\theta^j = \gamma_\phi^j \cos\phi / r \quad (IV.20)$$

where $j=0, 1; 1=1, 2, \dots, n$. The first of these superscripts (0) corresponds to a particular solution and the remaining n superscripts correspond to homogeneous solutions.

For homogeneous solutions:

$$\Delta \epsilon_{\theta}^1 = \epsilon_{\theta}^1 \quad (\text{IV.21})$$

$$\Delta K_{\theta}^1 = K_{\theta}^1 \quad (\text{IV.22})$$

and for particular solution:

$$\Delta \epsilon_{\theta}^0 = \epsilon_{\theta}^0 - \epsilon_{\theta}^i \quad (\text{IV.23})$$

$$\Delta K_{\theta}^0 = K_{\theta}^0 - K_{\theta}^i \quad (\text{IV.24})$$

Where the subscript i refers to a previous solution state.

For elastic-plastic solution process the previous solution state is also called a residual state.

For homogeneous solutions,

$$\Delta N_{\phi}^1 = N_{\phi}^1 \quad (\text{IV.25})$$

$$\Delta M_{\phi}^1 = M_{\phi}^1 \quad (\text{IV.26})$$

and for particular solution:

$$\Delta N_{\phi}^0 = N_{\phi}^0 - N_{\phi}^i \quad (\text{IV.27})$$

$$\Delta M_{\phi}^0 = M_{\phi}^0 - M_{\phi i} \quad (IV.28)$$

Eq. (III.91) and Eq. (III.94) are now solved:

$$\begin{aligned} \Delta \varepsilon_{\phi}^j = & \left[(\Delta N_{\phi}^j - C_{12} \Delta \varepsilon_{\theta}^j - K_{12} \Delta K_{\theta}^j) D_{11} \right. \\ & \left. - (\Delta M_{\phi}^j - K_{12} \Delta \varepsilon_{\theta}^j - D_{12} \Delta K_{\theta}^j) K_{11} \right] \end{aligned} \quad A_{11} \quad (IV.29)$$

$$\begin{aligned} \Delta K_{\phi}^j = & \left[(\Delta M_{\phi}^j - K_{12} \Delta \varepsilon_{\theta}^j - D_{12} \Delta K_{\theta}^j) C_{11} \right. \\ & \left. - (\Delta N_{\phi}^j - C_{12} \Delta \varepsilon_{\theta}^j - K_{12} \Delta K_{\theta}^j) K_{11} \right] \end{aligned} \quad A_{11} \quad (IV.31)$$

where various coefficients C_{11} , C_{12} , C_{22} , K_{11} , K_{12} , K_{22} , D_{11} , D_{12} , D_{22} are solved by integrating Eq. (III.97) through the thickness using Simpson's rule; A_{11} is determined from Eq. (III.96)

Now ΔN_{θ}^j and ΔM_{θ}^j are similarly determined from Eq. (III.92) and Eq. (III.94) respectively.

Thus:

$$M_{\theta}^j = M_{\theta i} + \Delta M_{\theta}^j$$

$$N_{\theta}^j = N_{\theta i} + \Delta N_{\theta}^j \quad (\text{IV.32})$$

$$\varepsilon_{\phi}^j = \varepsilon_{\phi i} + \Delta \varepsilon_{\phi}^j \quad (\text{IV.33})$$

$$K_{\phi}^j = K_{\phi i} + \Delta K_{\phi}^j \quad (\text{IV.34})$$

The subsequent development of a numerical scheme for the direct integration of a set of first order ordinary differential equations, given by Eqs. (IV.12) to (IV.17), require a much clearer perspective with regard to the treatment of $(n)^{\text{th}}$ and $(n+1)^{\text{th}}$ iteration values. Eqs. (IV.12) to (IV.17) are therefore reorganized in the following form.

Let:

$$\{F_i\} = \text{Vector of the fundamental variables of Eqs. (IV.12) to (IV.17), } i=1,2,\dots,6 \\ = \{w_{\phi}, \gamma_{\phi}, M_{\phi}, Q_{\phi}, U_{\phi}, N_{\phi}\}^T.$$

$$\{R_{i,j}\} = \text{Matrix that contains constants and } (n)^{\text{th}} \text{ iteration values of all variables and their derivatives in Eq. (IV.12) to (IV.17), } i=1,2,\dots,6; j=1,2,\dots,12. \\ (\text{see table IV.1 for components of this matrix}).$$

$$\{A_j\} = \text{Vector of } (n+1)^{\text{th}} \text{ iterates of fundamental and auxiliary variables in Eqs. (IV.12) to (IV.17); } j=1,2,\dots,6. \\ = \{\varepsilon_{\theta}, K_{\theta}, \varepsilon_{\phi}, K_{\phi}, N_{\theta}, M_{\theta}\}^T.$$

$\{L_i\}$ = Vector of $(n)^{th}$ iterates of the fundamental and auxiliary variables that are not multiplied by coefficients of $(n+1)^{th}$ iterates in Eqs. (IV.12) to (IV.17).

Where

$$L_1 = L_2 = L_3 = 0 \quad (IV.35)$$

$$L_4 = r \left[\left\{ K_\phi N_\phi - K_\phi N_\theta - \frac{2}{R_\phi} \gamma_\phi^2 N_\phi + \frac{\gamma_\phi Q_\phi}{R_\phi} \right\}^{(n)} - P_n \right] \quad (IV.36)$$

$$L_5 = \frac{1}{2} \left\{ \gamma_\phi^2 \right\}^{(n)} \quad (IV.37)$$

$$L_6 = - \left\{ \frac{\gamma_\phi N_\phi}{R_\phi} \right\}^{(n)} - P_\phi \quad (IV.38)$$

The set of first order ordinary differential equations are now organized as:

$$\{F_{i,s}\}^{(n+1)} = \left[R_{i,j} \right]^{(n)} \left\{ \frac{F_i}{A_i} \right\}^{(n+1)} + \{L_i\}^{(n)} \quad (IV.39)$$

Where $i = 1, 2, \dots, 6$ and

$j = 1, 2, \dots, 12$

Table IV.1 Components of Matrix $R_{i,j}$

$$R_{1,2} = 1$$

$$R_{4,10} = r N_{\phi}^{(n)}$$

$$R_{1,5} = \frac{1}{R_{\phi}}$$

$$R_{4,11} = \sin \phi + r K_{\theta}^{(n)}$$

$$R_{2,10} = 1$$

$$R_{5,1} = - \frac{1}{R_{\phi}}$$

$$R_{3,3} = - \frac{\cos \phi}{r}$$

$$R_{5,2} = - \gamma_{\phi}^{(n)}$$

$$R_{3,4} = 1$$

$$R_{5,9} = 1$$

$$R_{3,12} = \frac{\cos \phi}{r}$$

$$R_{6,2} = N_{\phi}^{(n)}$$

$$R_{4,2} = \frac{r}{R_{\phi}} \left\{ N_{\phi}^{(n)} \gamma_{\phi}^{(n)} - Q_{\phi}^{(n)} \right\}$$

$$R_{6,4} = - \frac{1}{R_{\phi}}$$

$$R_{4,4} = \frac{r}{R_{\phi}} \gamma_{\phi}^{(n)}$$

$$R_{6,6} = \frac{\gamma_{\phi}^{(n)}}{R_{\phi}} - \frac{\cos \phi}{r}$$

$$R_{4,6} = \frac{r}{R_{\phi}} \left\{ 1 + (\gamma_{\phi}^2)^{(n)} + R_{\phi} K_{\phi}^{(n)} \right\}$$

$$R_{6,11} = \frac{\cos \phi}{r}$$

$$R_{4,8} = r N_{\theta}^{(n)}$$

All other components of the matrix $[R_{i,j}]$ have a zero value.

In the expanded form Eq. (IV.43) is written as:

$$\left\{ \begin{array}{c} F_{1,s} \\ F_{2,s} \\ \vdots \\ F_{6,s} \end{array} \right\}^{(n+1)} = \left[\begin{array}{cccccc} R_{1,1} & R_{1,2} & \cdots & R_{1,12} & \cdots & R_{1,12} \\ R_{2,1} & R_{2,2} & \cdots & R_{2,12} & \cdots & R_{2,12} \\ \vdots & \vdots & \ddots & \vdots & \ddots & \vdots \\ \vdots & \vdots & \ddots & \vdots & \ddots & \vdots \\ \vdots & \vdots & \ddots & \vdots & \ddots & \vdots \\ R_{6,1} & R_{6,2} & \cdots & R_{6,12} & \cdots & R_{6,12} \end{array} \right]^{(n)} \left\{ \begin{array}{c} G_1 \\ G_2 \\ \vdots \\ G_{12} \end{array} \right\}^{(n+1)} + \left\{ \begin{array}{c} L_1 \\ L_2 \\ \vdots \\ L_6 \end{array} \right\}^{(n)} \quad (IV.40)$$

$$\text{Where } \{G_j\} = \left\{ \frac{F_i}{A_i} \right\}, \quad i=1,2,\dots,6; \quad j=1,2,\dots,12 \quad (IV.41)$$

It is customary to regard $\{L_i\}^{(n)}$ as a load vector and, hence, is considered only during direct integrations of the particular solutions. Once a solution is known for an iteration then the middle surface strains and curvatures are used to evaluate the strain increments at every point through the thickness using the following expressions:

$$\Delta \epsilon_{\phi} = (\epsilon_{\phi} - \epsilon_{\phi i}) = (\bar{\epsilon}_{\phi} - \bar{\epsilon}_{\phi i}) - z (\bar{K}_{\phi} - \bar{K}_{\phi i}) \quad (IV.42)$$

$$\Delta \varepsilon_\theta = (\varepsilon_\theta - \varepsilon_{\theta i}) = (\bar{\varepsilon}_\theta - \bar{\varepsilon}_{\theta i}) + z (\bar{K}_\phi - \bar{K}_{\phi i}) \quad (\text{IV.43})$$

Where z is the coordinate through the thickness, $\bar{\varepsilon}_\phi$, $\bar{\varepsilon}_\theta$, \bar{K}_ϕ , \bar{K}_θ , are some of the auxiliary variables at the middle surface.

Subscript i refers values of these auxiliary variables at the previous solution state.

4.5 Statement of Chapter.

The equations (IV.39) are now in the appropriate form to be used with the non-linear integration scheme that is developed in a subsequent chapter. All quantities of Eqs. (IV.39) are non-dimensionalized in Appendix B.

CHAPTER V

NUMERICAL INTEGRATION SCHEME FOR LINEAR ANALYSIS

5.0 Intent of Chapter.

In this chapter the suppression technique for linear elastic analysis is reviewed. This is done separately in this chapter in order to avoid repetition of certain salient features of this technique that would be common to both linear and non-linear analysis. More detailed discussions of the numerical integration process including suppression can be found in (11) to (14).

5.1 Linear Analysis Method Background.

The numerical integration problem is first set-up such that the fundamental variables are those appearing on the boundaries. Then the boundary value problem is transformed into a set of initial value problems; solutions to each of these initial value problems are called partial solutions.

A problem arises in the use of numerical integration. The solutions are of the exponential type and accuracy is lost in integrating over long path lengths. To overcome this problem the multisegment method (12) or the suppression technique (13) and (14) can be used. These methods provide uniform accuracy everywhere along the integration path.

In the multisegment method the region of integration is subdivided into a number of segments. The stiffness of each segment is obtained by successively setting each fundamental

variable at the beginning of the segment equal to unity while others are set equal to zero. Having the stiffness of previously integrated segments, one can reassemble the segments by solving a set of simultaneous equations. The number of these equations equals the number of fundamental variable times the number of shell segment, plus one. Kalnins and Lestini (67) adopted a Newton-Raphson scheme with the multisegment method of numerical integration for the large deflection analysis of elastic shells of revolution.

The suppression technique alleviates the numerical problem of error propagations by recombining the independent initial value problems (partial solutions) when necessary as the integration proceeds. They are recombined in such a way that the components of the erroneous growing solutions at the point in question are eliminated. With this technique, the solutions are all of comparable magnitude when the integration process arrives at the far edge of the shell. Whenever the partial solutions have become large compared with the initial conditions, the suppression is accomplished by requiring that linear combination of the partial solutions sequentially satisfy sets of artificial initial conditions with small magnitude at various points along the meridian of the shell. Thus, for each segment the number of equations solved equals the number of fundamental variables. For the linear elastic analysis of shells the partial solutions can be linearly combined to obtain the final solution.

An extension of the suppression technique to non-linear shell analysis is presented in the following in which the quasi-linearization technique described in chapter IV is used in such a way that the final recombination of partial solutions becomes possible.

In the numerical integration scheme, a standard Runge-Kutta Gill procedure in conjunction with Hamming's predictor-corrector method is used to solve the system of first order differential equations.

5.2 Description of Suppression Process.

In the suppression technique for a system of order $2j$, j quantities are assumed at the initial point and j boundary conditions are satisfied at the terminal point. The correct solution corresponds to some other set of initial values that produce boundary quantities satisfying the terminal boundary conditions.

Partial solutions for j homogeneous and one particular solution designated by s_0 , s_1 , ..., s_j are carried simultaneously by assuming j initial values and prescribing j boundary conditions at the initial point. The growth of extraneous solutions is controlled by selecting suppression points at locations where magnitudes of the fundamental variables have exceeded a prescribed limit which is based upon the desired level of accuracy. At each suppression point artificial boundary conditions are satisfied and a set of coefficients are chosen and stored. The resulting

suppressed solution is used to restart the integration process and the integration is carried out until another suppression point is required. The artificial boundary conditions are once again satisfied at this new suppression point and a set of coefficients required for recombination are determined for the present suppression point. These coefficients are used to modify the set of coefficients at the previous suppression points. This process is repeated until the terminal point at the far end of the shell is reached where the terminal boundary conditions are satisfied. The set of coefficients for recombination determined to satisfy the terminal boundary conditions are used to determine the final set of coefficients at all previous suppression points. The process is completed by performing direct integration between all the suppression points, using these initial conditions vectors, with recombination of partial solution after integration to determine the final solution.

5.3 Basic Suppression Technique.

The detailed mathematical treatment of the integration process for the linear elastic analysis of shells of revolution is outlined in the following. The fundamental variables are as defined in Chapter II.

Let the partial solution matrix P be defined as follows:

$$\begin{bmatrix} P \end{bmatrix} = \begin{bmatrix} W_{\phi, so} & W_{\phi, si} & W_{\phi, sj} \\ Y_{\phi, so} & Y_{\phi, si} & Y_{\phi, sj} \\ M_{\phi, so} & M_{\phi, si} & M_{\phi, sj} \\ Q_{\phi, so} & Q_{\phi, si} & \dots & Q_{\phi, sj} \\ U_{\phi, so} & U_{\phi, si} & U_{\phi, sj} \\ N_{\phi, so} & N_{\phi, si} & N_{\phi, sj} \end{bmatrix} \quad (V.1)$$

Where the subscript ϕ on the fundamental term refers to meridional direction, comma denoted derivative, s represents arc lengths along the meridian of the shell, a zero (0) identifies a particular solution and the numbers $1, 2, \dots, j$ identify j homogeneous conditions.

The partial solution matrix given by Eq, (V.1) is written as:

$$\{P_k\} = \{P_0, P_1, \dots, P_j\} \quad (V.2)$$

Where $K = 0, 1, 2, \dots, j$

Each of the vectors P_k is composed of $(j+1)$ boundary conditions and $(j+1)$ initial conditions at the initial point. The $(j+1)$ initial conditions are given by vectors I_0 and I_j as follows:

$$l_0 = \begin{Bmatrix} 0 \\ 0 \\ \vdots \\ \vdots \\ \vdots \\ 0 \end{Bmatrix}, l_1 = \begin{Bmatrix} 1 \\ 0 \\ \vdots \\ \vdots \\ \vdots \\ 0 \end{Bmatrix}, l_2 = \begin{Bmatrix} 0 \\ 1 \\ \vdots \\ \vdots \\ \vdots \\ 0 \end{Bmatrix}, \dots, l_j = \begin{Bmatrix} 0 \\ \vdots \\ \vdots \\ \vdots \\ \vdots \\ l_{jj} = 1 \end{Bmatrix}$$

(v.3)

Thus, a partial solution vector $\{p_k\}$ in Eq. (v.2) is given by:

$$\{p_j\} = \left\{ \frac{B_j}{l_j} \right\}, \quad \{p_0\} = \left\{ \frac{B_0}{l_0} \right\}$$

(v.4)

Once j boundary conditions are known at the initial point, j initial conditions are chosen according to Eqs. (v.3) thus converting the boundary problem to an initial value problem according to Eqs. (v.4).

Furthermore, let P_m^n be the matrix of partial solutions \tilde{P} at suppression point m after n suppressions have been made. The value $m = 1$ can be represented as the base or the initial point. The shell equations are integrated numerically from base to point where the extraneous solutions become so large that it is necessary to suppress them. It was found convenient to represent the shell equations in a non-dimensionalized form which provided a balanced set of equations that were used for suppression. The first point at which suppression was carried out is denoted by $m = 2$. The extraneous solutions are suppressed by requiring that the partial solutions satisfy sets of independent conditions. The magnitudes of the conditions must be small compared to the values of the unsuppressed partial solutions at the suppression point. At a suppression point the artificial boundary conditions are represented by the vectors $\{A_k\}$ with the element A_{kk} ($k=0, 1, \dots, j$). A convenient selection of artificial boundary values is as follows:

$$\{A_0\} = \begin{Bmatrix} t_{00} = 0 \\ 0 \\ 0 \\ 0 \\ \vdots \\ \vdots \\ 0 \end{Bmatrix}, \quad \{A_1\} = \begin{Bmatrix} t_{11} = 1 \\ 0 \\ \vdots \\ \vdots \\ 0 \end{Bmatrix}, \quad \{A_j\} = \begin{Bmatrix} 0 \\ \vdots \\ 0 \\ \vdots \\ A_{11} = 1 \\ \vdots \\ 0 \end{Bmatrix}, \quad \{A_j\} = \begin{Bmatrix} 0 \\ \vdots \\ \vdots \\ \vdots \\ \vdots \\ A_{jj} = 1 \end{Bmatrix}$$

(V.5)

As outlined before it should be noted that for a system of order $2j$, only j boundary conditions are satisfied at the terminal or the suppression point. In other words out of $2j$ quantities in the matrix \bar{P} only j quantities need be chosen in order to obtain appropriate suppression coefficients. The choice of these j quantities is arbitrary but chosen in such a way that the suppression process is most efficient. It has been found that a choice of higher magnitude j values produces an efficient suppression process.

Let us assume that the j quantities to be chosen out of the matrix \bar{P} are denoted by \bar{Q} and are as follows for a system of $2j=6$ and $j=3$:

$$\bar{Q} = \begin{bmatrix} (1) & (2) & (3) \\ M_{\phi,s_1} & M_{\phi,s_2} & M_{\phi,s_3} \\ (1) & (2) & (3) \\ Q_{\phi,s_1} & Q_{\phi,s_2} & Q_{\phi,s_3} \\ (1) & (2) & (3) \\ N_{\phi,s_1} & N_{\phi,s_2} & N_{\phi,s_3} \end{bmatrix} = [q_1, q_2, q_3] \quad (V.6)$$

Let the unsuppressed quantities $\{q_i\}$ ($i = 0, 1, \dots, j$) where $\{q_i\}$ are vectors of \bar{Q} , represent the fundamental variables at the suppression point, i. e. at a point at which extraneous solution can not be tolerated, so that the following artificial boundary conditions are satisfied. Here again, as before, a 0 designates a particular solution and $j=1, 2, \dots$ correspond to homogeneous solutions.

$$[\bar{Q}] \{ \bar{q}_i \} + \{ q_K \} = \{ t_K \} \quad (K = 0, 1, \dots, j)$$

$$\text{or } \sum_{i=1}^j Q_{ki} \{ q_i \} + \{ q_K \} = \{ t_K \} \quad (v.7)$$

This will yield a set of suppression coefficients:

$$H_{kj} = \begin{bmatrix} \bar{q}_{0i} & \bar{q}_{11} & \bar{q}_{1j} \\ \vdots & \vdots & \vdots \\ \vdots & \vdots & \vdots \\ \vdots & \vdots & \vdots \\ \vdots & \ddots & \vdots \\ \vdots & \vdots & \vdots \\ \bar{q}_{0j} & \bar{q}_{1j} & \bar{q}_{jj} \end{bmatrix}; \quad \begin{matrix} K=0,1,\dots,j \\ i=1,2,\dots,j \end{matrix} \quad (v.8)$$

Each solution will yield a set of H_{1k} values so that the suppressed solution can be written as:

$$\bar{s}_K = s_K + \sum_{i=1}^j B_{ki} s_i \quad (K = 0, 1, \dots, j) \quad (v.9)$$

\bar{s}_K is the suppressed partial solution vector and s_K is the unsuppressed partial solution vector. It is necessary to point out here that at the m^{th} suppression point H_{k1}^m suppression coefficients obtained are used not only to suppress the solution at the m^{th} suppression point in question but also to resuppress all the

previous suppression points from the base to the m^{th} suppression point ($m=1, 2, \dots, t$). This marching process is continued until the terminal point is reached. At the terminal point only the particular solution need be suppressed to the real or terminal boundary conditions $\{ T_0^t \}$, so that the unsuppressed values $\{ T_K \}$ can be combined as follows:

$$\{ \bar{T}_K \} = \{ T_K \} + \sum_{i=1}^j H_{01}^t \{ T_1 \} \quad (\text{V.10})$$

where $\{ \bar{T}_K \}$ represents the final solution.

5.4 Statement of Chapter.

The suppression technique presented above is applicable only to linear elastic problems. In chapter that follow this technique has been extended to non-linear elastic and non-linear elastic-plastic problems in which certain salient features of the suppression technique of this chapter will be used.

CHAPTER VI

NUMERICAL INTEGRATION OF QUASILINEARIZED EQUATIONS

6.0 Intent of Chapter.

In this chapter is developed an algorithm for the non-linear analysis of shells of revolution, Eq. (IV.41) with non-dimensionalized terms is to be used in that development. An extension of this numerical integration algorithm for elastic-plastic analysis is also presented.

6.1 Suppression Scheme for Non-linear Elastic Analysis.

6.1.1 Application of Quasilinearization. The quasilinearization method consists of the determinations of successive iterations converging to the true solution. This method is advantageous in that the unknown values for the current iterate occur linearly in the equations. The coefficients of this current iterate may contain previous iterations to the unknown, thereby, the solution to the non-linear problem is obtainable with very little difficulty.

The quasilinearized set of non-linear first order ordinary differential equations derived in chapter III have in general the following characteristics:

- (1) They contain coefficients in terms of the previous iteration as well as the current iteration.
- (2) Each equation of the system is composed of:
 - (a) terms containing the previous iteration values (defined by the matrix $[R_{i,j}]$ in Eq. (IV.41) multiplied by the derivatives of the fundamental variables of the current iteration (defined

by the vector $\{F_{i,s}\}$ of Eq. (IV.41); and:

- (b) terms containing only the iterates of the previous solution and the loading terms defined by vector $\{L_i\}$ of Eq. (IV.41).
- (3) This system of equations is formulated to suit the elastic-plastic algorithm.
- (4) The vector $\{G\}$ of Eq. (IV.43) contains the current or $(n+1)$ th iterates of the fundamental as well as the auxiliary variables.
- (5) These system of equations contain auxiliary variables of the previous and current iterations.

6.1.2 Application of Suppression Scheme. The partial solutions for the non-linear analysis are represented at the $(n+1)$ th iteration, namely:

$$\begin{aligned}
 [F_{i,s}^p]^{(n+1)} &= [F_{i,s}^0 \ F_{i,s}^1 \ F_{i,s}^2 \ \dots \ F_{i,s}^r]^{(n+1)} \\
 &= \begin{bmatrix} w_{\phi,s}^0 & w_{\phi,s}^1 & w_{\phi,s}^r \\ \gamma_{\phi,s}^0 & \gamma_{\phi,s}^1 & \gamma_{\phi,s}^r \\ M_{\phi,s}^0 & M_{\phi,s}^1 & M_{\phi,s}^r \\ Q_{\phi,s}^0 & Q_{\phi,s}^1 & Q_{\phi,s}^r \\ U_{\phi,s}^0 & U_{\phi,s}^1 & U_{\phi,s}^r \\ N_{\phi,s}^0 & N_{\phi,s}^1 & N_{\phi,s}^r \end{bmatrix}^{(n+1)} \quad (VI.1)
 \end{aligned}$$

Where superscript $p=0,1,2,\dots,r$ identifies a particular solution and r homogeneous solutions.

Eq. (IV.42) is rewritten in the following form with the superscript p representing each of the $(r+1)$ partial solutions:

$$\left\{ \begin{array}{c} F_{1,s}^p \\ F_{2,s}^p \\ \vdots \\ F_{6,s}^p \end{array} \right\}^{(n+1)} = \left[\begin{array}{cccc} R_{1,1} & R_{1,2} & \dots & R_{1,12} \\ R_{2,1} & R_{2,2} & \dots & R_{2,12} \\ \vdots & \vdots & \ddots & \vdots \\ R_{6,1} & R_{6,2} & \dots & R_{6,12} \end{array} \right]^{(n)} \left\{ \begin{array}{c} G_1^p \\ G_2^p \\ \vdots \\ G_{12}^p \end{array} \right\}^{(n+1)} + \left\{ \begin{array}{c} L_1 \\ L_2 \\ \vdots \\ L_6 \end{array} \right\}^{(VI.2)}$$

It should be noted that the (n) th iterates in $[R_{i,j}]^{(n)}$ remain same for r homogeneous and one particular solution. The vector $\{L_i\}^{(n)}$ will disappear for the r homogeneous solutions.

The various partial solution vectors $\{F_{i,s}^p\}^{(n+1)}$ are sub-vector of $\{D\}^{(n+1)}$. In the suppression process the definitions of initial conditions vectors, artificial boundary condition vectors etc. will be the same as defined for linear analysis in the previous chapter. Likewise, the process of recombination described in the previous chapter is the same.

As outlined in Eqs. (IV.41) to (IV.43) the vectors $\{G_j^p\}^{(n+1)}$ and $\{L_i\}^{(n)}$ and the matrix $[R_{i,j}]^{(n)}$ are composed of the fundamental as

well as the auxiliary variables determined for their respective iterations. To determine the auxiliary variables of the $(n+1)$ th iteration in the vector G_j^P , it is necessary to use the constitutive relations corresponding to elastic or elastic-plastic material behavior as outlined in chapter V. For instance, in chapter V it has been shown that the fundamental and the auxiliary variables are inter-related through partial stiffness coefficients which must be determined at every meridional point during the integration process. A discussion on the non-linear elastic-plastic algorithm is the subject of Appendix D. It should be noted that iterations on both geometric and material non-linearities occur simultaneously in the solution algorithm.

For the first iteration to the non-linear elastic solution, the linear elastic suppressed partial solutions are used as the assumed values required. Likewise, the non-linear elastic set of suppressed partial solutions are used as initial assumptions for the first iteration of the elastic-plastic solution scheme. In view of the quazilinearized form of the shell equations and the incremental nature of the elastic-plastic analysis the linear super-position of the homogeneous and the particular terms as described in section 6.2 becomes possible.

6.1.3 Complexities of Non-linear Elastic-Plastic Analysis:

As has been stated in the previous section, the quazilinearized form of Sander's shell governing equations that were derived in Chapter II can be used in an elastic-plastic analysis since the use

of elastic constitutive relations was avoided in their derivation.

In this section is discussed the specific manner in which the elastic-plastic constitutive relations are used along with the quasilinearized differential equations and the suppression technique.

The auxiliary variables ε_θ , κ_θ , ε_ϕ , κ_ϕ , N_θ , M_θ , are evaluated at every meridional integration point as before. In addition the partial stiffness coefficients E_{ij} are evaluated at each meridional integration location at several points through the thickness. With the Von-Mises Yield criteria used, eleven points through the thickness were necessary to achieve the desired accuracy in the solution. With E_{ij} values known at each point through the thickness, their weighted effects C_{ij} , D_{ij} and K_{ij} , as defined in Chapter V, were evaluated at the meridional integration point using the trapezoidal integration rule. It is essential to store C_{ij} , D_{ij} and K_{ij} terms in addition to the auxiliary variables, defined earlier. This is necessary in order to calculate all partial solutions at the meridional point. This integration process is subsequently continued along the shell meridian following the suppression technique described in previous sections.

6.2 Non-linear Multisegment Numerical Integration Technique.

The multisegment method of analysis for large deflection elastic problems has been developed by Kalnins (67), for large deflection elastic-plastic problems by Girdean (9). This technique is outlined in the following in order to establish a direct analytical comparison with the suppression technique.

The system of first order ordinary differential equations are represented by:

$$\frac{dy}{dx} = f \{ x, y^1(x), y^2(x), \dots, y^n(x), h(x) \} \quad (VI.3)$$

where $y(x)$ are the fundamental variables and $h(x)$ denotes the non-homogeneous terms in the interval ($a < x < b$) with the boundaries a and b . It is assumed that the values of $n/2$ elements of each vector $y(a)$ and $y(b)$ are known boundary conditions. The interval is divided into equal segments M in order that the extraneous growth of the solutions can be controlled at the end of these segments by satisfying the terminal boundary conditions.

At the initial edge the boundary value problem is converted into an initial value problem. The direct integration is performed within each segment for all segments within the interval upto b where the boundary condition must be satisfied. If T_1 and T_{M+1} are the transformation matrices, then:

$$T_1 y(a) = Y(a) \quad (VI.4)$$

$$T_{M+1} y(b) = U(b)$$

$$Y_i(x) = \begin{bmatrix} \frac{\partial y^1(x)}{\partial y^1(x_i)} & \frac{\partial y^1(x)}{\partial y^2(x_i)} & \cdots & \frac{\partial y^1(x)}{\partial y^j(x_i)} & \cdots & \frac{\partial y^1(x)}{\partial y^n(x_i)} \\ \frac{\partial y^2(x)}{\partial y^1(x_i)} & \frac{\partial y^2(x)}{\partial y^2(x_i)} & \cdots & \frac{\partial y^2(x)}{\partial y^j(x_i)} & \cdots & \frac{\partial y^2(x)}{\partial y^n(x_i)} \\ \vdots & \vdots & \ddots & \vdots & \ddots & \vdots \\ \frac{\partial y^n(x)}{\partial y^1(x_i)} & \frac{\partial y^n(x)}{\partial y^2(x_i)} & \cdots & \frac{\partial y^n(x)}{\partial y^j(x_i)} & \cdots & \frac{\partial y^n(x)}{\partial y^n(x_i)} \end{bmatrix} \quad (VI.5)$$

The j^{th} column of $Y_i(x)$ can be regarded as a set of new variables. A set of simultaneous first-order differential equations is integrated from x_i to x_{i+1} forming the matrix $Y_i(x_{i+1})$. The required first-order differential equations are then obtained by differentiating Eq. (VI.3):

$$\frac{d}{dx} \left\{ \frac{dy(x)}{dy^j(x)} \right\} = \frac{d}{dy^j(x_i)} f \left\{ x, y^1(x), y^2(x), \dots, y^n(x), h(x) \right\} \quad (VI.6)$$

The solution to the non-linear problem is the limit to which the iterative solution to Eq. (VI.6) converges. The solution of the linearized problem is chosen as the initial trial solution.

$$y_i(x_{i+1}) - y^a(x_i) - y^a(x_{i+1}) = -z_i(x_{i+1}) \quad (VI.7)$$

$$z_i(x_{i+1}) = y^c(x_{i+1}) - y_i(x_{i+1}) - y^t(x_i) \quad (VI.8)$$

Where $y^a(x)$ are the values of the iterated solution state, $y^c(x)$ are the values of the integrated solution state from x_i to x_{i+1} and $y^t(x_i)$ are the initial values of the solution.

These evaluations are carried at the end of every segment S_i , $i = 1, 2, \dots, M$ thus representing M matrix equations which contain $M+1$ unknown vectors: $y^a(x_i)$, $i=1, 2, \dots, M+1$.

Since there are n boundary condition exactly specified, the number of unknowns become the same as the number of equations. Consequently the combined system of equations for all i is solved uniquely for $y^a(x_i)$ using the Gaussian elimination technique. The choice of the control of the extraneous growth of the solution is in the predetermined selection of the size of equal segments.

6.3 Suppression Scheme vs Multisegment Method.

The suppression technique developed in Section 6.1 for large deflection elastic and large deflection elastic-plastic problems will be an improvement over the multisegment method described in Section 6.2 for the following reasons:

- (1) In the multisegment method of analysis the selection of the size of each segment is the only way to control the extraneous

growth of the solution.

In the suppression technique the growth of the extraneous solutions is controlled based on a criteria imposed on the growth of one or all variables. The choice of the suppression point is thus arbitrary and the suppression points can be unevenly spaced.

(2) In the multisegment method of analysis it is necessary to handle ($n \times n$) matrices for inversions as well as for solving simultaneous equations. In the suppression technique the order of matrices for inversions is reduced by one half.

(3) In the multisegment method of analysis the unknown fundamental variables are determined through a solution of a set of $M \times n/2$ equations by a technique such as the Gaussian elimination technique.

In the suppression technique the solution of the problem develops in a marching process so that only $n/2$ equations at the terminal point would be considered. In fact that process occurs automatically when the inversion process in item 2 occurs at the terminal point. Instead, (M!) inner products are taken of two matrices at each suppression point.

(4) In the multisegment method of analysis for large deflection problems the determinations of the Jacobian matrices at the end of each segment requires a complex solution scheme and requires increased storage since at the end of the interval a Gaussian elimination scheme is necessary to obtain the solution to the problem.

In the suppression technique presented in Section 6.1 the quasilinearization of the shell equation and the suppression technique

are complementary. Once a system of equations have been quazilinearized it is a simple matter to apply the suppression technique. Thus a clear improvement is inherent.

6.4 Statement of Chapter.

A numerical method of analysis for the large deflection elastic-plastic analysis of symmetrically loaded shells of revolution has now been described. In the chapter that follows a set of example problems have been solved for the purpose of verification of the method of analysis.

CHAPTER VII

RESULTS

In this chapter a brief description of boundary condition is included. Then a set of four numerical examples are presented which provide comparison with published results. The spectrum of these examples chosen cover membrane and bending behavior of various types of shell configurations. For instance, a torus example provides excellent validation of small deflection and large deflection analysis. The examples of spherical and cylindrical shell exhibit membrane behaviour with large deflection elastic-plastic behaviour and various strain hardening properties. An annular plate having bending behavior was analyzed with small deflection elastic, large deflection elastic and large deflection elastic-plastic consideration using a perfectly plastic material behavior providing good agreement with experimental and previous theoretical research. These comparisons, therefore, validate the numerical methods developed in the forgoing chapters.

7.1 Boundary Conditions.

Treatment of shell equations requires careful considerations of boundary conditions at the base (initial edge) and at the apex (final edge). A total of six boundary conditions must be known in order to solve the boundary value problem in symmetrically loaded axisymmetric shells of revolution. As defined in chapter II the six fundamental variables to be used to satisfy these boundary

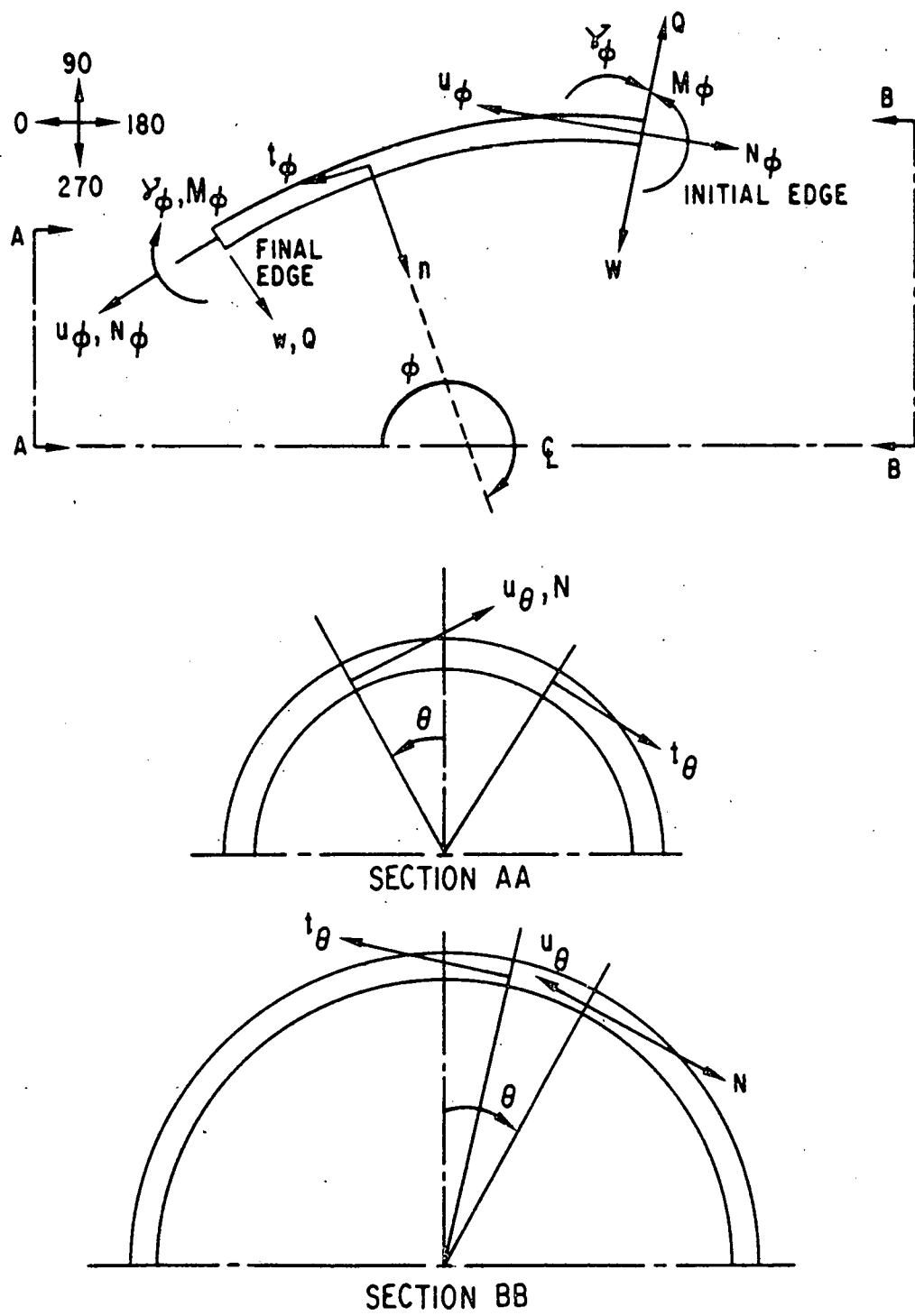


Figure 7.1. Shell Boundary Condition Nomenclature

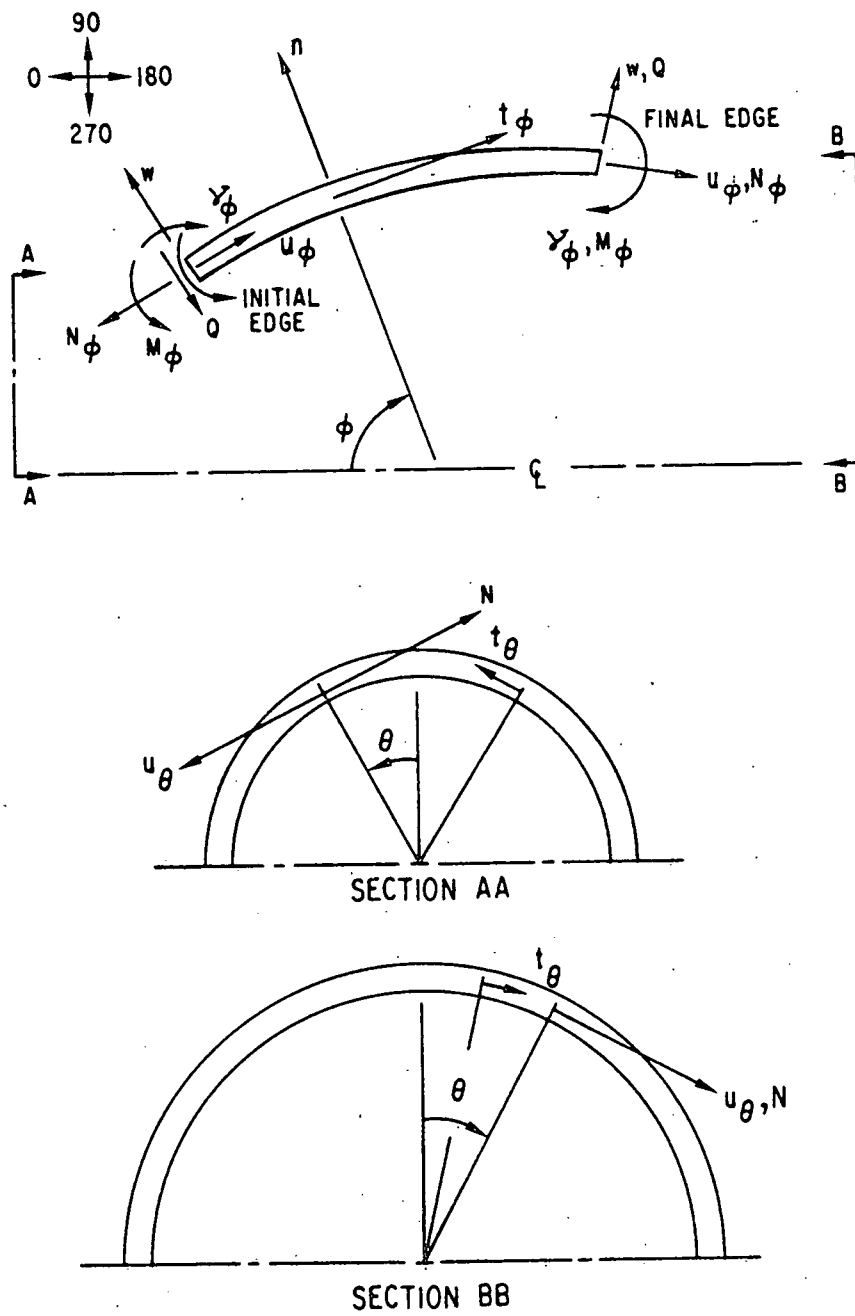


Figure 7.2. Shell Boundary Condition Nomenclature

conditions are $w, \gamma_\phi, M_\phi, Q_\phi, U_\phi$ and N_ϕ . Figs 7.1 and 7.2 show the sign conventions at the initial edge and at the final edge. Note the change in the direction of the normal from Fig. 7.1 to Fig. 7.2 depending upon the choice of the initial edge of the shell. Consistent with the shell behavior three of the six fundamental variables are chosen at each of the initial and the final edge of the shell. The suppression scheme used in chapter V and VI requires selection of the remaining three variables at the initial edge for prescribing arbitrary values in order to convert the boundary value problem into initial values problem.

7.2 Torus Under External Pressure.

For verification of large deflection theory, a torus under external pressure appeared to be a very good example. The problem was investigated earlier by Kalnins and Lestini (67) who used multi-segment method of integration on Reisner-Meisner's Shell equations. The results presented here used the suppression technique, that was developed in chapter VI, for the numerical integration of Sander's non-linear shell equations (7). It should be mentioned here that Sander's (7) assumptions in his development of the non-linear shell theory are identical to Reisner-Meisner's non-linear shell theory used by Kalnins (67).

The geometrical and material constants of the torus problem according to the nomenclature of Fig. 7.3 were taken as follows:

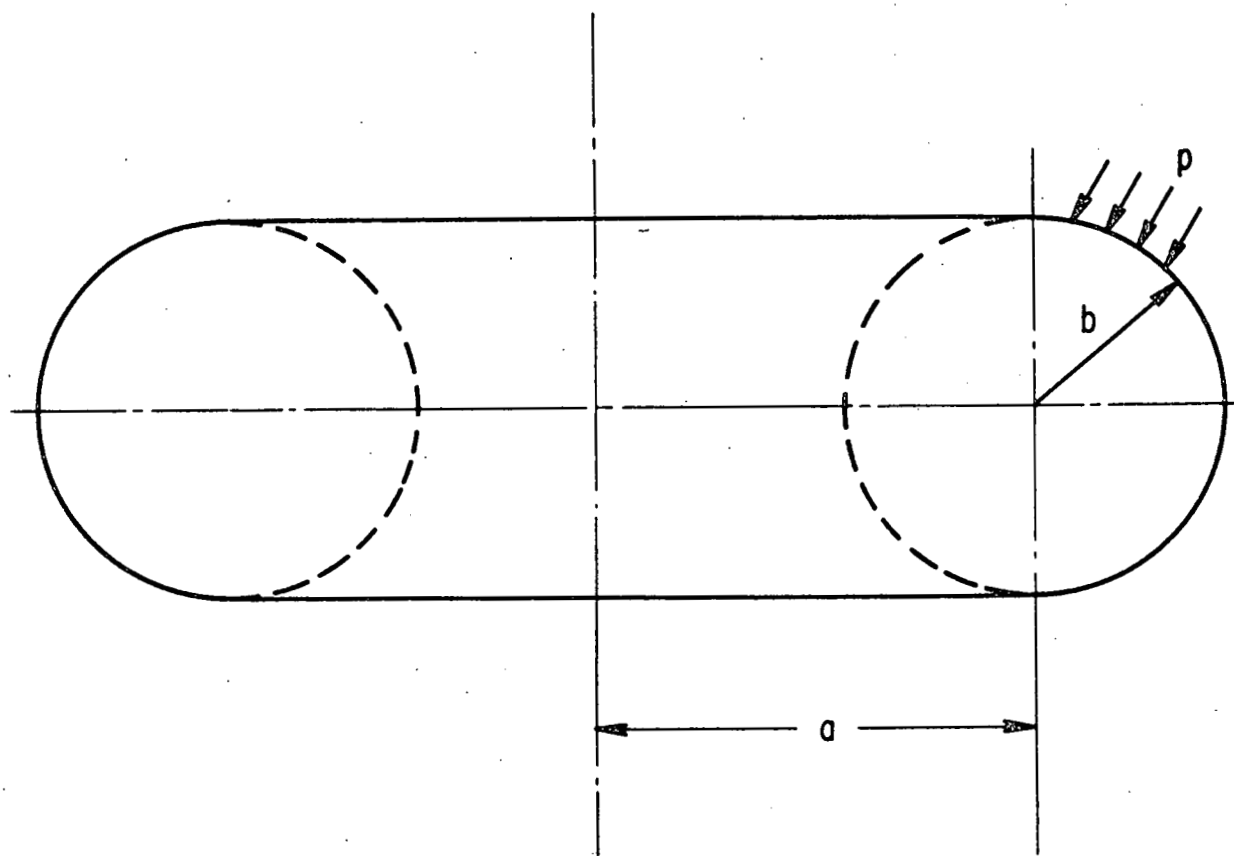


Figure 7.3. Torus Under External Pressure

$$\frac{a}{b} = 1.5$$

$$\frac{h}{b} = 0.01$$

$$\frac{p}{E} = 0.00001$$

$$E = 30 \times 10^6 \text{ psi}$$

$$\gamma = 0.3$$

$$\phi = 90^\circ \text{ (initial edge)}$$

$$\phi = 270^\circ \text{ (final edge)}$$

Boundary Conditions:
(at inner and final edge)

$$\gamma_\phi = 0.0$$

$$Q_\phi = 0.0$$

$$u_\phi = 0.0$$

Initial Conditions:
(at inner edge)

$$w_\phi = 1.0$$

$$M_\phi = 1.0$$

$$N_\phi = 1.0$$

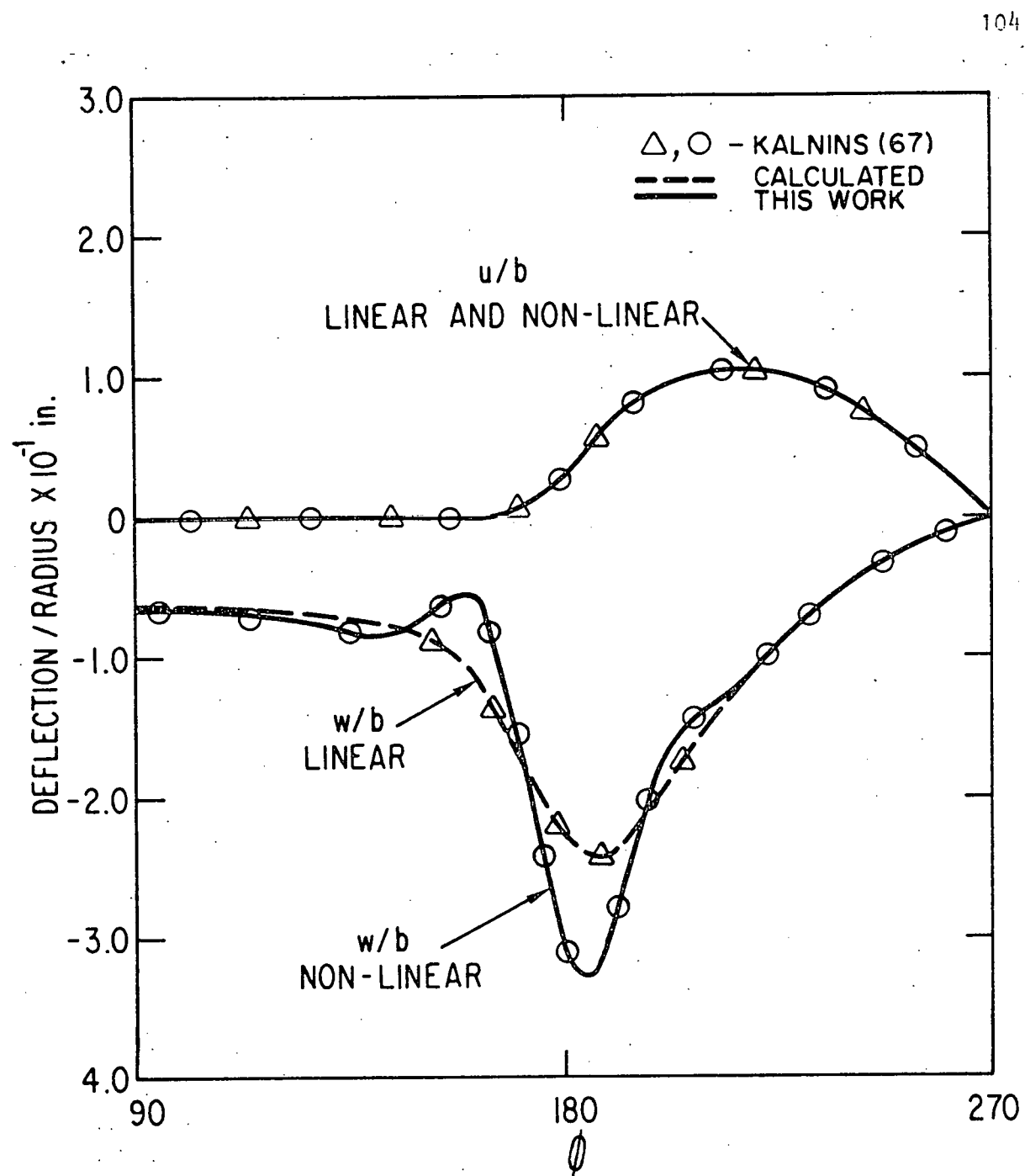


Figure 7.4. Elastic Deflection Behavior of a Torus

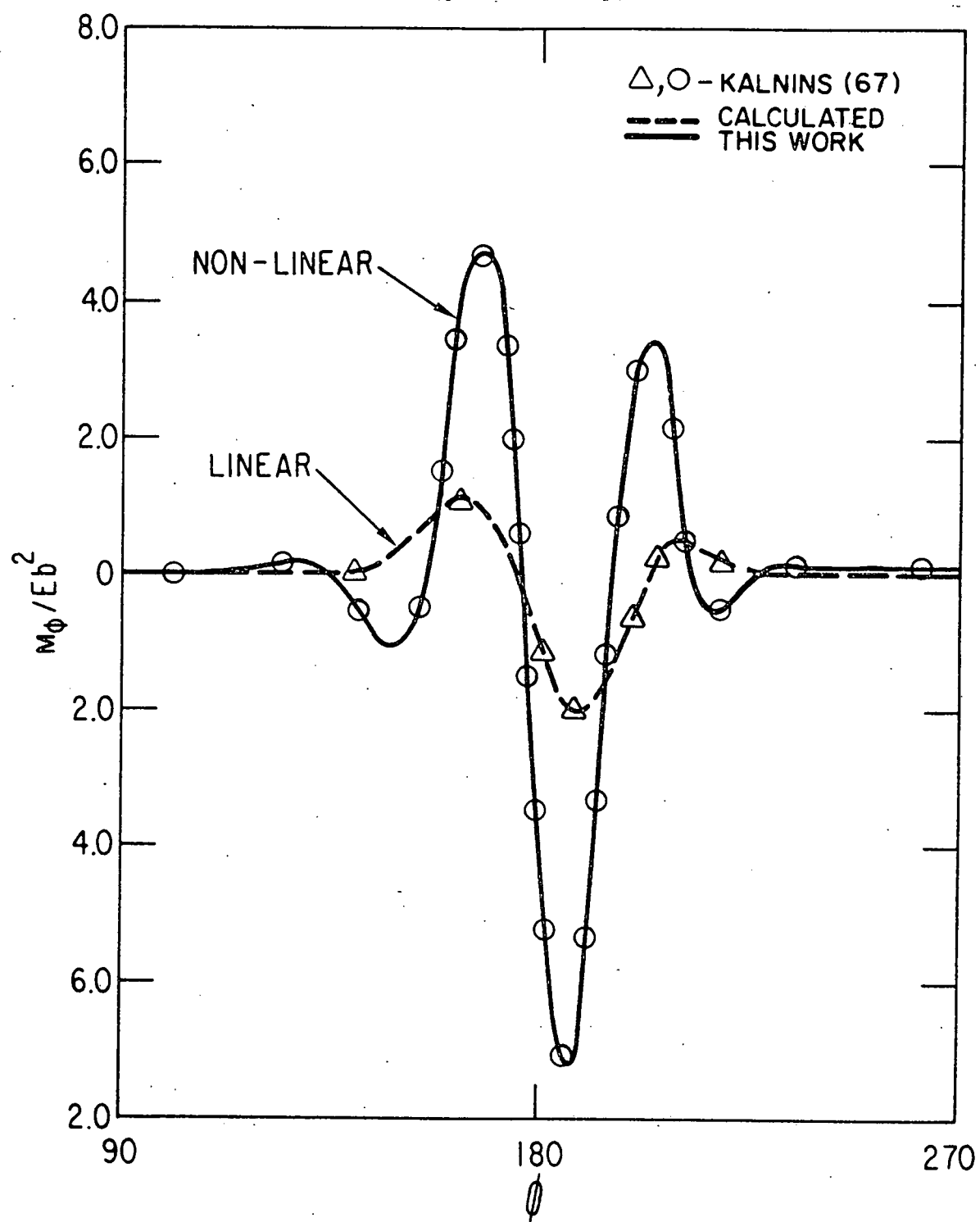


Figure 7.5. Elastic Meridional Moment Distribution of a Torus

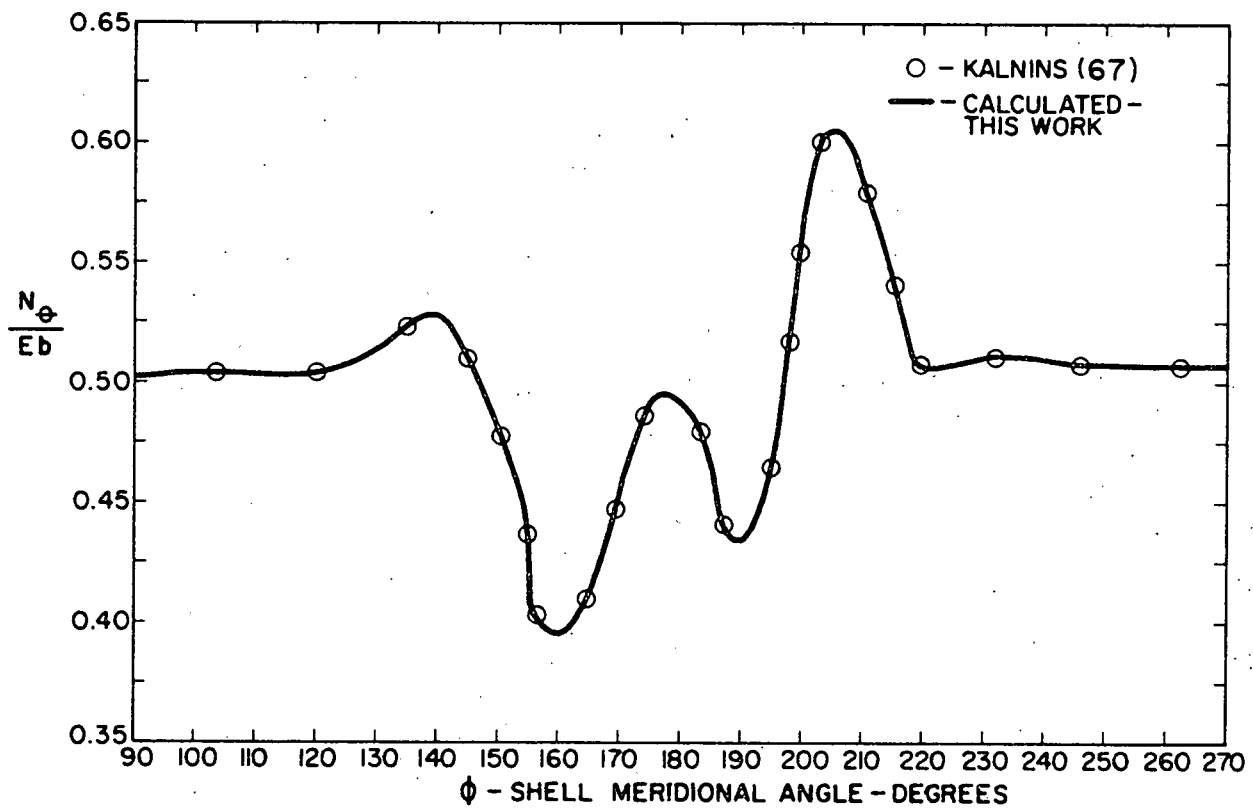


Figure 7.6. Elastic Circumferential Membrane Force Distribution in Torus

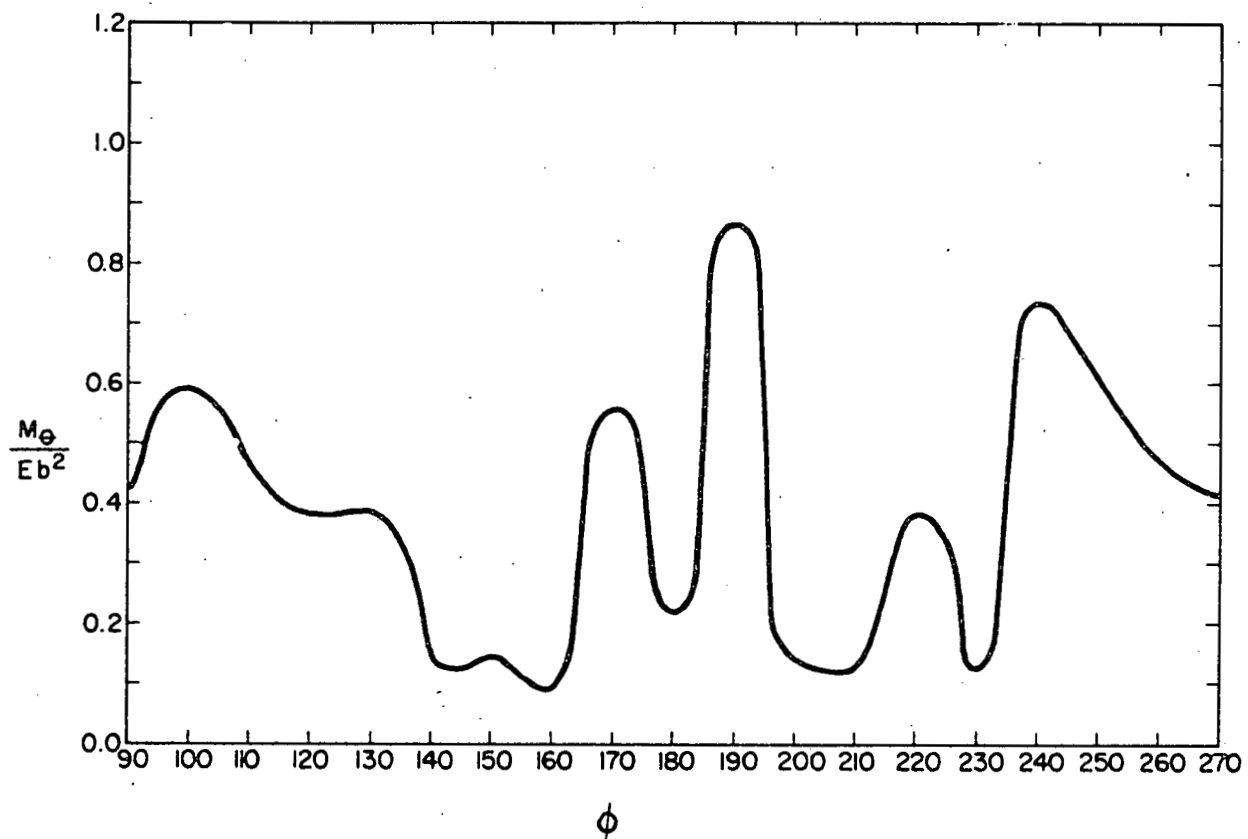


Figure 7.7. Circumferential Bending Moment Distribution in Torus

Results were first obtained for linear-elastic behavior. For the non-linear elastic analysis the results of the linear elastic analysis were used as initial iterates. The convergence of the non-linear elastic solution was obtained with desired accuracy within about three iterations. For this analysis no incremental approach was necessary since the quazilinearization of shell equations made possible the integration of non-linear shell equations for one step total applied load. The non-dimensionalization of the shell theory further improved the stability of the solution. The suppression technique of Chapter VI was found to be a good analytical tool in integrating non-linear shell equations.

The results of the torus problem are plotted in Fig. 7.4 to 7.7 and show excellent agreement with Kalnin's results in (67). The dotted curves indicate linear elastic solution and solid curves indicate non-linear elastic solution in these figures. Fig. 7.4 is a plot between deflection and meridional angle ϕ . The dotted line indicates linear elastic solution and solid line indicates non-linear elastic solution. The solutions differed from those tabulated in (67) by a maximum of two percent difference. Fig. 7.5 is a plot between meridional moment resultant and the meridional angle ϕ and shows good agreement with Kalnins results in (67). Fig. 7.6 is a plot between circumferential membrane force resultant and the meridional angle ϕ showing similar agreements. Fig. 7.7 is a plot of circumferential bending moment result and meridional angle ϕ . It

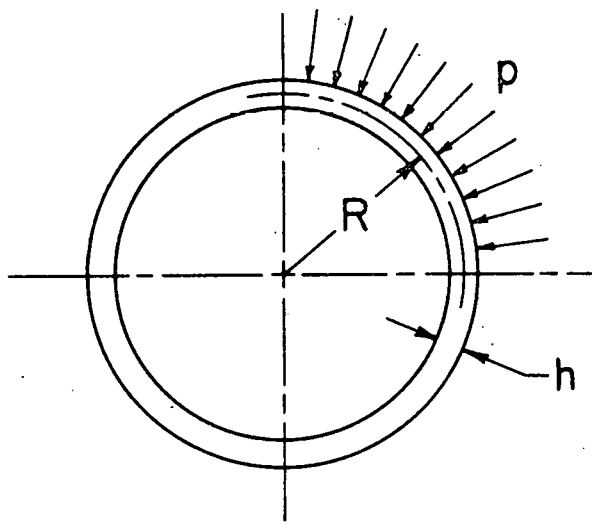


Figure 7.8. Spherical Membrane Under External Pressure

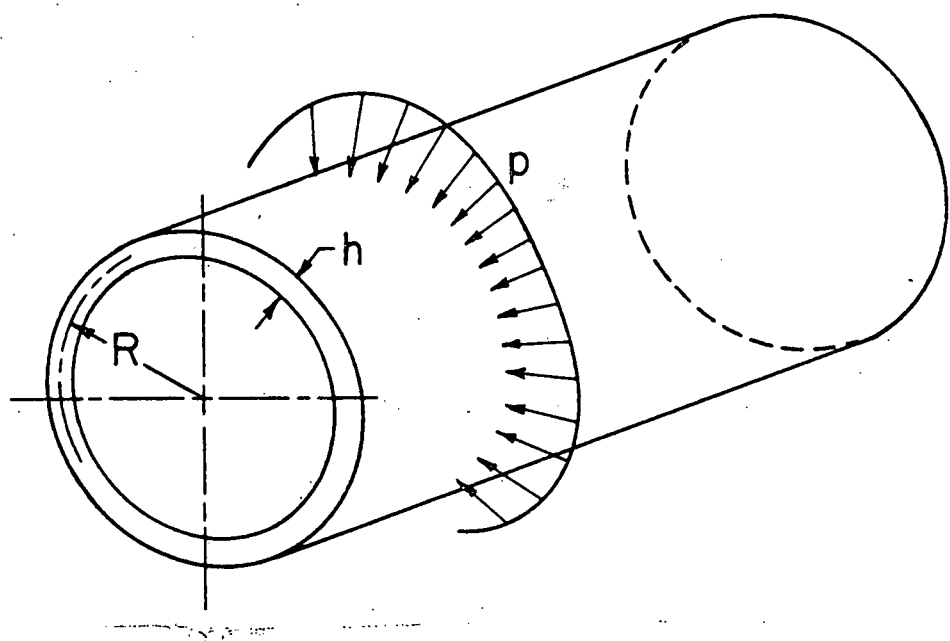


Figure 7.9. Cylindrical Membrane Under External Pressure

is noteworthy that high variations in fundamental variables occur approximately between meridional angles of 150° to 225° .

7.3 Spherical Membrane Under External Pressure.

For the elastic-plastic analysis understanding and verification of results it was considered useful to analyze a spherical membrane under external pressure. The geometric and material parameters used according to the nomenclature of Fig. 7.8 are as follows:

$$\phi = 0^{\circ} \text{ (initial edge)}$$

$$\phi = 90^{\circ} \text{ (final edge)}$$

$$R = 20.0 \text{ inches}$$

$$h = 0.5 \text{ inches}$$

$$E = 30 \times 10^6 \text{ psi}$$

$$v = 0.3$$

$$\sigma_y = 28300 \text{ psi (yield stress)}$$

$$p = 2000 \text{ psi}$$

$$\sigma = 410000 \text{ psi (elastically calculated stress)}$$

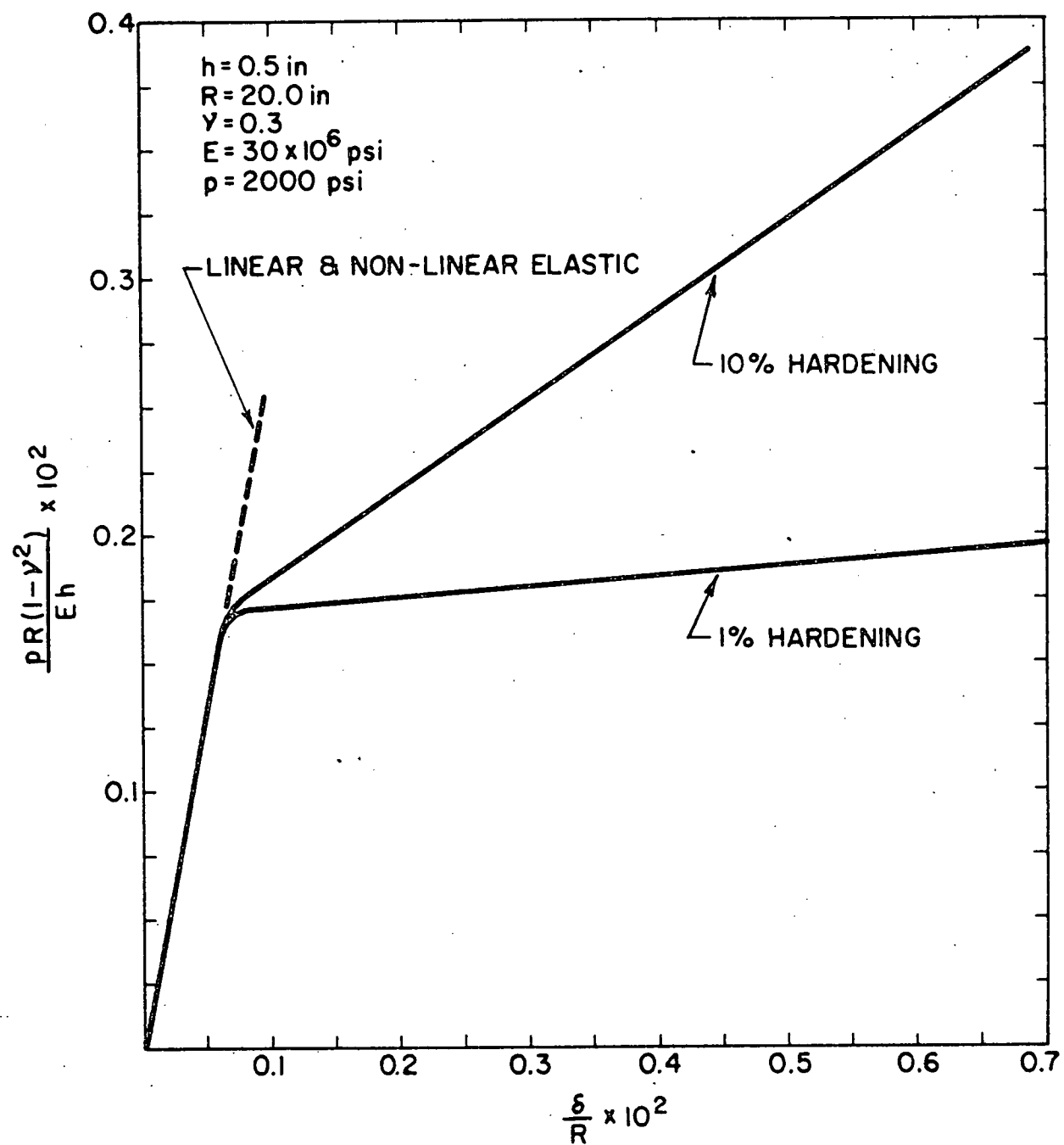


Figure 7.10. Deflection Relationship of Spherical Membrane Under External Pressure

Boundary Conditions (at inner and final edge)	Initial Conditions (at inner edge)
$\gamma_\phi = 0.0$	$w_\phi = 1.0$
$Q_\phi = 0.0$	$M_\phi = 1.0$
$U_\phi = 0.0$	$N_\phi = 1.0$

Strain-hardening properties of the material were included in the elastic-plastic analysis. The results of the large-deflection elastic-plastic analysis are reported in Fig. 7.10 which is a relationship between load and deflection. The results of this analysis were carried far beyond the deflection values reported in Fig. 7.10 and exhibited stability of the solution for very large deflections. Fig. 7.10 shows the relationship between load and deflection for two different percentage (1% and 10%) of strain-hardening. It is indicated that the spherical membrane showed considerable resistance to applied load with increased strain-hardening.

7.4 Cylindrical Membrane Under External Pressure.

Another example of elastic-plastic analysis chosen was that of a cylindrical membrane subjected to external pressure. The geometric parameters used according to the nomenclature of Fig. 7.9 are as follows:

$$\phi = 90^\circ$$

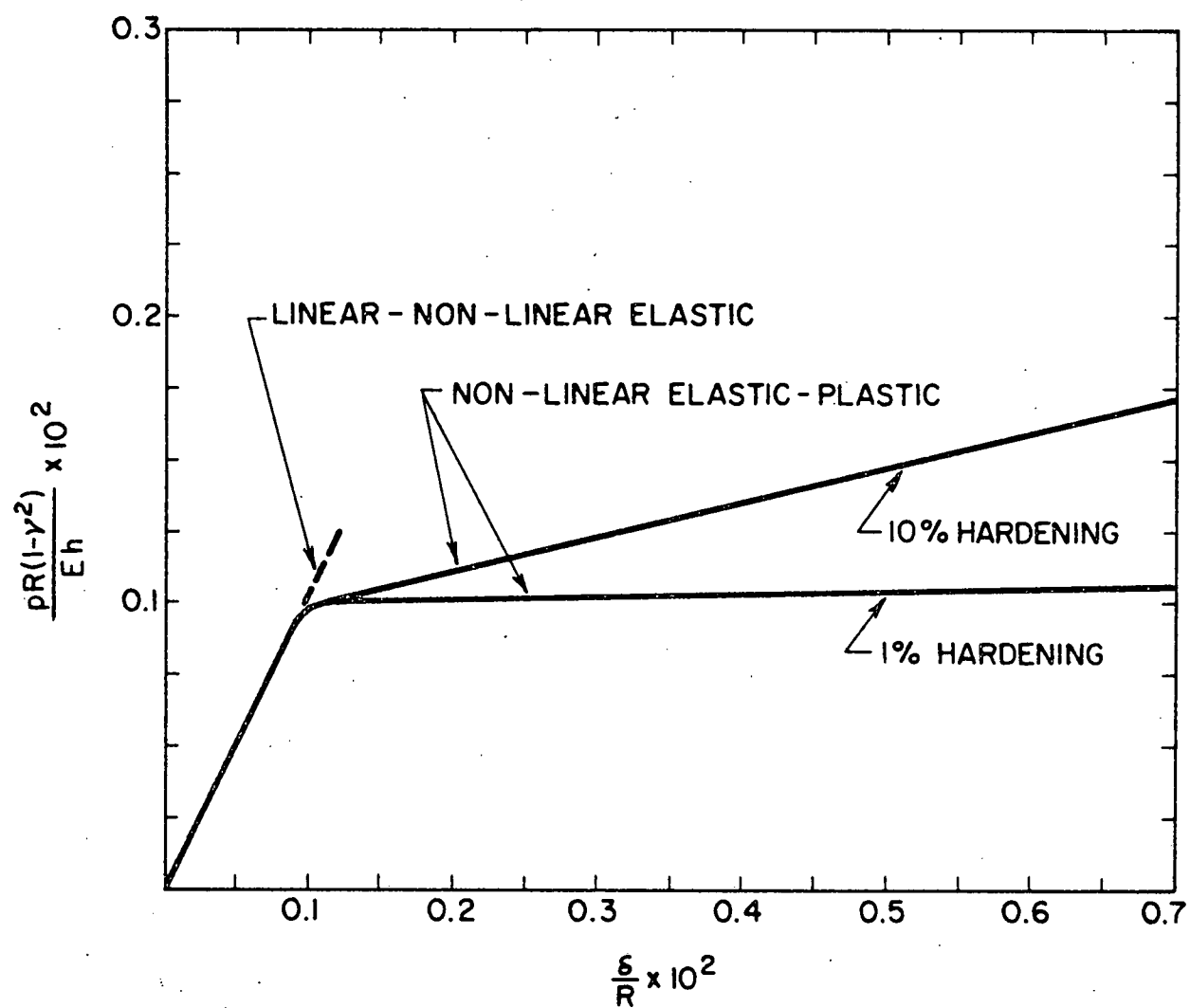


Figure 7.2. Load Deflection of Cylindrical Membrane Under External Pressure

R = 20.0 inches

h = 0.5 inches

L = 10.0 inches

E = 30×10^6 psi

v = 0.3

σ_y = 28300. psi (yield stress)

p = 1000. psi

σ = 40000. psi (elastically calculated stress)

Boundary Conditions
(at initial and final edge)

γ_ϕ = 0.0

Q_ϕ = 0.0

U_ϕ = 0.0

Initial Conditions
(at inner edge)

w_ϕ = 1.0

M_ϕ = 1.0

N_ϕ = 1.0

Since the elastically calculated stress of cylindrical membrane example was the same as in the spherical membrane example, it provided an interesting study of the elastic-plastic analysis results. As for the spherical membrane example the results for cylindrical membrane example were computed for different strain-hardening percentages (1% and 10%). Results of the elastic-plastic analysis of cylindrical membrane are reported in Fig. 7.11, which is a relationship between load and deflection.

7.4 Annular Plate Subjected to Inner Edge Deflection.

Nomenclature of this problem is as indicated in Fig. 7.12. It is shown that the annular plate is simply supported at the outer edge and is free at the inner edge. Edge deflections were applied at the inner edge. Since this problem exhibits considerable bending and non-linear effects it was considered ideal to verify large deflection elastic-plastic analysis results.

This problem of annular plate was earlier analyzed experimentally and theoretically by Ohashi, Murakami and Endo (79) who used large deflection theory in their theoretical analysis. They used a perfectly plastic material in their theoretical and experimental analysis. In the theoretical analysis of (79) Von-Mises yield criterion was used with Prandt-Reuss's flow rule. The geometrical and material parameters used were as follows:

$$a = 100 \text{ mm}$$

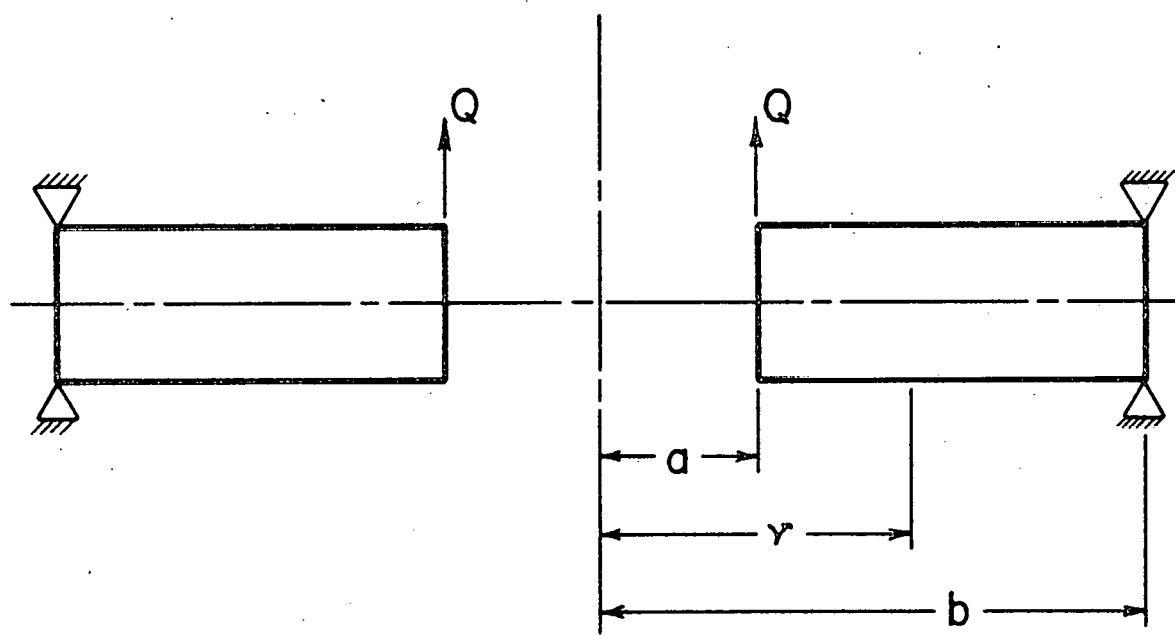


Figure 7.12. Annular Plate Nomenclature

$$b = 200 \text{ mm}$$

$$h = 10 \text{ mm}$$

$$v = 0.28$$

$$E = 20890 \text{ Kg/mm}^2$$

$$H' = 0.0 \text{ (perfectly plastic)}$$

$$\sigma_y = 30.1 \text{ Kg/mm}^2$$

Hutula (65) also analyzed this problem using a large deflection theory and under the conditions similar to (79). Their results showed good agreement with experimental and theoretical results of (79). In the experimental analysis of annular plate in (79) a mild steel specimen was used which behaved more closely like a perfectly plastic material.

The large deflection elastic-plastic analysis of this annular plate was also analyzed in this work to verify the techniques developed in earlier chapters. Since local unloading was allowed in this analysis it was possible to go beyond the range to which the analysis was carried out in (79). This analysis was carried out to the same range of loading to which Hutula (65) carried his results. Following boundary

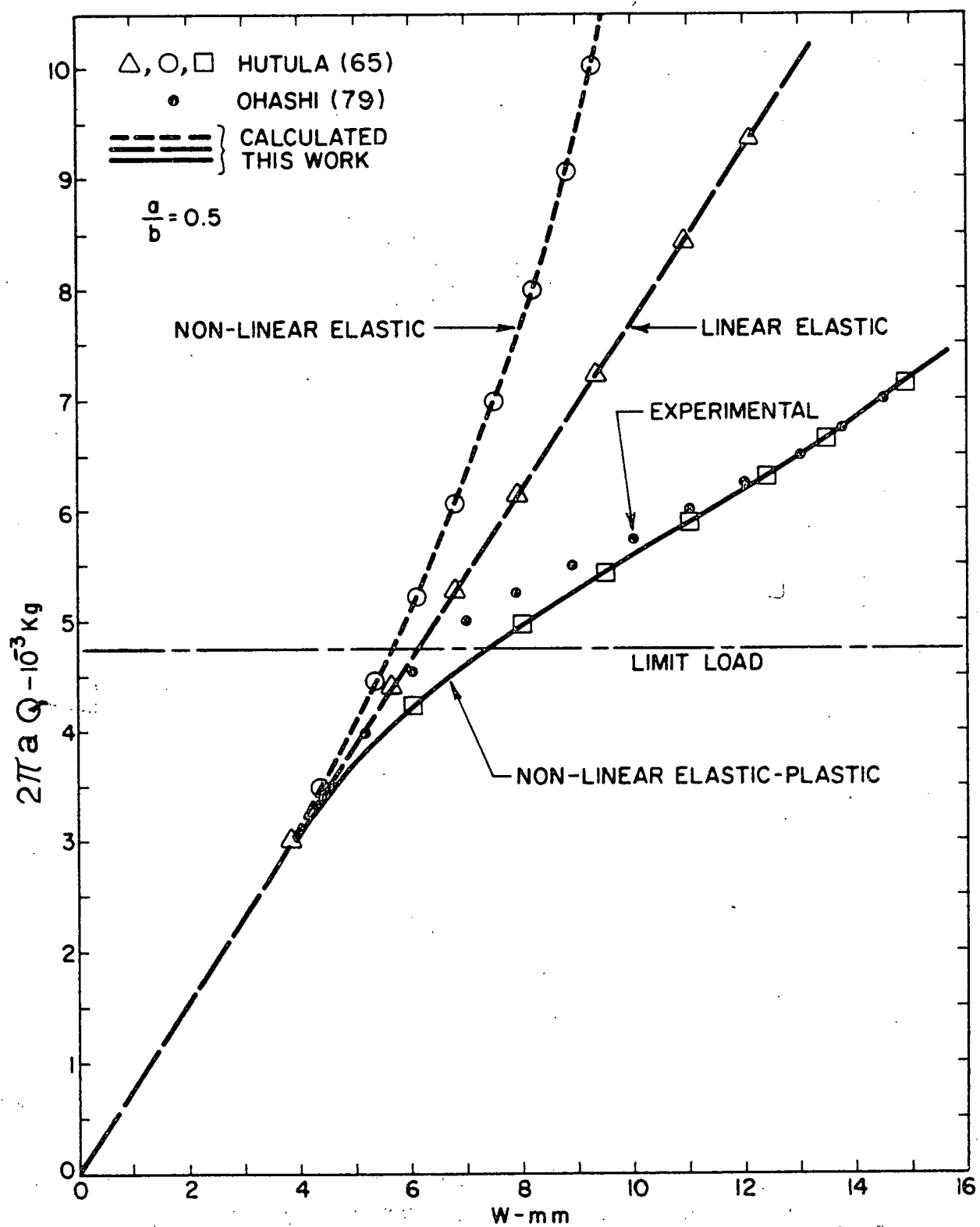


Figure 7.13. Relation Between Total Load and Deflection of Annular Plate

boundary conditions and initial conditions were used in the analysis.

Boundary Conditions

At initial edge

$$w_\phi = w_{\phi i} \text{ (specified)}$$

$$N_\phi = 0.0$$

$$M_\phi = 0.0$$

Initial Conditions

$$\gamma_\phi = 1.0$$

$$Q_\phi = 1.0$$

$$U_\phi = 1.0$$

At final edge

$$w_\phi = 0.0$$

$$N_\phi = 0.0$$

$$M_\phi = 0.0$$

The results of this analysis are reported in Fig. 7.13.

First a linear elastic analysis was carried out which showed good agreement with the results of Hutula (65) as shown in Fig. 7.13.

The results of non-linear elastic analysis also compared very well with those of Hutula (65). As shown in Fig. 7.13 the non-linearity is quite evident as indicated by linear elastic and non-linear elastic results.

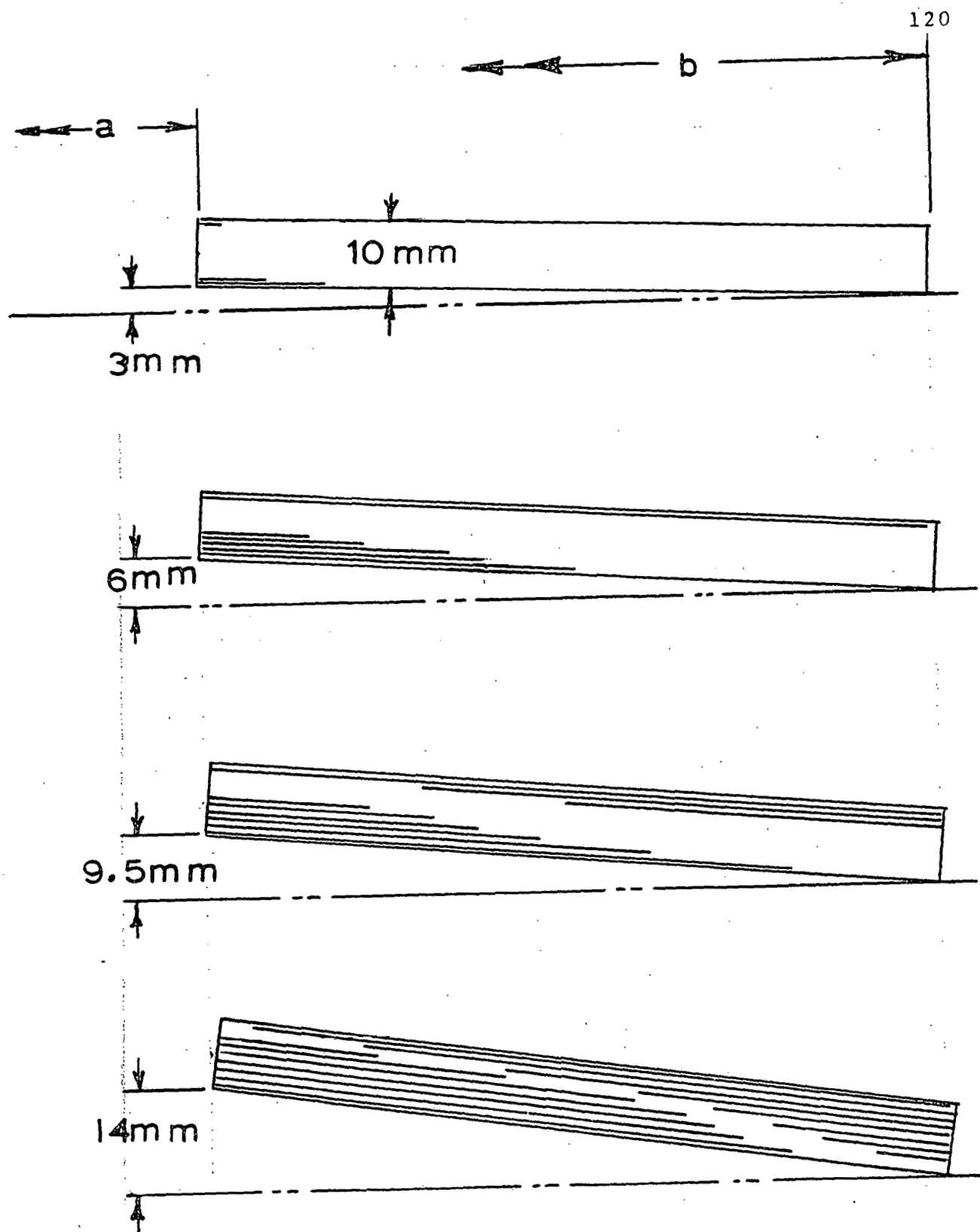


Fig. 7.14 Elastic-Plastic Histogram of Annular Plate

The theoretical results of this analysis and those of Ohashi (79) and Hutula (65) compare very well with the experimental results of (79) in the large deflection range. However, some apparent disagreement with experimental results, of the order of about 8%, can be seen in the small deflection range. This difference can be expected since the material properties and the plasticity constitutive relations are based on uniaxial experimental data and thus may not match fully with biaxial load deflection results. A histogram of the spread of the plastic zone in the deformed annular plate is given in Fig. 7.14.

CHAPTER VIII

CONCLUSIONS AND RECOMMENDATIONS

Improvements in methods of large deflection elastic-plastic analysis of shells and other structures continue to be of interest. With the developments in the previous chapters an improved numerical suppression scheme is now available for the large deflection elastic-plastic analysis of axisymmetric shells of revolution subjected to symmetric loadings. Results presented in the previous chapter indicate the accuracy of this numerical scheme. It appears to be possible to extend this method for more complicated situations.

8.1 Summary of Study. Quazilinearization of Sander's non-linear shell equations is presented for the first time. With these quazi-linear equations the suppression scheme for numerical integrations has been developed to solve non-linear boundary-value problems; in particular the problem of the large deflection elastic-plastic response of shells of revolution. This suppression scheme has been used in conjunction with a Newton-Raphson iteration method for the constitutive relations. Convergence process at the yield surface in elastic-plastic problems is thus obtained.

8.2 Discussion of Results. The large deflection elastic analysis results for a torus presented in the previous chapter show excellent agreement with the results obtained by Kalnins (67) who adopted the multisegment method of numerical integration in that work.

It was not possible to obtain experimental verification of the results for torus. For large deflection elastic-plastic analysis of an annular plate, also reported in the previous chapter, agreement has been obtained with experimental results as well as with previous analytic results using the multisegment method obtained by Hutula (65). For the annular plate problem a perfectly plastic material behavior was assumed. A set of examples were also presented that included strain-hardening material effects.

8.3 Limitations. Although non-linear problems have been solved with the suppression scheme, such problems have been limited only to axisymmetric shell behavior. The method of quazilinearization has been developed for shells of revolution using the first order effects of the Taylor series expansion of a function. Large deflection elastic-plastic analysis can be carried out only with incremental loadings. For each incremental load the entire suppression process must be used in a space-wise marching process to find a new solution state.

A set of three boundary conditions must be specified at each end of the shell, any set of arbitrary values can be specified for the three remaining variables at the initial edge. The analysis is limited to static dead weight or/and pressure loadings. However any symmetric edge loadings can be specified by transforming them into edge boundary conditions.

Only isotropic material properties were considered and no thermal effects were included. However, strain hardening can be accounted

differently at different points of the shell depending upon the magnitude of the plastic strain effects.

8.4 Possible Extensions.

- a. With the present method of analysis thermal loadings can be included by proper modifications of the shell governing equations and the constitutive relations.
- b. Dynamic effects may be added with the present method of analysis by inclusion of inertia effects in the governing shell equations. However, a modal superposition analysis in the elastic-plastic regimes is not possible. Direct time-integration would have to be used.
- c. A convenient means of specifying arbitrary loadings is to use Fourier Series distributions. Due to the non-linear nature of elastic-plastic analysis it is not a straight forward process to superpose Fourier harmonics in order to analyze arbitrary loaded elastic-plastic problems.
- d. It is possible to include cyclic thermal loading effects by proper modifications of the elastic-plastic constitutive relations. This will also allow a study of thermal ratchetting and plastic-creep problems.
- e. A study is recommended in which various other yield functions and hardening laws are used.

8.5 General Conclusions. Through the application of a quasilinearization algorithm it has become possible to extend the suppression scheme of numerical integrations to nonlinear problems. Since, for a suppression process, a criteria must be selected on limiting the extraneous growth of the solution, the degree of stability and/or accuracy will depend upon the criteria. No extensive studies were carried out to find optimum rules for such a criteria.

The suppression method is known to be computationally superior to the multi-segment method for linear problems. Until now it had

not been possible to use the suppression method for nonlinear shell problems except in a strictly incremental fashion. Although no comparison of efficiency were made in this study, it is expected that the suppression method will be as comparatively efficient for nonlinear problems as it is for linear problem. The large deflection elastic solution of a torus presented in the previous chapter is indicative of the need to be concerned about the accuracy of non-linear shell solutions.

APPENDIX A

STRESS PRELIMINARIES

A.1 Stress Tensor.

$$\sigma_{ij} = \begin{bmatrix} \sigma_{11} & \sigma_{12} & \sigma_{13} \\ \sigma_{21} & \sigma_{22} & \sigma_{23} \\ \sigma_{31} & \sigma_{32} & \sigma_{33} \end{bmatrix} = \begin{bmatrix} \sigma_x & \tau_{xy} & \tau_{xz} \\ \tau_{yx} & \sigma_y & \tau_{yz} \\ \tau_{zx} & \tau_{zy} & \sigma_z \end{bmatrix} \quad (A.1)$$

Stress tensor can be resolved into following additive components:

$$\sigma_{ij} = \sigma'_{ij} + \sigma''_{ij} \quad (A.2)$$

where

$$\sigma''_{ij} = \begin{bmatrix} \sigma_m & 0 & 0 \\ 0 & \sigma_m & 0 \\ 0 & 0 & \sigma_m \end{bmatrix} = \begin{bmatrix} \frac{1}{3}(\sigma_x + \sigma_y + \sigma_z) & 0 & 0 \\ 0 & \frac{1}{3}(\sigma_m + \sigma_y + \sigma_z) & 0 \\ 0 & 0 & \frac{1}{3}(\sigma_x + \sigma_y + \sigma_z) \end{bmatrix} \quad (A.3)$$

$$\left[\begin{array}{ccc}
 \frac{2\sigma_x - \sigma_y - \sigma_z}{3} & \tau_{xy} & \tau_{xz} \\
 \tau_{xy} & \frac{-\sigma_x + 2\sigma_y - \sigma_z}{3} & \tau_{yz} \\
 \tau_{xz} & \tau_{yz} & \frac{-\sigma_x - \sigma_y + 2\sigma_z}{3}
 \end{array} \right] \quad (A.4)$$

This is the deviatoric component of stress tensor.

or

$$\sigma'_{ij} = \sigma_{ij} - \frac{1}{3} \delta_{ij} \sigma_{kk} \quad (A.5)$$

$$\delta_{ij} = 1 \text{ for } i = j$$

$$= 0 \text{ for } i \neq j$$

$$\sigma_{kk} = \sigma_{11} + \sigma_{22} + \sigma_{33} = \sigma_x + \sigma_y + \sigma_z \quad (A.6)$$

$$\sigma'_{12} = \sigma_{12} - \frac{1}{3} (0) (\sigma_{11} + \sigma_{22} + \sigma_{33}) = \tau_{xy} \quad (A.7)$$

$$\sigma'_{11} = \sigma_{11} - \frac{1}{3} (1) (\sigma_{11} + \sigma_{22} + \sigma_{33}) = \frac{2\sigma_{11} - \sigma_{22} - \sigma_{33}}{3} \quad (A.8)$$

A.2 Stress Invariant.

The second invariant of the deviatoric component of stress tensor has significance in plasticity theory. The term 'invariant' derives from the fact that magnitudes of these quantities are independent of the particular set of coordinate axes being considered.

In index notation, second invariant can be written as:

$$J_2^1 = \frac{1}{2} \sigma_{ij}^1 \sigma_{ij}^1 \quad (A.9)$$

$$= \frac{1}{2} (\sigma_{1j}^1 \sigma_{1j}^1 + \sigma_{2j}^1 \sigma_{2j}^1 + \sigma_{3j}^1 \sigma_{3j}^1)$$

$$= \frac{1}{2} \left[(\sigma_{11}^1 + \sigma_{12}^1 + \sigma_{13}^1)^2 + (\sigma_{12}^1 + \sigma_{22}^1 + \sigma_{23}^1)^2 \right.$$

$$\left. + (\sigma_{13}^1 + \sigma_{23}^1 + \sigma_{33}^1)^2 \right]$$

Since

$$\sigma_{11}^1 + \sigma_{22}^1 + \sigma_{33}^1$$

$$= \frac{\sigma_{11}^1 - \sigma_{22}^1 - \sigma_{33}^1}{3} + \frac{\sigma_{22}^1 - \sigma_{11}^1 - \sigma_{33}^1}{3} + \frac{\sigma_{33}^1 - \sigma_{22}^1 - \sigma_{11}^1}{3}$$

$$= 0 \quad (A.10)$$

$$(\sigma'_{11} + \sigma'_{22} + \sigma'_{33})^2 = 0 = \sigma'^2_{11} + \sigma'^2_{22} + \sigma'^2_{33} + 2(\sigma'_{11}\sigma'_{22} + \sigma'_{11}\sigma'_{33} + \sigma'_{22}\sigma'_{33}) \quad (A.11)$$

$$\sigma'^2_{11} + \sigma'^2_{22} + \sigma'^2_{33} = -2(\sigma'_{11}\sigma'_{22} + \sigma'_{11}\sigma'_{33} + \sigma'_{22}\sigma'_{33}) \quad (A.12)$$

$$J'_2 = \frac{1}{2} [\sigma'^2_{11} + \sigma'^2_{22} + \sigma'^2_{33} + 2(\sigma'^2_{12} + \sigma'^2_{23} + \sigma'^2_{13})] \quad (A.13)$$

$$J'_2 = -[\sigma'_{11}\sigma'_{22} + \sigma'_{11}\sigma'_{33} + \sigma'_{22}\sigma'_{33} - (\sigma'^2_{12} + \sigma'^2_{23} + \sigma'^2_{13})] \quad (A.14)$$

$$J'_2 = -[\sigma'_x\sigma'_y + \sigma'_x\sigma'_z + \sigma'_y\sigma'_z - \sigma^2_{xy} - \sigma^2_{yz} - \sigma^2_{xz}] \quad (A.15)$$

A.3 Effective Stress.

Effective stress can be written as:

$$\sigma = C_1 \sqrt{(\sigma_x - \sigma_y)^2 + (\sigma_y - \sigma_z)^2 + (\sigma_z - \sigma_x)^2 + 6(\tau_{xy}^2 + \tau_{xz}^2 + \tau_{yz}^2)}$$

$C_1 = \frac{1}{3}$, the effective stress is equal to the octahedral shear stress;

$C_1 = \frac{1}{\sqrt{6}}$, the effective stress is equal to the square of

second invariant J_2' of the deviatoric component of the stress tensor.

$C_1 = \frac{1}{\sqrt{2}}$ then for a uniaxial stress, for which σ_x is the axial stress and all of the other stress components are zero, $\bar{\sigma} = \sigma_x$

$$\sigma_x' = \frac{2 \sigma_x - \sigma_y - \sigma_z}{3} = \frac{(\sigma_x - \sigma_y) + (\sigma_x - \sigma_z)}{3} \quad (A.16)$$

$$\sigma_y' = \frac{2 \sigma_y - \sigma_x - \sigma_z}{3} = \frac{(\sigma_y - \sigma_z) - (\sigma_x - \sigma_y)}{3} \quad (A.17)$$

$$\sigma_z' = \frac{2 \sigma_z - \sigma_x - \sigma_y}{3} = \frac{-(\sigma_y - \sigma_z) - (\sigma_x - \sigma_z)}{3} \quad (A.18)$$

A.4 Strain Preliminaries.

$$\epsilon_{ij}' = \epsilon_{ij}'' + \epsilon_{ij}''' \quad (A.19)$$

$$\epsilon_{ij}''' = \begin{bmatrix} \epsilon_m & 0 & 0 \\ 0 & \epsilon_m & 0 \\ 0 & 0 & \epsilon_m \end{bmatrix} \quad (A.20)$$

where $\epsilon_m = \frac{1}{3} (\epsilon_x + \epsilon_y + \epsilon_z)$

deviatoric strain tensor

$$\epsilon_{ij} = \begin{bmatrix} \frac{2\epsilon_x - \epsilon_y - \epsilon_z}{3} & \frac{\gamma_{xy}}{2} & \frac{\gamma_{xz}}{2} \\ \frac{\gamma_{xy}}{2} & \frac{2\epsilon_y - \epsilon_z - \epsilon_x}{3} & \frac{\gamma_{yz}}{2} \\ \frac{\gamma_{xz}}{2} & \frac{\gamma_{yz}}{2} & \frac{2\epsilon_z - \epsilon_x - \epsilon_y}{3} \end{bmatrix} \quad (A.21)$$

$$\epsilon_{12} = \frac{\gamma_{xy}}{2}$$

$$\epsilon_{13} = \frac{\gamma_{xz}}{2}$$

$$\epsilon_{23} = \frac{\gamma_{yz}}{2}$$

(A.22)

It is important to note that in both plasticity and creep the assumption of incompressibility is made. This means that when only the inelastic portion of the total strain is considered:

$$\epsilon_m = 0$$

$$\text{or } \epsilon_{ij}'' = 0$$

$$\text{and } \epsilon_{ij}' = \epsilon_{ij}$$

The second invariant, I_2' , of the deviatoric component of the strain tensor is in the case of in-elastic strains equal to the second invariant, I_2 , of the strain tensor:

$$I_2' = I_2 = \frac{1}{2} \epsilon_{ij} \epsilon_{ij} \quad (A.23)$$

$$I_2 = - \left[\epsilon_x \epsilon_y + \epsilon_x \epsilon_z + \epsilon_y \epsilon_z - \frac{\gamma_{xy}^2}{4} - \frac{\gamma_{xz}^2}{4} - \frac{\gamma_{yz}^2}{4} \right] \quad (A.24)$$

Effective Strain

$$\bar{\epsilon} = C_2 \sqrt{(\epsilon_x - \epsilon_y)^2 + (\epsilon_y - \epsilon_z)^2 + (\epsilon_z - \epsilon_x)^2 + \frac{3}{2}(\gamma_{xy}^2 + \gamma_{xz}^2 + \gamma_{yz}^2)} \quad (A.25)$$

$C_2 = \frac{2}{3}$, the effective strain is equal to the octahedral shear strain

$C_2 = \frac{1}{\sqrt{6}}$, square of the effective strain is equal to the second invariant I_2 of the strain tensor, provided only in-elastic

strains are being considered.

In case of uniaxial strain:

$$\epsilon_y = \epsilon_z = -\frac{1}{2} \epsilon_x \quad (A.26)$$

Since $\epsilon_m = 0$

Therefore $\bar{\epsilon} = \epsilon_x$ for a uniaxial test provided that $C_2 = \frac{\sqrt{2}}{3}$

A.5 Deviatoric Stress Tensor.

$$\sigma'_{ij} = \sigma_{ij} - \frac{1}{3} \delta_{ij} \sigma_{kk} \quad (A.27)$$

$$\sigma'_{ij} = \begin{bmatrix} \frac{2\sigma_{11} - \sigma_{22} - \sigma_{33}}{3} & \sigma_{12} & \sigma_{13} \\ \sigma_{12} & \frac{-\sigma_{11} + 2\sigma_{22} - \sigma_{33}}{3} & \sigma_{23} \\ \sigma_{13} & \sigma_{23} & \frac{-\sigma_{11} - \sigma_{22} + 2\sigma_{33}}{3} \end{bmatrix} \quad (A.28)$$

Second Invariant

$$J'_2 = \frac{1}{2} \sigma'_{ij} \sigma'_{ij} \quad (A.29)$$

$$= - \left[\sigma'_{11} \sigma'_{22} + \sigma'_{11} \sigma'_{33} + \sigma'_{22} \sigma'_{33} - \sigma_{12}^2 - \sigma_{23}^2 - \sigma_{13}^2 \right].$$

Effective Stress

$$\bar{\sigma} = C_1 \sqrt{(\sigma_{11} - \sigma_{22})^2 + (\sigma_{22} - \sigma_{33})^2 + (\sigma_{33} - \sigma_{11})^2} + 6 (\sigma_{12}^2 + \sigma_{13}^2 + \sigma_{23}^2) \quad (A.30)$$

$$C_1 = \frac{1}{3}, \frac{1}{\sqrt{6}}, \frac{1}{\sqrt{2}} \quad \text{maintain choice.}$$

APPENDIX B

NON-DIMENSIONALIZED SHELL EQUATION

AND

TREATMENT OF SINGULARITIES AT SHELL APEX

B.1 Significance of Non-dimensionalization.

There are two significant advantages in dealing with the non-dimensionalized form of shell equations. First, the treatment of singularities at the shell apex which is often difficult to handle in the analysis becomes convenient with the non-dimensionalization of the shell equations.

Second, non-dimensionalized shell equations serve as a convenient tool in speeding up the numerical integration process. Thus, a convenient means of representation by which the control of the large magnitudes of the growing extraneous solution as well as improving the accuracy of the numerical integration schemes is provided.

The terms that are non-dimensionalized initially are as follows:

$$w^* = \frac{w_\phi}{R_s},$$

$$U^* = \frac{U_\phi}{R_s},$$

$$R_{\phi}^* = \frac{R_{\phi}}{R_s} , \quad R_{\theta}^* = \frac{R_{\theta}}{R_s} ,$$

$$s^* = \frac{s}{R_s} , \quad r^* = \frac{r}{R_s} ,$$

$$h^* = \frac{h}{R_s} , \quad \frac{\partial}{\partial s^*} = R_s \frac{\partial}{\partial s}$$

$$p^* = \frac{p(1 - v^2)}{Eh} \cdot R_s = \frac{p(1 - v^2)}{Eh^*}$$

Where,

R_s = R for cylinder and sphere
 $= b$ for torus etc.

$$\epsilon_{\theta}^* = \epsilon_{\theta} = \frac{\cos\phi}{r^*} u^* + \frac{\sin\phi}{r^*} w^* \quad (B.1)$$

$$\gamma_{\phi}^* = \gamma_{\phi} \quad (B.2)$$

$$\kappa_{\theta}^* = \kappa_{\theta} R_s = \frac{\cos\phi}{r^*} \gamma_{\phi}^* \quad (B.3)$$

$$M_{\phi}^* = \frac{M_{\phi} h}{D}, \quad M_{\theta}^* = \frac{M_{\theta} h}{D}$$

$$N_{\phi}^* = \frac{N_{\phi}}{K}, \quad N_{\theta}^* = \frac{N_{\theta}}{K}$$

Where,

$$D = \frac{Eh^3}{12(1-v^2)} \quad (B.4)$$

$$K = \frac{Eh}{1-v^2} \quad (B.5)$$

$$M_{\theta}^* = v M_{\phi}^* + (1-v^2) h^* \kappa_{\theta}^* \quad (B.6)$$

$$N_{\theta}^* = v N_{\phi}^* + (1-v^2) \epsilon_{\theta}^* \quad (B.7)$$

$$\epsilon_{\phi}^* = N_{\phi}^* - v \epsilon_{\theta}^* \quad (B.8)$$

$$\kappa_{\phi}^* = \frac{M_{\phi}^*}{h^*} - v \kappa_{\theta}^* \quad (B.9)$$

B.2 Non-dimensionalized Governing Shell Equations.

Non-dimensionalized linear set of first order governing shell equations are:

$$w^*, s^* = \frac{U_\phi^*}{R_\phi^*} - \gamma_\phi^* \quad (B.10)$$

$$\gamma_\phi^*, s^* = \frac{M_\phi^*}{h^*} - v K_\theta^* = K_\phi^* \quad (B.11)$$

$$M_\phi^*, s^* = \frac{\cos\phi}{r^*} (M_\theta^* - M_\phi^*) + \frac{12 (r^* Q_\phi^*)}{r^* h^*} \quad (B.12)$$

$$\begin{aligned}
 (r^* Q_\phi^*), s^* &= N_\theta^* \sin\phi + \frac{r^* N_\phi^*}{R_\phi^*} + r^* \kappa_{\theta 0}^* N_\theta^* + r^* N_{\theta 0}^* \kappa_\theta^* + r^* \kappa_{\phi 0}^* N_\phi^* \\
 &+ r^* N_{\phi 0}^* \kappa_\phi^* + \frac{r^*}{R_\phi^*} \gamma_{\phi 0}^{*2} N_\phi^* + \frac{2r^*}{R_\phi^*} N_{\phi 0}^* \gamma_{\phi 0}^* \gamma_\phi^* - \frac{r^*}{R_\phi^*} Q_{\phi 0}^* \gamma_\phi^* \\
 &- \frac{r^*}{R_\phi^*} \gamma_{\phi 0}^* Q_\phi^* - r^* \kappa_{\theta 0}^* N_{\theta 0}^* - r^* \kappa_{\phi 0}^* N_{\phi 0}^* - \frac{2r^*}{R_\phi^*} \gamma_{\phi 0}^{*2} N_{\phi 0}^* \\
 &+ \frac{r^*}{R_\phi^*} Q_{\phi 0}^* \gamma_{\phi 0}^* - p^* r^* \quad (B.13)
 \end{aligned}$$

$$U_\phi^*, s^* = \epsilon_\phi^* - \frac{w^*}{R_\phi^*} - \frac{1}{2} \gamma_\phi^{*2} \quad (B.14)$$

$$\begin{aligned}
 N_{\phi,s}^* &= \frac{\cos\phi}{r^*} (N_{\theta}^* - N_{\phi}^*) - \frac{r^* Q_{\phi}^*}{R_{\phi}^* r^*} + \frac{1}{R_{\phi}^*} \{ \gamma_{\phi 0}^* N_{\phi 0}^* + \gamma_{\phi 0}^* (N_{\phi}^* - N_{\phi 0}^*) \\
 &\quad + N_{\phi 0}^* (\gamma_{\phi}^* - \gamma_{\phi 0}^*) \} \\
 &= \frac{\cos\phi}{r^*} (N_{\theta}^* - N_{\phi}^*) - \frac{r^* Q_{\phi}^*}{R_{\phi}^* r^*} + \frac{1}{R_{\phi}^*} \{ \gamma_{\phi 0}^* N_{\phi 0}^* + N_{\phi 0}^* \gamma_{\phi}^* \} \\
 &\quad - \frac{1}{R_{\phi}^*} \gamma_{\phi 0}^* N_{\phi 0}^*
 \end{aligned} \tag{B.15}$$

B.3 Singularities at the Apex of Shells.

Since at the apex of the shell $r=0$ and r occurs in the denominator of the shell equations, it is essential to have some means of correcting such singularities while maintaining the accuracy during the numerical integration process. If we consider the shell apex as smooth rather than pointed, then these singularities can be removed conveniently. If the shell apex is smooth then obviously $\phi=0$. The non-dimensionalization of the shell equations has helped in reducing this problem to fewer number of the governing equations. Further, it should be noted that during the non-dimensionalization the governing equation for $Q_{\phi,s}$ has been rearranged to help remove the singularities from that equation.

From symmetry at the apex in the axisymmetric shells of revolution it is recognized that:

$$u = 0$$

$$\text{and } \gamma = 0 \quad (B.16)$$

$$\phi = 0 \quad r = 0$$

and if there is no concentrated load at the apex $Q_\phi = 0$.

Since the meridional and circumferential directions are not distinct at the apex:

$$N_\theta = N_\phi$$

$$M_\theta = M_\phi \quad (B.17)$$

$$\epsilon_\theta = \epsilon_\phi$$

$$(B.18)$$

$$\text{and } \kappa_\theta = \kappa_\phi$$

Hence, with the above conditions and with the rearranging of only one governing equation to be $(r Q)_s$, rather than Q_ϕ , the non-dimensionalization of the shell equations has helped in removing

the singularities at the apex. There are other ways that this could have been done. For instance the shell region at the apex can be regarded as a shallow spherical shell.

APPENDIX C

SHELL CONFIGURATIONS

1. Cylinder.

R	= radius of cylinder
ϕ	= 90°
r	= R
R_ϕ	= ∞
R_θ	= R
L	= Length of cylinder
S	= L

2. Sphere.

R	= radius of sphere
ϕ	= angle of normal to the middle surface measured from axis of revolution.
r	= R
R_ϕ	= R
R_θ	= R

3. Torus.

a	= distance of torus center measured from axis of symmetry.
b	= radius of torus.

ϕ = angle of normal to the middle surface measured from the axis of revolution.
 r = $a+b \sin\phi$
 R_ϕ = b
 R_θ = $a+b \sin\phi$
 s = Distance measured along meridian middle surface.

4. Cone.

R_ϕ = ∞
 s = Distance measured along the meridian
 ϕ = angle of normal to the middle surface measured from the axis of revolution.
 a = distance of initial edge from the axis of revolution.
 α = Cone angle
 R_θ = $b \tan \alpha$
 b = Length on the meridian.
 r = $a+b \sin\alpha$

5. Annular Plate.

ϕ = 0
 a = initial edge
 r = $a+b \sin\alpha$

b = distance between initial and final edge.

α = 90°

R_ϕ = ∞

R_θ = r

APPENDIX D

DEFINITION OF HARDENING

The nature of incremental plastic analysis is such that a set of strain values must be assumed with which the iteration procedure must start. These assumed values of strains should be reasonably close approximation, to the behavior, preferably, in order to speed the convergence process. The procedure to be used for predicting the magnitude of the strains must also be consistent with the material behavior. The available material curves have been constructed based on uniaxial loading experiments and, thus, can not fully describe biaxial or multiaxial stress behavior.

Let $\bar{\sigma}$ be the calculated effective stress and $\bar{\sigma}_y$ the corresponding yield point stress. β is the slope of elastic-plastic portion of the bilinear stress-strain curve and is some measure of strain hardening of the material.

The total strain is composed of elastic and plastic component of strain.

$$\epsilon = \epsilon^e + \epsilon^p \quad (D.1)$$

$$\bar{\sigma} = \bar{\sigma}_0 + \beta E (\varepsilon - \varepsilon_y) \quad (D.2)$$

$$= \bar{\sigma}_0 + \beta E (\varepsilon^e + \varepsilon^p - \varepsilon_y)$$

$$= \bar{\sigma}_0 + \beta E \left(\varepsilon^p + \frac{\bar{\sigma}}{E} - \frac{\bar{\sigma}_0}{E} \right)$$

$$\bar{\sigma} = \bar{\sigma}_0 + \frac{E}{K} \varepsilon^p \quad (D.3)$$

Where $K = \frac{1-\beta}{\beta}$ as defined in Fig. (D.1)

But:

$$\bar{\sigma}^2 = \sigma_\phi^2 - \sigma_\phi \sigma_\theta + \sigma_\theta^2 = H^2 \text{ (say)} \quad (D.4)$$

Where H is the hardening modulus.

or:

$$\bar{\sigma} = H = \bar{\sigma}_0 + \frac{E \varepsilon^p}{K} \quad (D.5)$$

Taking the derivative with respect to ε^p

$$\frac{\partial \bar{\sigma}}{\partial \varepsilon^p} = H' = \frac{E}{K} \quad (D.6)$$

Hence, H is the slope of the effective stress-plastic strain diagram. It can be determined from the available material experimental data.

Corresponding to a load increment let the stress increments be represented by $d\sigma_\phi$ and $d\sigma_\theta$ for stress components σ_ϕ and σ_θ and the corresponding strain increments by $d\varepsilon_\phi$ and $d\varepsilon_\theta$.

At a given load level P_a the linear elastic solution is obtained. The maximum stress value for all points through the meridian and radial direction is located. If this maximum stress value of effective stress is larger than the yield stress it is scaled down to the yield stress. The load P_a is also correspondingly scaled down to P_b .

At the value of P_b the non-linear elastic solution is determined. The maximum stress value is once again located. This maximum effective stress value is scaled to the yield stress and the scalar factor α is determined such that:

$$\sigma_y = \alpha \bar{\sigma}_{\max} \quad (D.7)$$

The scalar factor is now used to scale the entire solution and a load P_c is determined. The non-linear elastic solution is once again obtained at the load level P_c by direct integration of governing shell equations. This process is repeated until the non-linear elastic solution is at the yield point at which the load level is P_y .

The resulting value of P_y is the load level at which the plastic solution load steps must begin. The solution at this load level is stored as residuals indicated by the subscript (1). A load increment ΔP_n is now taken and the total load at this load step is:

$$P_n = P_m + \Delta P_n \quad (D.8)$$

Where n is the current increment number and m the previous increment number. At the first load step $P_m = P_y$ such that,

$$P_1 = P_y + \Delta P_1 \quad (D.9)$$

A study of the Newton-Raphson algorithm has indicated that this incremental load step must be small enough to maintain the stress point near the yield surface and within the scope of this algorithm to bring it to the yield surface. The entire solution is now scaled to this load level $P_m + \Delta P_n$.

The effective stress values of this scaled solution at every point along the meridian and radial direction are now checked against the yield stress of the material. If a point is elastic then, the corresponding assumed values of stress and strain increments are given by:

$$d\sigma_\phi = \sigma_\phi - \sigma_{\phi i} \quad (D.10)$$

$$d\sigma_\theta = \sigma_\theta - \sigma_{\theta i} \quad (D.11)$$

$$\bar{\sigma} = \sigma_{\phi}^2 - \sigma_{\phi} \sigma_{\theta} + \sigma_{\theta}^2 \quad (D.12)$$

$$d\bar{\sigma} = \bar{\sigma} - \bar{\sigma}_i \quad (D.13)$$

$$d\epsilon_{\phi} = \frac{1}{E} (d\sigma_{\phi} - v d\sigma_{\theta}) \quad (D.14)$$

$$d\epsilon_{\theta} = \frac{1}{E} (d\sigma_{\theta} - v d\sigma_{\phi}) \quad (D.15)$$

$$d\epsilon = 0 \quad (D.16)$$

However if a point is plastic the entire calculation procedure is in the incremental form.

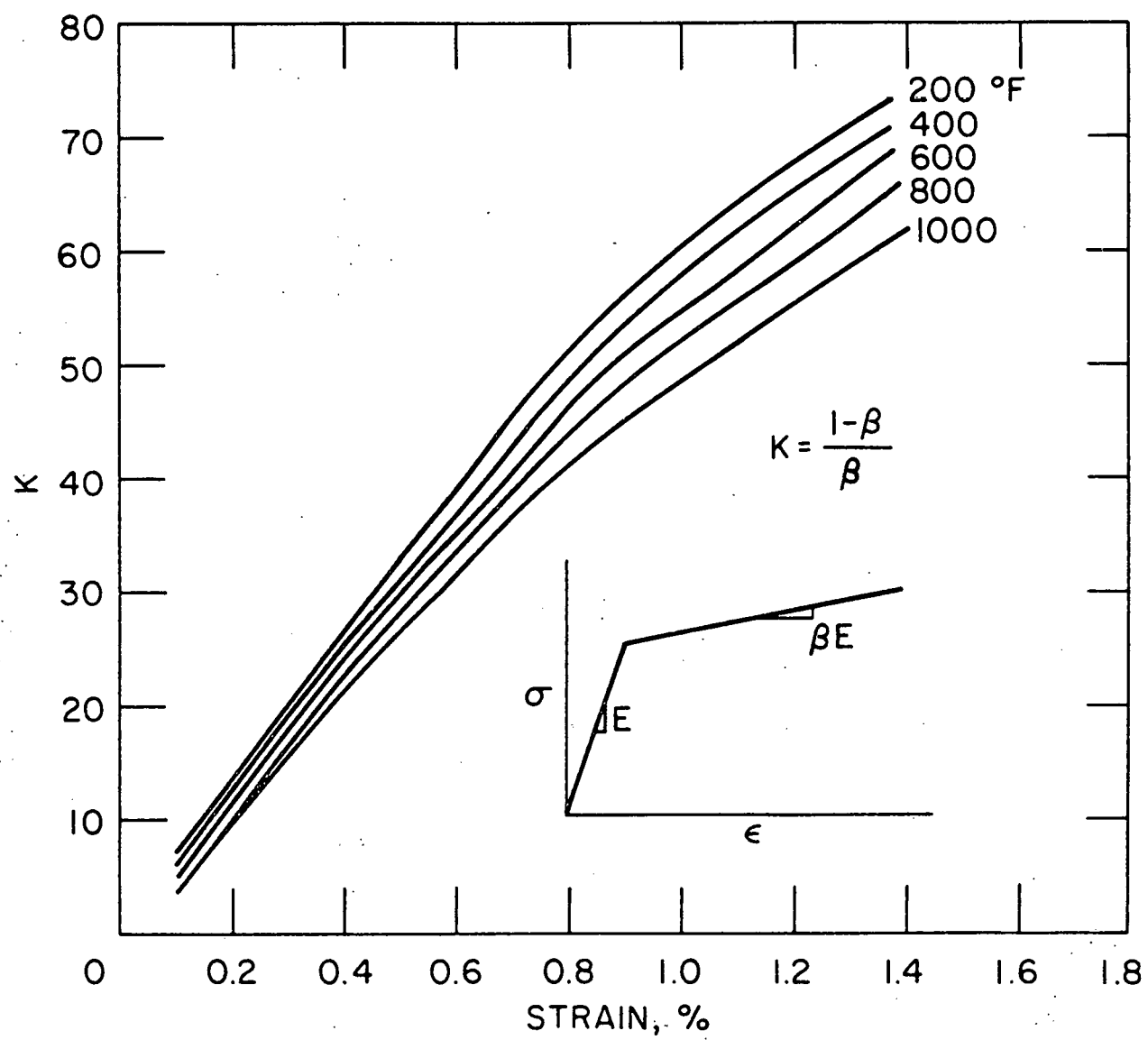


Figure D.1. Bilinear Strain Hardening Properties of SS304 Material.

BIBLIOGRAPHY

1. Hill, R., Mathematical Theory of Plasticity, Oxford, Clarendon Press (1964).
2. Green, A. E. and Naghdi, P. M., "A General Theory of an Elastic-plastic Continuum," *Arch. Rational Mech. Anal.*, Vol. 18, 1965, pp. 251-281.
3. Lee, E. H., "Elastic-plastic Deformation at Finite Strain," *3. Applied Mechanics*, 36(1) (March 1969), p. 1-6.
4. Wu, R. W. H. and Witmer, E. A., "Finite-element Analysis of Large Transient Elastic-plastic Deformations of Simple Structures with Application to the Engine Rotor Fragment Containment/Deflection Problem," NASA-CR-120886, ASRL TR154-4 (January 1972).
5. Koiter, W. T., "On the Nonlinear Theory of Thin Elastic Shells," *Proc. Koninklyke Nederl. Akad. van Wetensch. (Ser. B)*, 69:1-54, No. 1, 1966.
6. Naghdi, P. M. and Nordgren, R. P., "On the Nonlinear Theory of Elastic Shells under the Kirchoff's Hypothesis," *Quarterly Applied Mathematics*, 21:49-59 (1963).
7. Sanders, J. L., "Nonlinear Theories for Thin Shells," *Quarterly Applied Mathematics*, 21:21:36 (1963).
8. Biricikoglu, V. and Kalnins, A., "Large Elastic Deformations of Shells with the Inclusion of Transverse Normal Strains," *Int. Journal of Solids and Structures*, 7:(5), May 1971, pp. 431-444.
9. Gerdeen, J. C., et. al, "Large Deflection Analysis of Elastic-Plastic Shells using Numerical Integration," *AIAA Journal*, 9(6) (June 1971), p. 1012-1018.
10. Kalnins, A., "Analysis of Shells of Revolution Subjected to Symmetrical and Nonsymmetrical Loads," *ASME Journal of Applied Mechanics*, 31:(3) (September 1964). p. 467-476.
11. Goldberg, J. E. and Bogdanoff, J. F., "Static and Dynamic Analysis of Nonuniform Concave Shells under Symmetrical and Unsymmetrical Conditions," *Proc. Sixth Symposium on Ballistic Missile and Aerospace Technology*, Los Angeles, 1, Academic Press New York, 1961, p. 219-238 v. 1.

12. Kalnins, A. and Lestini, J. F., "On Linear Analysis of Elastic Shells of Revolution," ASME Journal of Applied Mechanics, Trans, 34(1) March 1967, p. 59-64.
13. Leonard, J. W., "Dynamic Response of Initially Stressed Membrane Shells," ASCE Journal of the Engineering Mechanics Div., 95(EM5) (October 1969), p. 1231-1253.
14. Carter, R. L., Robinson, A. R., and Schnobrich, W. C., "Free Vibrations of Hyperboloidal Shells of Revolution," ASCE Journal of the Engineering Mechanics Div., 95 (EM5) (October 1969) p. 1033-1052.
15. Marcal, P. V. and Pilgrim, W. R., "A Stiffness Method for Elastic-Plastic Shells of Revolution," Journal of Strain Analysis 1(4):339-350 (1966).
16. Marcal, P. V., "Large Deflection Analysis of Elastic-Plastic Shells of Revolution," AIAA/ASME 10th Structures, Structural Dynamics, and Materials Conference, New Orleans, April 14-16, 1969, p. 369-379.
17. Marcal, P. V., "Finite Element Analysis of Combined Problems of Nonlinear Material and Geometric Behavior," Computational Approaches in Applied Mechanics, ASME (1970), Computer Conf. IIT, 1969, E. Sevin, ed., p. 133-149.
18. Marcal, P. V., "Large Deflection analysis of Elastic-plastic Plates and Shells," Proc. of the First International Conference on Pressure Vessel Technology, Part I, Desigh and Analysis, Delft, Netherlands, (1969), P. 75-87, ASME.
19. Yaghmam, S., "Incremental Analysis of Large Deformations in Mechanics of Solids with Applications to Axisymmetric Shells of Revolution," NASA CR-1350 (June 1969).
20. Gerdeen, J. C., "Nonlinear Elastic-plastic analysis of Shells of Revolution," Special Report, Battelle Memorial Institute, Columbus, Ohio (August 1968).
21. Mulcahey, T. M., "An Assessment of Kinematic Hardening Thermal Ratchetting," Journal of Engineering Materials and Technology, TRANS, ASME, Vol. 96, (July 1974). pp. 214-221.
22. Bree, J., "Ratchet and Fatigue Mechanisms in Sealed Fuel Pins for Nuclear Reactors," TRG Report 1214 (D), 1966.

23. Leech, J. W., pian, T. H. H., Witmer, E. A., and Herrmann, W., "Dynamic Response of Shells to Externally-Applied Dynamic Loads." Massachusetts Institute of Technology, ASD- TDR-62-610, 1962.
24. Pugh, C. E., et al. Currently Recommended Constitutive Equations for Inelastic Design Analysis of FFTF Components, 1972, ORNL-TM-3602.
25. McLellan, D., L., "Prediction of Stress-Strain Behavior at Various Strain Rates and Temperatures." 7th International Symposium of High Speed Testing; The Rheology of Solids, Boston, Massachusetts, March 17-18, 1969. Applied Polymer Symposia No. 12, 1969, p. 137-163.
26. Leech, J. W., "Finite Difference Calculation Method for Large Elastic-Plastic Dynamically-Induced Deformations of General Thin Shells." Massachusetts Institute of Technology, AFFDL-TR-66-171, December 1966.
27. Leech, J. W., Witmer, E. A., and Pian, T. H. H., "Numerical Calculation Technique for Large Elastic-Plastic Transient Deformations of Thin Shells." AIAA Journal, Vol. 6, No. 12, Dec. 1968, pp. 2352-2359.
28. Morino, L., Leech, J. W., and Witmer, E. A., "PETROS 2: A New Finite-Difference Method and Program for the Calculation of Large Elastic-Plastic Dynamically-Induced Deformations of General Thin Shells." Massachusetts Institute of Technology, ASRL, TR 152-1 (BRL CR 12) December 1969.
29. Morino, L., Leech, J. W., and Witmer, E. A., "An Improved Numerical Calculation Technique for Large Elastic-Plastic Transient Deformations of Thin Shells." Journal of Applied Mechanics, Vol. 38, No. 2, June 1971, pp. 423-436.
30. Atluri, S., Witmer, E. A., Leech, J. W., and Morino, L. "PETROS 3: A Finite-Difference Method and Program for the Calculation of Large Elastic-Plastic Dynamically-Induced Deformations of Multilayer Variable-Thickness Shells." Massachusetts Institute of Technology, ASRL TR 152-2, (BRL CR 60), November 1971.

31. Pirotin, S. D., Morino, L., Witmer, E. A., and Leech, J. W., "Finite-Difference Analysis for Predicting Large Elastic-Plastic Transient Deformations of Variable-Thickness Soft-Bonded Thin Shells." Massachusetts Institute of Technology, ASRL TR 152-3, Dec. 1971.
32. Huffington, N. J., Jr., "Blast Response of Panels." BRL TN 1702 August 1968.
33. Massard, J. M., "General Inelastic Response of Layered Shells." Lockheed Missiles and Space Co., (GIRLS I and IA, Report L-H-66-12), (GIRLS II, Report L-41-66-6). September 1966.
34. Roth, R. S., Muskat, R., and Grady, P. J., "Unsymmetrical Bending of Shells Of Revolution-- A Digital Computer Program." Avco Corp., Wilmington, Massachusetts., Report KHDR-6, Feb., 1965.
35. Stern, P., "SADISTIC IV-Stresses and Displacements in Layered Orthotropic Shells of Revolution with Temperature Dependent Properties." Lockheed Missiles and Space Co., Sunneyvale, Calif. Report L-41-66-7, Hardening Technology Studies II, September 1966.
36. Wrenn, B. G., Sobel, L. H., and Silbsy, W., "Nonsymmetrical and Nonlinear Response of thin Shells." Lockheed Missiles and Space Co., Report LMSC-B-72-67-3, Dec. 1967.
37. Silbsy, W., Sobel, L. H., and Wrenn, B. G., "Nonsymmetrical and Nonlinear Dynamic Response of Thin Shells, Vol. 1, User's Manual for STAR (Shell Transient Asymmetric Response)." Lockheed Missiles and Space Co., Report LMSC-B-70-68-19, Dec. 1968.
38. Hubka, W. F., "A Calculation Method for the Finite Deflection, Elastic-Plastic Dynamic Response of Shells of Revolution." Kaman Nuclear Report No. KN-69-26(M), January 1969.
39. Bushnell, D., "Stress, Stability, and Vibration of Complex Shells of Revolution: Analysis @ User's Manual for BOSOR 3." Lockheed Missiles and Space Co., SAMSO TR 69-375, September 1969
40. Ball, R. E., "A Program for the Nonlinear Static and Dynamic Analysis of Arbitrarily-Loaded Shells of Revolution." Conference on Computer-Oriented Analysis of Shell Structures, Palo Alto, Calif., Paper 37, p. 10-14, 1970.

41. Kalnins, A., "FREE Vibration of Rotationally Symmetric Shells." J. Acoustical Soc. Am., Vol. 36, No. 7, July 1964, pp. 1355-1365.
42. Svalbonas, V., and Angrisano, N., "Numerical Analysis of shells, Volume 1: Unsymmetric Analysis of Orthotropic Reinforced Shells of Revolution," NASA CR-61299, Sept. 1969.
43. Cohen, G. A., "Computer Program for Analysis of Imperfection Sensitivity of Ring-Stiffened Shells of Revolution." NASA CR-1801, October 1971.
44. Archer, J., "Consistent Matrix Formulations for Structural Analysis Using Finite-Element Techniques." AIAA Journal, Vol. 3, October 1965, pp. 1910-1918.
45. Argyris, J. H., "Continue and Discontinue--- An Apercu of Recent Developments of the Matrix Displacement Methods." Proceedings of the First AFFDL Conference on Matrix Methods in Structural Mechanics, ARRD-TR-66-80, December 1965, pp. 11-190.
46. Cappelli, A. P., Nishimoto, T. S., and Radkowske, P. R., "Analysis of Shells of Revolution Having Arbitrary Stiffness Distributions." AIAA J. Vol. 7, No. 10, Oct. 1969, p. 1909-1915.
47. Schaeffer, H. G., "Computer Programs for Finite-Difference Solutions of Shells of Revolution under Asymmetric Loads." NASA TN D-3926, 1967.
48. Greene, B. E., Jones, R. E., McLay, R. W., and Strome, D. R., "Dynamic Analysis of Shells Using Doubly-Curved Finite Elements." Proc. 2nd. AFFDL Conference on Matrix Methods in Structural Mechanics, AFFDL-TR-68-150, Oct. 1968, pp. 185-212.
49. MacNeal, R. H. (Editor), "NASTRAN: Theoretical Manual; User's Manual; Programmer's Manual; and Demonstration Problem Manual." NASA Documents respectively, SP-221, SP-222, SP-223, SP-224, 1969.
50. Klein, S. and Sylvester, R. J., "The Linear Elastic Dynamic Analysis of Shells of Revolution by the Matrix Displacement Method." Proceedings of the First AFFDL Conference in Matrix Methods in Structural Mechanics, AFFDL-TR-66-80, December 1968, pp. 299-328.

51. Kotanchik, J. J.; Yeghiayan, R. P., Witmer, E. A., and Berg, B. A., "The Transient Linear Elastic Response analysis of Complex Thin Shells of Revolution Subjected to Arbitrary External Loadings, by the Finite Element Program SABORS/DRASTIC." SAMSO TR 70-206 (MIT-ASRL TR 146-10) AD 709189, April 1970.
52. Clough, R. W. and Wilson, E. L., "Dynamic Finite Element Analysis of Arbitrary Thin Shells." Conference on Computer-Oriented Analysis of Shell Structures at Lockheed Palo Alto Research Laboratory, August 1970, Paper 40, p. 10-14.
53. Key, S. W. and Beisinger, Z. E., "The Transient Dynamic analysis of Thin Shells by the Finite Element Method." Third AFFDL Conference on Matrix Methods in Structural Mechanics, October 1971.
54. Stephens, J. A., Martinez, J. E., Tillerson, J. R. Hong, J. H., and Haisler, W. E., "Nonlinear Dynamic Analysis of Shells of Revolution by the Matrix Displacement Method." Dept. of Aerospace Eng., Texas A & M University, Report 69-77, FEB. 1970.
55. Stricklin, J. A., Martinez J. E., Tillerson, J. R., Hong, J. H., and Haisler, W. E., "Nonlinear Dynamic Analyses of Shells of Revolution by the Matrix Desplacement Method." AIAA Journal, Vol. 9, No. 4, April 1971, pp. 629-636.
56. Dalus, W. L., Ip, C., and VanDerlinden, J. W., "Design Considerations of Elastic-Plastic Structures Subjected to Dynamic Loads." AIAA/ASME 11th Structures, Structural Dynamics & Materials Conf., April 22-24, 1970, Denver, Colorado.
57. Wu, R. W-H., and Witmer, E. A., "Finite-Element Analysis of Large Elastic-Plastic Transient Deformations of Simple Structures," AIAA Journal, Vol. 9, No. 9, September, 1971, pp. 1719-1724.
58. Zienkiewicz, O. C., and Parekh, C. J., "Transient Field Problems: Two-Dimensional and Three-Dimensional Analysis by Isoparametric Finite Elements." Intl. Journal for Numerical Methods in Engineering, Vol. 2, 1970, pp. 61-71.
59. Liepins, A. A., "Asymmetric Nonlinear Dynamic Response and Buckling of Shallow Spherical Shells." NASA CR-1367, June 1969.

60. Turner, M. J., Dill, H., Martin, H. C., and Melosh, R. J., "Large Deflection Analysis of Complex Structures Subjected to Heating and External Loads." *J. Aero Space Sciences*, Vol. 27, Feb. 1960, pp. 97-106.
61. Crank, J., and Nicolson, P., "A Practical Method for Numerical Evaluation of Solutions of Partial Differential Equations of the Heat Conduction Type" *Proc. Camb. Phil. Soc.* 43, 50-67, 1947.
62. Hodge, P. G., "Computer Colutions of Plasticity Problems", University pf Minnesota - Contract N14-67-A-113-25, Project No. NR064-429, Report H1-3.
63. Hodge, P. G., Garg, V, K.M Anand, S. C., "A Finite Element Method for Plasticity Problems", University of Minnesota, Contract N14-67-A-113-25, Project NR064-429, Report AEM-H1-6, 1973.
64. Mendleson, A., Plasticity: Theory and Applications, the Macmillan Company, New York. 1968.
65. Hutula, David Norman,"Large Deflection Elastic-Plastic Analysis of Axisymmetric Shells of Revolution"Phd. Thesis-Michigan Technological University, University Microfilms Inc., Ann Arbor, Michigan.
66. Lee, E. S. et.al,"Application of Quazilinearization to the Solution of Non-linear Differential Equations" Kansas State University, Manhattan Kansas, July 1967.
67. Kalnins, A., Lestini, J. F., "On Non-linear Analysis of Elastic Shells of Revolution" *Journal of Applied Mechanics*, March, 1967- pp.59-64.
68. Bellman R., Functional equation in the Theory of Dynamic programming. V-Positivity and quasi-linearity." Proc. Nat Acad., Sci. 41, 743. 1955.
69. Kalaba R., J. Math. Mech., "On Non-linear Differential Equations- The Maximum Operation and Monotone Convergence", 8,519, 1959.
70. Lee, E. S., "Quasi-linearization, Non-linear boundary value problems and optimization." Chem. Eng. Sci., 21,183, 1966.

71. Diercks, D. et.al. "Results of Strain Hardening Experiments for Stainless Steel Material-Conducted at Argonne National Laboratory" - to be reported.
72. W. Prager and P. G. Hodge, Theory of Perfectly Plastic Solids, Wiley, New York, 1951.
73. D. C. Drucker, Some Implications of work Hardening and Ideal Ideal Plasticity, Quart. Appl. Math., 7, 1950., pp 411-418.
74. D. C. Drucker, A more Fundamental Approach to Plastic Stress-Strain relations, 1st U. S. Congress of Applied Mechanics, ASME, New York, 1952, pp. 487,491.
75. R. Von Mises, Mechanic der festes Koerper in Plastisch deformation Zustand, Goeltinger Nachr, Math. Phys., K1, 1913, pp. 582-592.
76. L. Prandt. Spannungsverteilung in Plastischen Koerpern, Proceedings of the 1st International Congress on Applied Mechanics, Delft, Technische Boekhandel en Druckerij, J. Waltman, Jr., 1925, pp 43-45.
77. E. Reuss, Beruecksichtigung der elastischen Formaenderungen in der Plastizitaetstheorie, Z. Angew. Math. Mech., 10, 1930, pp. 266-274.
78. W. Prager, "The Theory of Plasticity - A Survey of Recent Achievements," Proc. Inst. Mech. Engrs., London, 169, 41, 1955.
79. Ohashi, Y., Murkame, S., and Endo, A., "Elasto-plastic Binding of an Annular Plate at Large Deflection." Ingenieur-Archiv, v35, 1967, pp 340-350.
80. Zarghamee, M. S. and Robinson , R. R. "Free and Forced Vibration of Spherical Shells". Illinois University, Department of Civil Enginee ing. Structural Research. Series 293. July 1965. p:130.
81. Zarghamee, M. S. and Robinson, R. R. "Numerical Methods for Analysis of Free Vibration of Spherical Shells." AIAA Journal 7, July 1967. p. 1256-61.